CIV102 – Structures and Materials
An Introduction to Engineering Design
Course Notes

Allan Kuan
Michael P. Collins

September 2021

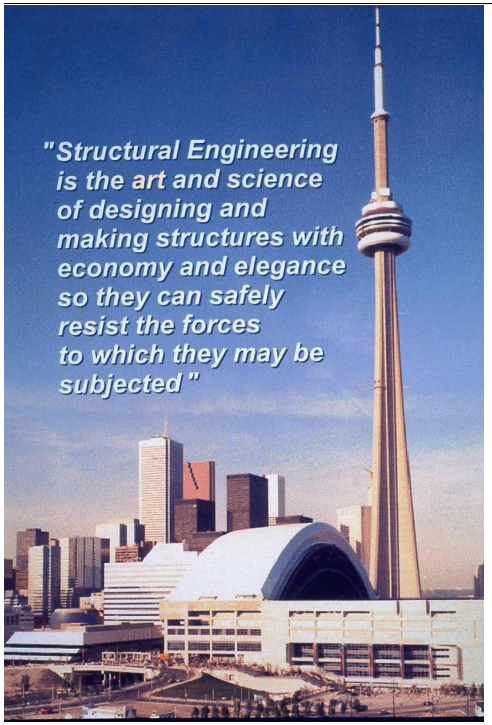

CIV102 – Structures and Materials
An Introduction to Engineering Design

University of Toronto
Division of Engineering Science
September 2021

Allan Kuan
Michael P. Collins

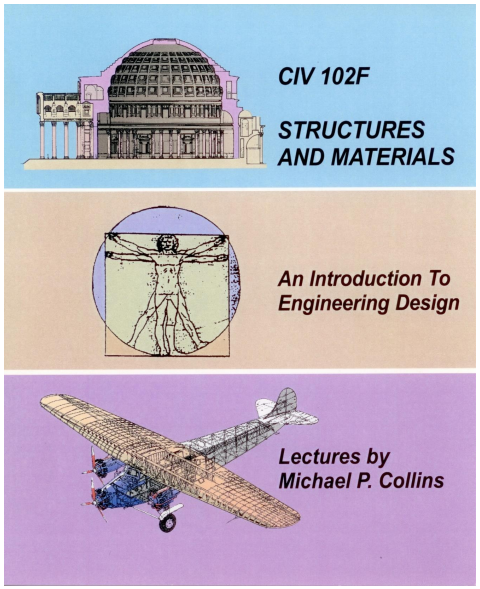

The previous cover of the course notes, used until 2020.

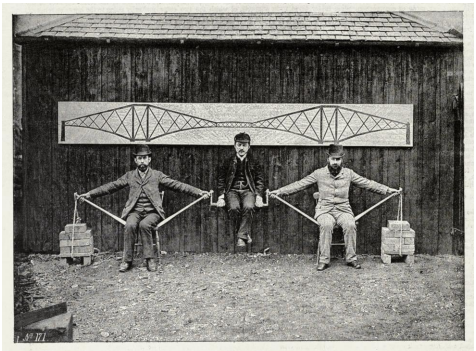

Living demonstration explaining the principles which allow the Firth of Forth railroad bridge to carry load. Designed by Benjamin Baker and John Fowler.

Table of Contents

Test of a 4 m deep reinforced concrete slab strip at the University of Toronto in 2015. This remains the largest reinforced concrete shear test ever performed.

Lecture 1 – The Three Principles of Engineering

The Three Principles of Engineering

"The four to twelve page Toike Oike we remember – with its notices of School events, reports of meetings, accounts of the exploits of School teams, messages from the Dean and occasional jokes – would scarcely seem to have the potential to convulse the University of Toronto. True the bound volume in the Engineering Society Office did have one issue with a short joke encircled in blue pencil. We understood that this had got the editor suspended – possibly even expelled. It is also true that in our fourth year Engineering Physics wrested control from the former editors, apparently meeting with little organized resistance, and produced Volume XXX (or possibly XXXI – there seems to have been some confusion). Luckily no one attempted to use this experiment as a launching pad for a career in journalism or politics. But one of the editors who remains active has just fearlessly restated the three fundamental Principles of Engineering presented in that 1939 manifesto:

1. $F = M \times A$
2. *You can't push on a rope.*
3. *A necessary condition for solving any given Engineering problem is to know the answer before starting*

Structural engineering is a branch of civil engineering which is interested in the analysis and design of structures which must safely carry forces. Some examples of civil structures designed by structural engineers, which are typically built out of steel, concrete, or timber, include buildings, bridges, tunnels, dams, and concrete offshore platforms. The principles used in structural engineering are also applicable to disciplines outside of civil engineering, such as aerospace engineering and biomedical engineering.

Before getting into the nuts and bolts of structural engineering, it is worth spending some time pondering the meaning of the ***Three Principles of Engineering*** in greater detail. As their name suggests, these principles apply, generally speaking, to all disciplines of engineering. They are particularly relevant to structural engineers however, as the collapse of significant structures – including those in Canada – have greatly influenced how engineering is practiced today. In fact, the Iron Ring ceremony, a ritual undergone by all engineers trained in Canada to affirm the duties and responsibilities of the profession, has its roots in the collapse of the Quebec Bridge in 1907.

The First Principle of Engineering, $\mathbf{F = M \times A}$, is Newton's second law of motion. It has practical applications in many branches of physics and engineering. For example, mechanical and aerospace engineers use it to design objects intended to move, such as transportation vehicles, spacecraft, or even robotic drones. Structural engineers on the other hand, typically make use of the special case of Newton's second law, which is when A, the acceleration of a body, is equal to 0. When this condition is satisfied, a system is said to be in a ***state of equilibrium***. The concept of equilibrium is fundamental to structural engineering, which is primarily interested in systems which do not accelerate except under exceptional circumstances, like during a severe earthquake.

Symbolically, the First Principle of Engineering represents the idea that engineers use mathematical models to understand and shape the world around them. Many branches of engineering do not use Newton's laws of motion but instead use their own discipline-specific set of tools which are also grounded in physics and math. Practicing engineers must master the application of these tools in their work, while engineers who work in research seek to develop new models and expand the body of knowledge of their respective field of engineering.

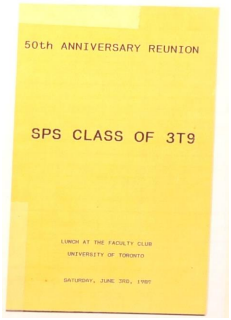

Fig.1.1 – Engineering Manifesto.

The Second Principle of Engineering, **"You can't push on a rope**", is very different from the First Principle. From a structural engineering perspective, a rope collapses when pushed because it is too flexible to carry a compressive (pushing) force. The technical reason why this occurs is because the rope ***buckles***. Buckling, which is discussed in greater detail later in the course, does not exclusively affect ropes, but can happen to any slender member is being subjected to a large compression force.

Buckling of slender compression members was the cause of failure of the Quebec Bridge, which collapsed during construction in 1907, killing 75 workers. The bridge, which was designed by the American engineer Theodore Cooper, had a similar shape as the Firth of Forth Railway Bridge which was at the time the longest cantilever truss bridge in the world. Baker and Fowler's bridge, shown in Fig. 1.2, used very large members to safely carry the large compression forces in the structure. Cooper, who ridiculed the Firth of Forth Railway Bridge for using excessive amounts of steel, instead used comparatively slender members in his design, which is shown in Fig. 1.3. These members, which buckled during construction, caused the failure shown in Fig. 1.4.

Fig. 1.2 – Baker and Fowler's Firth of Forth Railway Bridge. The two main spans are each 1700 feet long. Opened 1890.

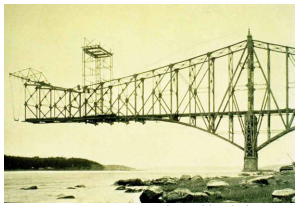

Fig. 1.3 – Cooper's Quebec Bridge during construction.

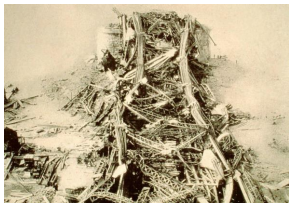

Fig. 1.4 – Cooper's Quebec Bridge after collapse.

Although the First Principle of Engineering celebrates the use of mathematical models in engineering, the Second Principle is a reminder to draw upon common sense and experience when working with the real world. The results of calculations – which can be simple calculations done by hand or complex simulations performed on a supercomputer – must be checked to ensure that they make sense. We know from our experience living in the real world that gravity pulls objects down, materials tend to expand when heated, light travels faster than sound, slender members buckle when pushed with great force, and so on. Calculations which suggest otherwise should generally not be trusted.

The Third Principle of Engineering is perhaps best summarized as **"To find the answer, you must know the answer"**. Although seemingly paradoxical, engineering is full of situations where this statement is true. For example, structural engineers often encounter the following dilemma: a bridge must be designed to carry loads which includes its own self-weight. However, its weight is not known until after the bridge has been designed, which in itself requires knowing its weight at the beginning of the design process. Without experience, resolving this paradox can be challenging and may even result in designs which are dangerously unsafe. Navigating through most engineering problems therefore requires a reasonable idea of what the final design will be before starting, i.e., the answer must be known before it is obtained.

The Third Principle of Engineering illustrates the value of experience when practicing engineering. It is also a reminder of the dangers of approaching new problems where one does not have any prior experience to act as a guide. The collapse of the Quebec Bridge, which was by far the longest bridge ever designed by Cooper, can partially be attributed to him straying from the Third Principle and attempting to find the answer without knowing what it should have been in the first place.

Lecture 2 – Basic Concepts: Newton, Pulling on Ropes, Units

Overview

In this chapter, a variety of basic concepts are introduced which permit simple structural systems to be understood from a mechanics-based perspective. Beginning from Newton's laws of motion, the idea of forces – such as the force due to gravity, and tension and compression forces transmitted through structural members – is discussed. By introducing the concept of a moment, a turning action which causes bodies to rotate, the three equations of equilibrium for two-dimensional systems are presented. The chapter concludes with a brief discussion about units.

Newton's Laws of Motion

Newton's three laws of motion are:

1. "Every body continues in its state of rest, or of uniform motion in a right line, unless it is compelled to change that state by forces impressed upon it". This can be mathematically expressed as:

$$\sum F = 0 \rightarrow a = 0 \tag{2.1}$$

2. "The change of motion is proportional to the motive force impressed; and is made in the direction of the right line in which that force is impressed"

$$F = ma \tag{2.2}$$

3. "To every action there is always opposed an equal reaction: or, the mutual actions of two bodies upon each other are always equal, and directed to contrary parts."

In Eq. (2.1) and (2.2), **F** is a force applied to the body, **m** is its mass (which is assumed to be constant), and **a** is the translational acceleration of the body. The first law of motion is especially relevant to the field of structural engineering, where the bodies considered are typically not accelerating despite being subjected to numerous forces.

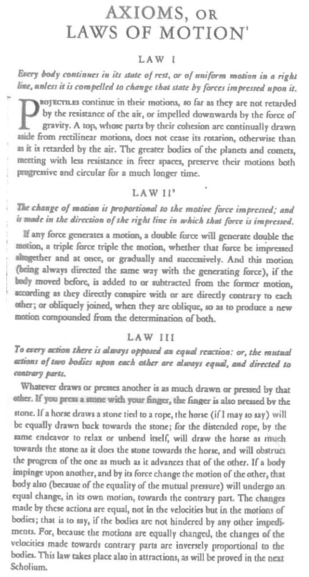

AXIOMS, OR
LAWS OF MOTION

LAW I

Every body continues in its state of rest, or of uniform motion in a right line, unless it is compelled to change that state by forces impressed upon it.

Projectiles continue in their motions, so far as they are not retarded by the resistance of the air, or impelled downwards by the force of gravity. A top, whose parts by their cohesion are continually drawn aside from rectilinear motions, does not cease its rotation, otherwise than as it is retarded by the air. The greater bodies of the planets and comets, meeting with less resistance in freer spaces, preserve their motions both progressive and circular for a much longer time.

LAW II

The change of motion is proportional to the motive force impressed; and is made in the direction of the right line in which that force is impressed.

If any force generates a motion, a double force will generate double the motion, a triple force triple the motion, whether that force be impressed altogether and at once, or gradually and successively. And this motion (being always directed the same way with the generating force), if the body moved before, is added to or subtracted from the former motion, according as they directly conspire with or are directly contrary to each other; or obliquely joined, when they are oblique, so as to produce a new motion compounded from the determination of both.

LAW III

To every action there is always opposed an equal reaction: or, the mutual actions of two bodies upon each other are always equal, and directed to contrary parts.

Whatever draws or presses another is as much drawn or pressed by that other. If you press a stone with your finger, the finger is also pressed by the stone. If a horse draws a stone tied to a rope, the horse (if I may so say) will be equally drawn back towards the stone; for the distended rope, by the same endeavor to relax or unbend itself, will draw the horse as much towards the stone as it does the stone towards the horse, and will obstruct the progress of the one as much as it advances that of the other. If a body impinge upon another, and by its force change the motion of the other, that body also (because of the equality of the mutual pressure) will undergo an equal change, in its own motion, towards the contrary part. The changes made by these actions are equal, not in the velocities but in the motions of bodies; that is to say, if the bodies are not hindered by any other impediments. For, because the motions are equally changed, the changes of the velocities made towards contrary parts are inversely proportional to the bodies. This law takes place also in attractions, as will be proved in the next Scholium.

Fig. 2.1 – Newton's three laws of motion.

Basic Definitions – Forces

The acceleration due to gravity caused by the pull of the Earth on a body is defined as **g**. Using Newton's second law, the gravitational force $\mathbf{F_g}$ which pulls an object with mass **m** towards the centre of the earth, is defined as:

$$F_g = mg \tag{2.3}$$

g varies around the world depending on the elevation of the ground, assuming a larger value closer to sea level and a smaller one at high elevations. A typical value of g which is accurate to three significant figures is **g = 9.81 m/s²**. This value is reasonably accurate over a wide range of elevations and will be used for all calculations in this course.

The main purpose of a structural member is to transmit forces from one location to another, like the rod shown in Fig. 2.2 which is being pulled with a force of 100 N on either side. The behaviour of the rod can be understood using Newton's first and third laws. Because the forces are equal in magnitude but pointing in opposite directions, the rod does not accelerate and is in a state of translational equilibrium. Furthermore, if the forces were caused by two people

pulling on the rod, they would feel the rod resist their applied force with an equal and opposite reaction force in order to maintain this state of equilibrium. A free body diagram drawn through any point along the rod would show that the internal force at every location is a pulling, or tensile, force of 100 N.

Fig. 2.2 – A body carrying 100 N of tension.

A member like the one shown in Fig. 2.2 which is carrying a pulling force acting through its axis is said to be in ***tension***. The opposite of tension is ***compression***, which is defined as a pushing force acting through the axis of a member like the one shown in Fig. 2.3. A free body diagram drawn through any point along the rod's length will reveal that the internal force at every location is a pushing, or compression, force of 100 N.

Fig. 2.3 – A body carrying 100 N of compression.

Components of Forces in Two Dimensions

When dealing with two-dimensional systems in the x-y plane, forces will generally produce an effect in both the horizontal (typically taken as x) and vertical (typically taken as y) directions. The actions of a force along these directions are called its x- and y- components respectively. A force **F** which is acting at an angle **θ** relative to the x axis, like the one drawn in Fig. 2.4, has components in the x- and y- direction, $\mathbf{F_x}$ and $\mathbf{F_y}$ respectively, defined as:

$$F_x = F\cos\theta \tag{2.4}$$

$$F_y = F\sin\theta \tag{2.5}$$

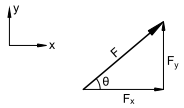

Fig. 2.4 – Components of a force.

The magnitude of the force is related to its components by Pythagoras' theorem:

$$F = \sqrt{(F_x)^2 + (F_y)^2} \tag{2.6}$$

Note: It often more convenient to define the x and y components of a force F using the side lengths of a similar triangle whose hypotenuse is parallel to F, instead of defining an angle θ. For example, for the force vector shown below in Fig. 2.5, defining sinθ = (b/c) and cosθ = (a/c) allows us to define the components as:

$$F_x = F\cos\theta = \frac{a}{c}F$$

$$F_y = F\sin\theta = \frac{b}{c}F$$

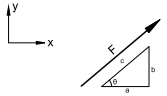

Fig. 2.5 – Determining the components of a force using a similar triangle.

Rotational Actions – Moments

In addition to causing translational motion, forces can also cause bodies to rotate. A ***moment*** is the turning effect produced by a force about a reference point when the line of action of the force does not pass through the defined point of reference. The moment $\mathbf{M_i}$ caused by a force about reference point **i** is defined as the product of the magnitude of the force **F** and the perpendicular distance between its line of action and the reference point, $\mathbf{d_i}$:

$$M_i = F \times d_i \tag{2.7}$$

Because a moment is defined based on a reference point, the moment produced by a force will be different when calculated about different reference points. For example, the 5 N force in Fig. 2.6 produces a counterclockwise moment of 5 N × 4 m = 20 Nm about point A and a clockwise moment of 5 N × 6 m = 30 Nm about point B.

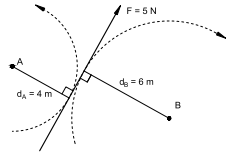

Fig. 2.6 – A 5 N force producing moments about points A and B.

A ***couple*** is special class of moments which occurs when two forces with the same magnitude **F** act in the opposite direction of each other while being separated by a perpendicular distance **d**. This produces a pure turning effect about every reference point in the x-y plane:

$$M = F \times d \tag{2.8}$$

A schematic of a couple is shown in Fig. 2.8.

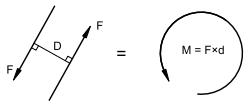

Fig. 2.8 – Definition of a couple.

*Note: Like moments, a **torque** is also a form of rotational force. A torque is a special case of a moment which acts through the axis of a prismatic object.*

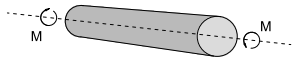

Fig. 2.7 – A moment acting about the axis of a prism, often referred to as a torque.

Note: Like forces, moments are considered as vectors, not scalars. Therefore, they are defined by both a magnitude, which may be in units of Nm, and a direction, which may be clockwise or counterclockwise.

Equations of Equilibrium

For two-dimensional systems, Newton's first law must be extended to include both translational and rotational equilibrium. Translational equilibrium requires the sum of all forces to equal zero in both the x- and y- directions so that there is no net translational acceleration:

$$\sum F_x = 0 \tag{2.9}$$

$$\sum F_y = 0 \tag{2.10}$$

Rotational equilibrium in the x-y plane also requires that the sum of all moments be equal to zero so that there is no rotational acceleration:

$$\sum M = 0 \tag{2.11}$$

Equations (2.9) to (2.11) are collectively referred to as the ***equations of equilibrium***. For a system which is in equilibrium, these equations are always satisfied regardless of the choice of coordinate system and reference point used to evaluate them.

Equilibrium of Forces which Meet at a Point

A special case of equilibrium is a system of forces which meet at a point, like the five forces shown in Fig. 2.9. Because each force passes through a common point, rotational equilibrium is guaranteed because the moment produced by each force about the point of intersection is equal to zero. Hence, only the two translational equations of equilibrium, Eq. (2.9) and (2.10), need to be satisfied for the system to be in equilibrium.

Frictionless Pulleys

Pulleys used together with cables are one of the simplest systems used in structural engineering. Consider the circular pulley with radius ***r*** shown in Fig. 2.10 which supports a rope being pulled with a force $\mathbf{T_1}$ on the left and $\mathbf{T_2}$ on the right. When the system is in equilibrium, the pulley will not rotate and hence the sum of moments must equal to zero. If it is assumed that there is no friction in the system, the moments produced by $\mathbf{T_1}$ and $\mathbf{T_2}$ about the centre of the pulley, $\mathbf{M_1}$ and $\mathbf{M_2}$ respectively, can be calculated as:

$$M_1 = T_1 \times r, \text{ acting counterclockwise}$$

$$M_2 = T_2 \times r, \text{ acting clockwise}$$

Taking the sum of all moments and setting them to equal to zero yields the following result:

$$\sum M_o = M_1 + M_2 = T_1 \times r - T_2 \times r = 0 \rightarrow T_1 = T_2 \tag{2.12}$$

Note: Equilibrium of a series of forces which meet at a point can be visualized by graphically rearranging the force vectors so that the tail of one vector connects with the tip of another. If a closed path can be formed by re-arranging the forces in this manner, the system is in equilibrium.

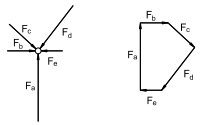

Fig. 2.9 – Five forces which meet at a point. They are in equilibrium because the force vectors can be rearranged to form a closed path. Note their lengths are proportionate to their magnitude.

Thus, the tension carried by a wire remains constant as it goes around a frictionless pulley. The pulley only serves to redirect the tension force carried by the wire.

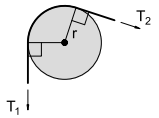

Fig. 2.10 – Free body diagram of an ideal pulley.

Dimensions and Units

In engineering, calculations are done using physical quantities which have units. In order to carry out these calculations correctly, it is necessary to become comfortable working with units and converting between them as needed.

It is important to distinguish between dimensions and units. ***Dimensions*** refer to the measurable physical quantities which describe a property – for example, the dimension of velocity is distance/time. ***Units*** are the means to describe dimensions according to some sort of standard reference. Using our example from before, common units used to measure velocity are metres per second (m/s) or kilometres per hour (km/h).

When performing calculations with physical properties, note the following rules:

1. Two quantities which are added together or subtracted from one other must have the same units
2. Quantities which are multiplied together or divided from each other will have their units multiplied or divided accordingly. For example, a velocity in m/s multiplied by a time in s will result in a distance in units of m.

In engineering, having a sense of what each unit means is necessary to interpret the correctness of a calculation and avoid unrealistic answers. Measurements of length and area are the most intuitive because of our experience working with objects and space in the real world. Units for weight and pressure are generally more difficult to visualize, but can still be interpreted using the following simple examples:

- 1 N is approximately the weight of a small apple
- 1 kN is approximately the weight of a football player
- 1 MPa is approximately the pressure applied to a notebook carrying the weight of an African bush elephant

Table 2.1 contains a list of common conversions which will occur in the course, and is reproduced in **Appendix E**.

Note: In CIV102, calculations will primarily be done using units of N or kN for forces, mm or mm^2 for geometric properties, MPa for stresses and kNm for bending moments. Calculations can be consistently done by working exclusively with units of mm, N and MPa.

Table 2.1 – Sample Unit Conversions

Working with SI units		
Lengths, Strains and Curvatures	Pressures and Stresses	Forces and Moments
1 m = 1,000 mm	1 Pa = 1 N/m^2	1 kN = 1,000 N
1 m^2 = 10^6 mm^2	1 kPa = 1 kN/m^2	1 MN = 10^6 N
1 m^3 = 10^9 mm^3	1 MPa = 1 MN/m^2	
	1 MPa = 1 N/mm^2	1 Nm = 1,000 Nmm
1 mm/m = 10^3 mm/mm		1 kNm = 10^6 Nmm
1 rad/m = 10^6 mrad/mm		
Working with other unit systems and other miscellaneous quantities		
1 foot = 12 inches	1 inch = 25.4 mm	
1 cubit = 18 inches	1 foot = 304.8 mm	9.81 m/s^2 = 32.2 feet/s^2
1 yard = 3 feet	1 mile = 1609 m	1 kNm = 0.738 kip ft
1 chain = 22 yards	1 ha = 2.47 acres	1 kNm = 8.85 kip in
1 furlong = 10 chains		
1 mile = 8 furlongs	1 kg = 2.20 lbs	1 hp = 746 Watt
1 mile = 1,760 yards	1 stone = 14.0 lbs	
		1 km/h = 0.278 m/s
1 acre = 10 square chains	1 lbs/ ft^3 = 16.02 kg/ m^3	1 km/h = 0.621 miles/h
1 square mile = 640 acres	100 lbs/ft^3 = 15.72 kN/m^3	1 knot = 1.852 km/h
1 ha = 10,000 square m		1 MPa = 145.0 psi
	1 N = 0.225 lbs (force)	1 kN/m^2 = 20.9 lbs/ft^2
	1 kip = 4.45 kN	

Lecture 3 – Building Bridges

Overview

In this chapter, the history of bridges is briefly discussed before the topic of suspension bridges is examined in more detail. The mechanics of how cable structures carry load is explained by using the concepts covered in Lecture 2.

Building Bridges

Bridges are structures which cross over obstacles such as rivers, roads, or cliffs and hence connect two locations which would otherwise be separated. The earliest bridges were used to cross over rivers and were built by simply felling a large tree and positioning the trunk over the water to span the distance between the two banks. More elaborate bridges were used by the Romans, who crossed over larger rivers by driving wood pieces into the riverbed and using them to support the longer deck, like the bridge shown in Fig. 3.1. Some examples of modern types of bridges are truss bridges, which consist of steel or timber pieces arranged in a lattice-like configuration, suspension bridges, which use steel cables to support a deck over long distances, and arch bridges built from stone or reinforced concrete. Many bridge systems will be introduced and discussed in further detail throughout the course, beginning with suspension bridges in this lecture.

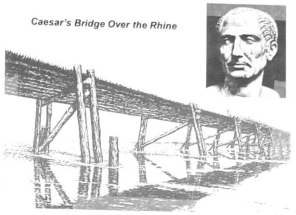

Fig. 3.1 – Caesar's Bridge over the Rhine.

Suspension Bridges

Suspension bridges, like the bridge designed by Thomas Telford shown in Fig. 3.2, use long cables carrying tension forces to support the bridge deck over significant distances. Improvements in construction methods and the increasing quality of steel cables has meant that many of the longest bridges in the world today are suspension bridges. Despite these advancements, the underlying mechanics of how these structures work remains grounded in the basic principles covered in the previous chapter.

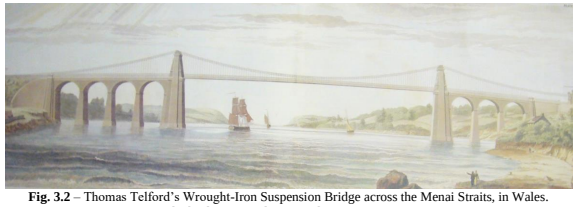

Fig. 3.2 – Thomas Telford's Wrought-Iron Suspension Bridge across the Menai Straits, in Wales. The bridge, opened in 1826, has a 177 m span.

Cable Forces in Suspension Bridges

For cable structures which carry hanging loads, the shape of the cables depends on how the loads are distributed. A cable which is not carrying any load besides its own self-weight is shown in Fig. 3.3. The shape that the cable assumes in this situation is called a ***catenary***. Accounting for this special shape can be important when designing cable

structures whose loading is dominated by the self-weight of the cables. A common example of such structures are power lines used to transmit electricity over long distances.

Fig. 3.3 – A hanging cable forming the shape of a catenary under its own weight.

When a load which is significant compared to the self-weight of the cable is hung at the midspan, the cable will change shape to form two straight lines. Having three weights will result in four straight lines, five weights will result in six straight lines, and so on. This progression is shown in Fig. 3.4, which shows how the shape of a hanging cable changes as the number of weights hung from it increase from one, to three, to five. Although the shape of the cable remains piecewise linear, the straight segments begin to approximate a smooth curve as the number of weights is increased. If the weights remain constant in value and the spacing between them approaches zero, the load is said to be ***uniformly distributed*** along the length of the structure. When this happens, the slope of the cable will vary linearly along the span and hence assume the shape of a ***parabola***.

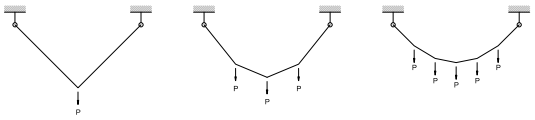

Fig. 3.4 – Change in cable shape as weights are added.

The tension in the cable at any location along the span can be determined by drawing a free body diagram. This is done by drawing the free body diagram so that its boundary cuts through the structure at the location of interest. Because the original structure was in equilibrium, the resulting substructures are also in equilibrium, and hence the three equations of equilibrium must be satisfied for each free body diagram. This is illustrated in Fig. 3.5, which investigates the tension in the cable between the first and second loads from the left by separating the structure at this location. Since the left and right substructures must both be in equilibrium, either free body diagram may be used to solve for the unknown tension in the wire, which has a vertical component of 3/2P.

Note: Although the shape of a cable under its own weight (a catenary) and a cable supporting a uniformly distributed load (a parabola) appear similar, the shapes are subtly different because of the differences in the loading. For a freely hanging cable, the load per unit length of the cable is constant, whereas for a cable supporting a uniform load, the load per unit length of the span is constant. Because the cable follows a curved profile, the self-weight of the cable is not constant along the length of the span, which results in the shape of the catenary.

Note: When drawing a free body diagram by cutting through a member, the internal forces which were carried by the member at the cut must be drawn onto the resulting free body diagram. This is because the internal forces are necessary for satisfying equilibrium of the structure at that point.

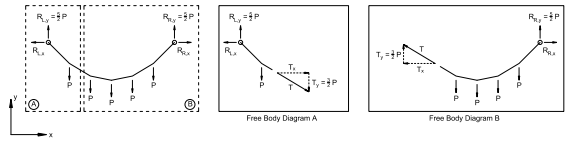

Fig. 3.5 – Analysis of tensile forces in a cable structure.

If a series of free body diagrams are drawn, like in Fig. 3.6, the variation in the tension force in the cable can be determined. Due to symmetry, only three free body diagrams need to be drawn to solve for the forces in the six straight segments of the structure, which are the forces at locations A, B and C.

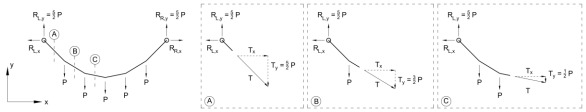

Fig. 3.6 – Calculating the variation of tension force in the cable using free body diagrams.

Determining the vertical component of the tension is a straightforward task if the vertical force carried by the two supports on the ends is known. They can be found by applying the three equations of equilibrium to a free body diagram of the whole structure, which results in reaction force of 5/2P on each side in this example. Once these support forces are known, equilibrium in the vertical direction requires that the vertical component of tension in the cable vary from a maximum of 5/2 P at the support, to a minimum of 1/2P at the midspan. If the spacing of the weights was reduced to approach zero, i.e., the load be uniformly distributed, the vertical component of force would reduce linearly from a maximum at the support to 0 at the midspan.

The horizontal component of force in the cable can be obtained using the other two equations of equilibrium. It should be noted however that in each of the free body diagrams shown in Fig. 3.6, the horizontal component of tension at the location of interest equals horizontal force supplied by the support. This allows us to conclude that the horizontal component of tension remains constant along the structure.

For a cable carrying tension, its inclination is a function of the relative size of its horizontal and vertical components. Under uniform loading, the vertical component of force in the cable varies linearly along its length while its horizontal component remains constant. Therefore, the slope of the cable will also vary linearly along its span, which results in the cable taking the shape of a parabola.

Note: Recall Fig. 2.4 which is reproduced below as Fig. 3.7. The slope of the force, and hence the cable, is equal to F_y divided by F_x.

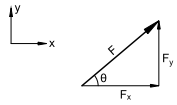

Fig. 3.7 – Components of a force.

Lecture 4 – Design of a Suspension Bridge

Overview

In this chapter, the equations of equilibrium are used to derive the cable forces in a uniformly loaded suspension bridge. The use of the resulting design equations is then illustrated using the Golden Gate Bridge as a real-life example

Analysis of Suspension Bridges

Consider the suspension bridge shown in elevation view in Fig. 4.1 which has a span ***L*** and a drape ***h***. The main cables support the loads carried by the deck, which is attached to the main cables using secondary hanger cables. The bridge supports a uniformly distributed load ***w*** which has units of force per unit length (i.e., kN/m). By examining a free body diagram of the whole structure, the vertical reaction forces provided by the towers at the ends of the bridge can be found by considering vertical and rotational equilibrium about the centre of the bridge:

$$\sum F_y = 0 \rightarrow R_{L,y} + R_{R,y} - wL = 0 \tag{4.1}$$

$$\sum M_{\text{midspan}} = 0 \rightarrow -R_{L,y} \times \left(\frac{L}{2}\right) + R_{R,y} \times \left(\frac{L}{2}\right) = 0 \tag{4.2}$$

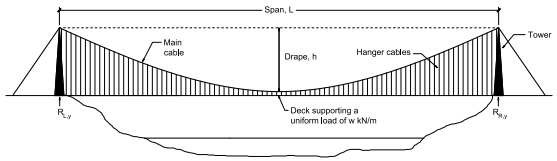

Fig. 4.1 – Elevation (side) view of a suspension bridge.

Equations (4.1) and (4.2) form a system of two equations and two unknowns, which are the reaction forces $\mathbf{R_{L,y}}$ and $\mathbf{R_{R,y}}$. Solving for the two unknowns leads to the conclusion that each support resists half of the total load carried by the bridge:

$$R_{L,y} = R_{R,y} = \frac{wL}{2} \tag{4.3}$$

Using this information, the equations of equilibrium can now be used to learn more about the forces in the cables between the supporting towers. Consider the free body diagram of half of the bridge, taken from the left support to the midspan, which is shown in Fig. 4.2.

Span: the horizontal distance between the two supports of a bridge.

Drape: The vertical distance between the highest and lowest points of the supporting cable.

Reaction Force: The force provided by a support in order to keep the structure in equilibrium.

Note: The result shown in Eq. (4.3) was rigorously proven using the equations of equilibrium. The same result could have been obtained by considering symmetry of the system.

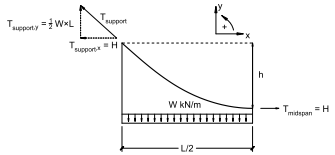

Fig. 4.2 – Analysis of forces in a cable. Note that T_{midspan} has no y-component because the cables are horizontal at midspan.

Applying the three equations of equilibrium to the free body diagram yields the following results:

$$\sum F_x = 0 \rightarrow -T_{\text{support, x}} + T_{\text{midspan}} = 0 \tag{4.4}$$

$$\sum F_y = 0 \rightarrow T_{\text{support, y}} - w \times \frac{L}{2} = 0 \tag{4.5}$$

$$\sum M_{\text{support}} = 0 \rightarrow T_{\text{midspan}} \times h - \left(w \times \frac{L}{2}\right) \times \frac{L}{4} = 0 \tag{4.6}$$

From Eq. (4.4), we can conclude that the horizontal component of tension, **H**, is constant in the cables. Furthermore, in Eq. (4.5), the vertical component of tension, **V**, is highest at the support and reduces to zero at the midspan. These observations are consistent with the results discussed in the previous chapter. Therefore:

$$T_{y,\max} = T_{\text{support, y}} = \frac{wL}{2} \tag{4.7}$$

Finally, re-arranging for H in Eq. (4.6) yields the following important result:

$$H = \frac{wL^2}{8h} \tag{4.8}$$

The maximum tension in the cables can be determined by calculating the net force from the vertical and horizontal components:

$$T_{max} = \sqrt{\left(T_{\text{x, max}}\right)^2 + \left(T_{y,\max}\right)^2} = \sqrt{\left(\frac{wL^2}{8h}\right)^2 + \left(\frac{wL}{2}\right)^2} \tag{4.9}$$

*Note: A distributed force **w** acting over a length **L** can be replaced by an equivalent point load which has the same magnitude and acts through the centroid of the distributed load. Some common examples are shown below:*

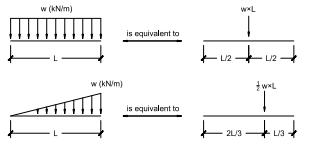

Note: In Eq. 4.6, the moments are calculated about the top-left corner of the free body diagram (i.e. at the support). The results of the derivation would not be affected if the moments were instead calculated about any other location.

*Note: The tension in the cables is lowest at the midspan of the bridge because $T_y = 0$ there. At this location, the tension in the cable is simply equal to **H**. Furthermore, the forces discussed in this chapter are the sum of the tensile forces carried by each main cable. Because there are usually two main cables in a suspension bridge, these forces should be divided by two when designing each individual cable.*

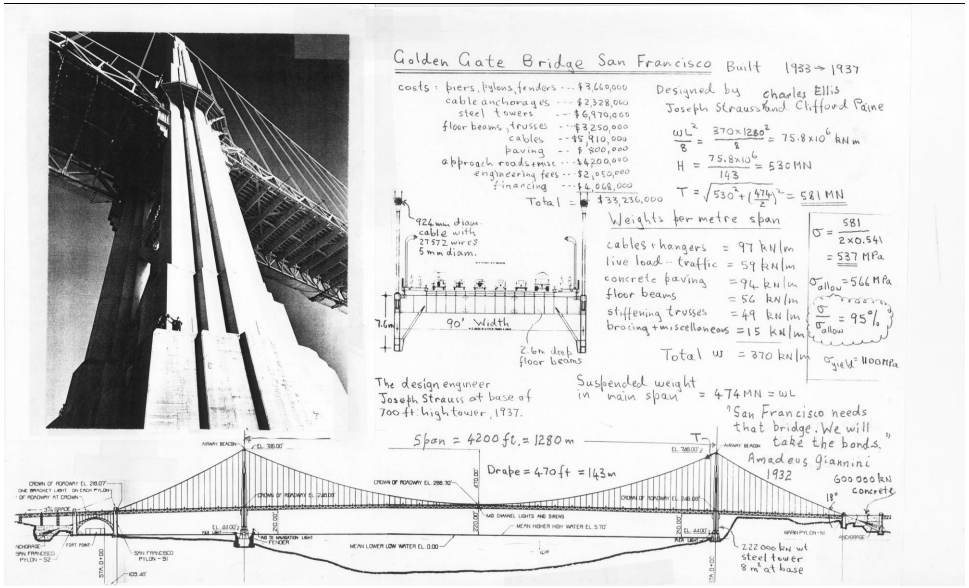

Fig. 4.3 – Design Calculations for the Golden Gate Bridge.

Lecture 5 – Stress, Strain, Hooke's Law and Young's Modulus

Overview

In this chapter, the basics of material behaviour are introduced. Hooke's law for linear elastic springs is discussed for simple structures subjected to tension or compression forces. After introducing the concepts of stress and strain, the Young's Modulus is introduced for relating the two for linear elastic materials. The spring constant for a member is demonstrated to be a product of its material stiffness and geometry.

Hooke's Law

In Robert Hooke's 1678 paper "Explaining the Power of Springing Bodies" he states, "The particles therefore that compose all bodies I do suppose to owe the greatest part of their sensible or potential extension to a vibrative motion." He suggested that the particles might vibrate back and forth one million times a second and protect their natural space.

After studying the behaviour of materials and springs, Hooke presented his findings as an anagram, *"ceiiinosssttuv"*, which, when decoded, spells out *"ut tensio, sic vis"*. This is a Latin phrase which translates to *"as the extension, so the force"*. Mathematically, Hooke's law explains that the restoring force in a spring, **F**, is proportionate to its change in length, **Δl**, by a constant **k:**

$$F = k\Delta l \tag{5.1}$$

Note: Although Hooke's law refers to the behaviour of springs, it is applicable to any structure which is subjected to direct tension or compression, such as a cable or a column.

In Eq. (5.1), the spring stiffness **k** has units of force per unit length, such as N/mm, and **F** acts in the opposite direction as **Δl**. A structure which obeys Hooke's law is said to be ***linear elastic***.

*Note: Because **F** and **Δl** are defined as the force and change in length in the direction of a prismatic member's axis, **k** is sometimes referred to as the **axial stiffness** of a member.*

Hooke's Law for Linear Elastic Materials – Stress, Strain and Young's Modulus

The spring constant of a member is affected by its shape and material composition. For example, a thin wire is easier to stretch than a thick wire made from the same material, and a rope made from a stiff material like steel is more difficult to stretch than a similarly shaped rope made from a softer material like plant fibre. To understand how the geometry of a member and its material properties contribute individually to the overall stiffness, we will introduce the concepts of stress and strain.

Stress is a physical quantity which describes the internal forces acting on a material. For a force **F** which is carried by a prismatic member with an undeformed cross-sectional area **A**, like the situation shown in Fig. 5.1, the engineering stress **σ** is defined as:

$$\sigma = \frac{F}{A} \tag{5.2}$$

Note: Although the definitions of stress and pressure appear to be similar, pressures refer to forces which are externally applied to a body (i.e. pressure applied to a surface), whereas stresses refer to internal forces which are carried by a structure (i.e. stress in a cable) or a material (i.e. stress in steel).

Fig. 5.1 – Terminology used to define stress.

Stress has dimensions of force per unit area and is typically described in units of MPa (MN/m² or N/mm²). Because of this, stress can be thought of as the normalized force per unit area experienced by a material.

Strain is a physical quantity which describes how much a material is being deformed. For a prismatic member with original length $\mathbf{L_o}$ which has elongated by a length **Δl**, like the situation shown in Fig. 5.2, the engineering strain **ε** is defined as:

$$\varepsilon = \frac{\Delta l}{L_o} \tag{5.3}$$

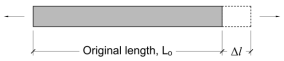

Fig. 5.2 – Terminology used to define strain.

Although strain is dimensionless, it is typically described in units of mm/mm, mm/m or even %. Because of this, strain can be thought of as the normalized change in length experienced by a material.

The benefits of using stress and strain to describe the forces and deformations in a material, instead of simply using the force and displacement of a structure, is because it allows the behaviour of structures to be compared even if they are different sizes. For example, a thin wire will intuitively break at a lower load than a thicker wire, but failure will occur at the same stress if they are both made from the same material.

Just like how Hooke's law states that the force and stretch of a spring are related by a constant, the stress felt by a linear elastic material is proportionately related to its strain by a constant **E**:

$$\sigma = E\varepsilon \tag{5.4}$$

E is called the ***Young's Modulus***, named after the English scientist Thomas Young. It has the same dimensions as stress and is commonly written in units of MPa. Fig. 5.3 shows the stress-strain relationship for several materials which have different values of **E**.

Note that the strains used in Eq. (5.4) are strains which are associated with a material deforming as it tries to carry stress. Materials may deform for other reasons, and in some circumstances, it may be necessary to distinguish between the strains associated with stress, and the strains caused by other effects. Some examples of strains which do not cause stress and should not be used in Eq. (5.4) are thermal strains caused by temperature effects, or shrinkage strains caused by water loss. Some of these effects are described in later chapters.

*Note: The **engineering stress** and **engineering strain** are defined using the undeformed geometry of the member. In reality, a member's cross-sectional area and length will change when it is carrying load. The **true stress** and **true strain** are the corresponding definitions of stress and strain when the deformed geometry is used instead. Although the true stress and true strain are more realistic indicators of a material's physical state, they cannot be easily measured, so the engineering definitions are used instead.*

*Note: Eq. (5.4), which relates the stress and strain in the material, is sometimes referred to an example of a constitutive relationship. Because **E** is a characteristic property of material which relates stress and strain, it is sometimes referred to as the **material stiffness**.*

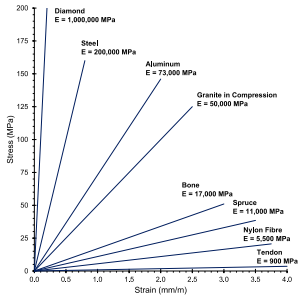

Fig 5.3 – Typical values of E for various materials.

Expressing k in Terms of Geometry and Material Stiffness

Hooke's law for linear elastic springs, Eq. (5.1), and its equivalent for linear elastic materials, Eq. (5.4), resemble each other because they both relate a force-based quantity (**F** or **σ**) and a displacement-based quantity (**Δl** or **ε**) by a stiffness-based quantity (**k** or **E**). Fig. 5.4 shows how these quantities are related to each other for linear elastic structures subjected to axial load:

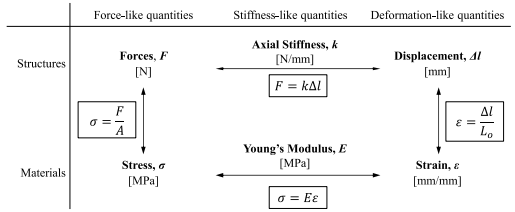

Fig. 5.4 – Relationships between structures and materials.

If the geometric properties **A** and $\mathbf{L_o}$, and material stiffness **E**, are known, then **k** for a member can be calculated by combining equations (5.2) to (5.4) and isolating for **F** and **Δl**. This results in the following relationship:

$$F = \frac{AE}{L_o}\Delta l \rightarrow k = \frac{AE}{L_o} \quad (5.5)$$

Therefore, the axial stiffness of a member **k** is proportionate to its cross-sectional area **A** and material stiffness **E**, and inversely proportionate to its length $\mathbf{L_o}$.

*Note: **k** will have units of N/mm if **A** is in mm², **E** is in MPa and $\mathbf{L_o}$ is in mm.*

Lecture 6 – Stress-Strain Response, Resilience, Toughness & Ductility

Overview

In this chapter, key material properties which are used in the design of structures are discussed. The complete stress-strain relationship for mild steel, a common material used in many steel and reinforced concrete structures, is presented.

Generalized Stress-Strain Behaviour

As materials are loaded to failure, they generally do not exhibit linear elastic behaviour for their entire life. Gradual accumulation of damage to the microstructure of the material and other material-specific internal effects cause the stress-strain curve to be nonlinear in general. Even materials which look and feel similar may have very different stress-strain properties. For example, Fig. 6.1 shows the stress-strain behaviour of three different types of steel whose stress-strain behaviour differs greatly due to the amount of carbon present.

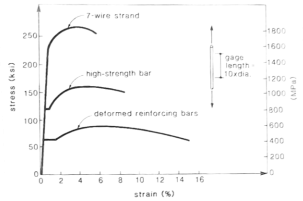

Fig. 6.1 – Stress-strain behaviour of different types of steel.

To describe key features of a material's stress-strain curve, engineers have defined ***material properties*** which serve as useful tools for evaluating and comparing different materials. Common aspects which are described by material properties include a material's weight, strength, stiffness, ductility and energy absorption capabilities. Fig 6.2, which shows the stress-strain curve of mild steel, illustrates many of the various material properties which are described below:

The ***strength*** of a material describes how much stress it can carry before failure occurs. Multiple definitions of strength exist to recognize the various stages of failure which a material experiences as it is loaded. The ***yield strength*** is defined as the stress which causes yielding to occur. The ***ultimate strength*** is defined as the largest stress which the material can carry before failure. Note that the strength of many materials in tension is different from their strength in compression.

Yielding: the state when a material, usually metals, begins to accumulate permanent deformations. When yielding begins, the strain will continue to increase even if the stress is held constant. The portion of the stress-strain curve which exhibits this behaviour is sometimes referred to as the ***yield plateau.***

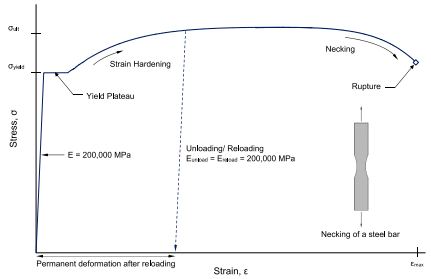

Fig. 6.2 – Stress-strain curve of mild steel in tension

The concept of ***ductility*** has several definitions, but generally refers to much a material can be deformed before it breaks. On a stress-strain curve, this refers to the largest strain a material can carry before fracturing. Materials which can sustain significant amounts of permanent deformation before failing are generally referred to as being ***ductile***, while those which cannot are referred to as being ***brittle***.

The slope of the linear elastic region of the stress-strain curve of a material is the ***Young's Modulus***, **E**. Materials which have a large Young's Modulus are generally referred to being ***stiff***, while those with a small Young's Modulus are called ***flexible***. Many materials such as steel tend to follow the slope of the linear elastic region when they are unloaded or reloaded, even after permanent deformations have occurred.

The complete stress-strain behaviour of mild steel (sometimes referred to as low-allow steel) can be roughly described as having three phases. For small strains, steel behaves in a linear elastic manner, and hence the stress and strain are related by the Young's Modulus. Once the stress reaches the yield stress, the material exhibits plastic behaviour along its yield plateau. For even larger strains, the stress-strain relationship is nonlinear, with some strengthening due to strain hardening, followed by softening as necking begins.

Strain Energy:

Strain energy is the energy stored in a structure or material as it is deformed. The strain energy **W** is defined as the area underneath the force-displacement curve of a structure, which is mathematically represented as:

$$W = \int F d\Delta l \quad (6.1)$$

Strain Hardening: the phenomenon where a material gains strength and stiffness when strained beyond its yield point.

Necking: the phenomenon where localization of tensile strains in a material causes the cross-sectional area to become noticeably smaller at one location causing it to resemble the shape of a neck. Usually precedes failure.

*Note: Deformations accumulated when a material is no longer behaving in a linear elastic manner tend to be permanent for many materials. These non-recoverable deformations are sometimes referred to as **plastic deformations** to contrast with the recoverable **elastic deformations**.*

Note: Eq. (6.1) is the integral of the force carried by the structure over the change in length it has experienced.

When a structure is loaded while it is behaving in a linear elastic manner, the area underneath the force-displacement curve will be a triangle. Thus, the strain energy for a material with axial stiffness **k** which has been elongated by **Δl** from its original length is calculated as:

$$W = \frac{1}{2}F\Delta l = \frac{1}{2}k(\Delta l)^2 \quad (6.2)$$

The area underneath the stress-strain curve of a material also represents an energy-based quantity, which is the strain energy density **U:**

$$U = \int \sigma d\varepsilon \quad (6.3)$$

U can be thought of as the energy stored in the material per unit volume and is typically expressed using units of MJ/m³. The strain energy density, **U**, is related to the strain energy, **W**, by the following equation:

$$W = U \cdot V_o \quad (6.4)$$

Where $\mathbf{V_o}$ is the original volume of the member before it has been deformed. When a material is behaving in a linear elastic manner, the area underneath the stress-strain curve is a triangle, which results in an alternative equation for the strain energy **W** if Eq. (6.3) and (6.4) are combined:

$$W = \int \sigma d\varepsilon \cdot V_o = \frac{1}{2}\sigma\varepsilon V_o \quad (6.5)$$

Having defined the strain energy, we can now define the ***resilience*** and ***toughness*** of a material. The maximum amount of energy which a structure or material can absorb before it exhibits permanent deformations is defined as its ***resilience***. The resilience of a material is calculated as the area under the stress-strain curve in the linear-elastic region. The ***toughness*** of a structure or material is a measure of how much energy it can absorb before breaking. The toughness of a material is hence defined as the area underneath the complete stress-strain curve.

Thermal Expansion

Materials tend to expand when heated and contract when cooled; the rate at which this occurs is a unique property of every material. The thermal strains experienced by a material, $\boldsymbol{\varepsilon_{th}}$, are related to the change in temperature **ΔT** by the ***coefficient of thermal expansion α*** according to the following equation:

$$\varepsilon_{th} = \alpha\Delta T \quad (6.6)$$

For example, if a 1200 mm long rod made of low alloy steel, which has $\alpha = 12\times10^{-6}$ /°C, was heated by 30°C, then it would experience a thermal strain of $(12\times10^{-6}) \times (30) = +\ 0.00036$ mm/mm. This corresponds to an elongation of 0.432 mm. Thermal strains can be significant for large structures – for example, large suspension bridges can change length by a few metres under large variations in temperature.

A table of useful material properties for many materials is found below, and is also reproduced in **Appendix A**.

Note: The strain energy density has units of MJ/m³ if the stress and strain are in units of MPa and mm/mm respectively. This is because 1 MPa = 1MN/m² = 1MNm/m³ = 1 MJ/m³.

Note: For a prismatic member, the undeformed volume V_o can be expressed as the product of the undeformed length L_o and the cross-sectional area A. Eq. (6.5) can then be rewritten as:

$$W = \frac{1}{2}\sigma\varepsilon AL_o$$

W will have units of J if σ is in MPa, ε is in mm/mm, A is in mm² and L_o is in m.

Note: If a member is free to expand or contract, then thermal strains do not lead to stresses developing in the material. However, if there is some sort of restraint which prevents it from changing sizes, then stresses will begin to develop, and the material may fail. One example of where this can happen is if a glass container with water inside is placed in a freezer. Under the cooler temperature, the container shrinks around the water, which is instead expanding as it freezes. Because the ice is preventing the glass from contracting, stresses begin to accumulate in the glass, and it may shatter.

Table 6.1 – Common Material Properties

Average Properties of Some Typical Materials Note that except for density, stiffness and coefficient of thermal expansion, all values have a considerable range

Material	Weight (kN/m³)	Stiffness E (MPa)	Tensile Strength (MPa) Yield	Tensile Strength (MPa) Ultimate	Compressive Strength (MPa)	Resilience (MJ/m³)	Toughness (MJ/m³) tens./comp.	Ductility Max. Elong. (%) Plastic/Elastic	α 10^{-6}/°C	Cost $/kg	Comment
Low Alloy Steel	77	200,000	420	560	420	0.44	135	25/0.21	12	0.60	Used in buildings, bridges, cars, etc.
High Tensile Steel	77	200,000	1650	1860	1650	6.8	55	4/0.83	12	1.50	Wire ropes, cables
High Alloy Steel	77	200,000	700	800	700	1.22	200	25/0.35	12	2.00	Pressure Vessels and tanks
Piano Wire	77	200,000	-	3000	-	22	22	0.2/1.50	12	1.50	Brittle material, not used in structures
Cast Iron	70	150,000	-	110	770	0.04	0.06/6	1/0.7	11	0.50	Traditional cast iron, moulded
Wrought Iron	75	185,000	200	350	200	0.11	90	30/0.11	12	1.00	99% pure iron, hammered, fibrous
Aluminum	27	69,000	40	80	60	0.012	19	40/0.06	24	1.80	Light, ductile, non-corrosive, soft metal
Aluminum Alloy	27	73,000	470	580	500	1.51	50	11/0.64	24	2.50	Used for canoes, aircraft, etc.
Copper	88	124,000	70	230	200	0.02	85	55/0.06	20	7.47	Very ductile metal – rounded curve
Bronze	79	105,000	200	390	350	0.2	40	12/0.19	17	2.80	Tin + copper alloy – stronger
Gold	189	82,000	40	220	180	0.01	80	50/0.05	14	40k	Heavy, expensive metal
Granite	26	52,000	-	11	140	0.001	0.01/0.26	0/0.02	8	0.15	Strongest and most durable building stone
Limestone	25	58,000	-	8	62	0.0006	0.01/0.09	0/0.01	6	0.03	Soft, useful building store
Slate	28	95,000	-	60	100	0.019	0.02/0.10	0/0.06		0.08	Stratified rock with high tensile strength
Brick	19	20,000	-	3	20	0.0002	0.01/0.03	0/0.01	9	0.10	Fired clay
Concrete	24	30,000	-	3	35	0.002	0.01/0.10	0/0.01	9	0.12	Mixture of cement, sand, stone, water
Glass	27	69,000	-	100	200	0.072	0.07/0.8	0/0.15	20	1.50	Solidified liquid sand
Oak	7.5	14,000	75	90	60	0.23	0.3/2.5	0.5/0.47	3	3.2	Strong, tough, heavy hardwood
Spruce	4.4	11,000	55	70	50	0.19	0.2/2.2	0.5/0.50	7	2.0	Light, strong, durable softwood
Tendon	10	900	70	80	-	2.7	4	1/7.8		-	Used as tension ties in mammals
Bone	20	17,000	150	180	180	0.66	1	0.5/0.9		-	Used as struts and beams in mammals
Rubber	9.2	7	-	20	20	15	20	4/300	500	2.0	Strange, useful material – low stiffness
Spider's Silk	10	4,000	-	1400	-	160	170	10/35		-	Most resilient material
Carbon Fibre	15	160,000	-	1800	-	10	10	0.1/1.1		50.0	Carbon fibre composites used in aircraft
Nylon Fibre	11	5,500	-	900	-	74	75	2/16	80	8.00	Excellent if stiffness not required
Kevlar Fibre	14	130,000	-	3600	-	50	60	1/2.7		50.00	Super material in many ways

Lecture 7 – "Explaining the Power of Springing Bodies"

Overview

Structures may vibrate when subjected to loads which move, or when disturbed from their equilibrium position. In this chapter, the basic behaviour of spring-mass systems under free vibration is introduced.

Free Vibration of Spring-Mass Systems

So far, we have primarily considered systems which are in a state of equilibrium and hence do not accelerate. However, structures will generally accelerate when subjected to time-varying loads or when disturbed from their equilibrium position. Consider the simplest case which was investigated by Hooke (shown in Fig. 7.1), which is a spring carrying a mass. Fig. 7.2, which illustrates his experiment in more detail, shows a linear elastic spring with a stiffness **k** attached to a mass **m**. The mass is considered to be significantly larger than the mass of the spring, which can be considered as weightless. For simplicity, the system will be analyzed without considering gravity, which will be re-introduced later in the chapter.

Suppose the mass **m** is pulled downwards from its resting position and then released. The mass will then vibrate up and down before eventually returning to its resting position. This is called ***free vibration and*** would theoretically continue forever were it not for factors such as air resistance and internal friction which eventually bring the vibration to a stop. The vertical position of the mass relative to its original location can be mathematically described using the time-varying function **x(t)**, and its vertical acceleration as it vibrates can be defined using another time-varying function **a(t)**. Note that the displacement **x(t)** is measured from the undeformed length of the spring and **x(t)** and **a(t)** are positive in the downwards direction.

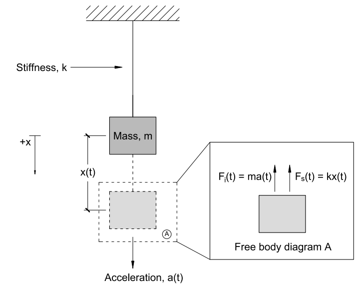

Fig. 7.2 – Analysis of a vibrating spring-mass system.

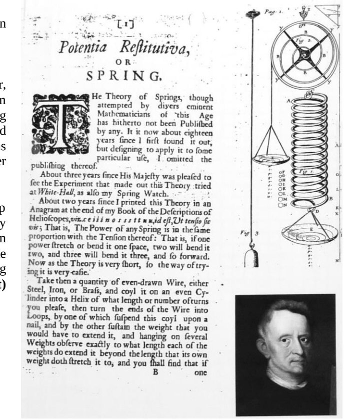
[1]

Potentia Restitutiva,

OR

SPRING.

THe Theory of Springs, though attempted by diyers eminent Mathematicians of this Age has hitherto not been Publiſhed by any. It it now about eighteen years ſince I firſt found it out, but deſigning to apply it to ſome particular uſe, I omitted the publiſhing thereof.

About three years ſince His Majeſty was pleaſed to ſee the Experiment that made out this Theory tried at *White-Hall*, as alſo my Spring Watch.

About two years ſince I printed this Theory in an Anagram at the end of my Book of the Deſcriptions of Helioſcopes, *viz. c e i i i n o s s s t t u u, id eſt, Ut tenſio ſic vis*; That is, The Power of any Spring is in the ſame proportion with the Tenſion thereof: That is, if one power ſtretch or bend it one ſpace, two will bend it two, and three will bend it three, and ſo forward. Now as the Theory is very ſhort, ſo the way of trying it is very eaſie.

Take then a quantity of even-drawn Wire, either Steel, Iron, or Braſs, and coyl it on an even Cylinder into a Helix of what length or number of turns you pleaſe, then turn the ends of the Wire into Loops, by one of which ſuſpend this coyl upon a nail, and by the other ſuſtain the weight that you would have to extend it, and hanging on ſeveral Weights obſerve exactly to what length each of the weights do extend it beyond the length that its own weight doth ſtretch it to, and you ſhall find that if

B one

Fig. 7.1 – Excerpt from Robert Hooke's 1678 paper "Explaining the Power of Springing Bodies".

Free body diagram A in Fig. 7.2 shows the forces applied to the mass if its acceleration and displacement are both acting downwards (positive). The forces which resist this motion are the inertial force, $\mathbf{F_i(t)}$ and the spring force $\mathbf{F_s(t)}$. As these are the only forces acting on the body, the two forces sum to zero, which produces the following equation:

Note: When the mass is vibrating, the inertial force is its resistance to being accelerated. Using Newton's second law, $F_i = ma(t)$.

$$F_i(t) + F_s(t) = 0 \rightarrow ma(t) + kx(t) = 0 \tag{7.1}$$

The acceleration **a(t)** is defined as the second derivative of the displacement **x(t)** with respect to time. This allows Eq. (7.1) to be written as just a function of **x(t)** and its derivatives:

*Note: Eq. (7.2) is called a **differential equation** because it relates a function, x(t), to one or more of its derivatives. Solving a differential equation means obtaining the unknown function x(t). In this case, the acceleration a(t) is related to x(t) by:*

$$a(t) = \frac{d^2x(t)}{dt^2}$$

$$m\frac{d^2x(t)}{dt^2} + kx(t) = 0 \tag{7.2}$$

Eq. (7.2) can be solved by assuming an answer for **x(t)**, and then verifying that our assumed function satisfies the differential equation. Consider the following function which is a sinusoid with amplitude of vibration **A**, angular frequency $\boldsymbol{\omega_n}$, and phase shift ϕ:

*Differential equations such as Eq. (7.2) have a useful property called **uniqueness**. This means that if a function x(t) satisfies the equation, and other conditions, then it is the only correct solution. The existence and uniqueness of solutions to differential equations is discussed further in more advanced calculus courses.*

$$x(t) = A\sin(\omega_n t + \phi) \tag{7.3}$$

The second derivative of **x(t)** with respect to time is then:

$$\frac{d^2x(t)}{dt^2} = -A\omega^2\sin(\omega_n t + \phi) \tag{7.4}$$

Substituting Eq. (7.3) and (7.4) into Eq. (7.2) and simplifying yields the following requirement for $\boldsymbol{\omega_n}$:

$$\omega_n = \sqrt{\frac{k}{m}} \tag{7.5}$$

The frequency of vibration of the spring-mass system when it is freely vibrating is related to the stiffness of system **k** and its mass **m** but is independent of other factors such as the amplitude of vibration and the initial disturbance. $\boldsymbol{\omega_n}$, is commonly referred to as the ***natural frequency*** of the system because it represents how quickly the system oscillates under free vibration and is purely defined by the system's inherent mechanical properties **k** and **m**. Stiffer systems, which have a large value of **k**, will hence have a high natural frequency and will vibrate quickly. On the other hand, systems with a higher mass have more inertia and will vibrate more slowly.

Note: ω_n has units of rad/s. Expressing the natural frequency in units of cycles per second requires converting ω_n to f_n using Eq. (7.6).

The natural frequency expressed in terms of cycles per second (hz), $\boldsymbol{f_n}$, and the natural period, $\mathbf{T_n}$, can be defined as:

Note: the period T is the time elapsed as one full cycle takes place.

$$f_n = \frac{1}{2\pi}\omega_n = \frac{1}{2\pi}\sqrt{\frac{k}{m}} \tag{7.6}$$

$$T_n = \frac{1}{f_n} = 2\pi\sqrt{\frac{m}{k}} \tag{7.7}$$

Note that when solving Eq. (7.2), we have not determined the values of the amplitude of vibration **A** or the phase shift ϕ. These parameters can be solved if the displacement and acceleration corresponding to t = 0 are known (i.e., x(t=0) = x_o and a(t=0) = a_o respectively). x_o and a_o are referred to as initial conditions.

Note: Solving for A and ϕ using the initial conditions, x_o and a_o will not be required in CIV102.

Consideration of Gravity

Although we neglected the presence of gravity when defining and solving Eq. (7.2), consider the effect of adding the gravitational force, which acts downwards, to the free body diagram in Fig. 7.2. The sum of forces can then be written as:

$$F_i(t) + F_s(t) = F_g = mg \tag{7.8}$$

Introducing the displacement **x(t)** and the acceleration **a(t)** results in a slightly modified version of Eq. (7.2):

$$m\frac{d^2x(t)}{dt^2} + kx(t) = mg \tag{7.9}$$

Again, this can be solved using a sinusoidal function. However, the mass will now oscillate around a value of x = Δ_o instead of x = 0:

$$x(t) = A\sin(\omega_n t + \phi) + \Delta_o \tag{7.10}$$

Substituting Eq. (7.10) into Eq. (7.9) results in the same equation for $\boldsymbol{\omega_n}$ as before and produces the following condition for $\boldsymbol{\Delta_o}$:

$$k\Delta_o = mg \tag{7.11}$$

Therefore, the system does not oscillate about the undeformed length of the wire when gravity is present. Instead, it oscillates about the resting position under the weight of the mass, which is $\boldsymbol{\Delta_o}$, the elongation of the spring due to the gravitational force. The inclusion of gravity does not influence the frequency of vibration, and hence our equations for $\boldsymbol{\omega_n}$, $\boldsymbol{f_n}$ and $\mathbf{T_n}$ are still valid.

A plot of the position of the mass over time, **x(t)**, is shown in Fig. 7.3. When reading the plot, note that downwards displacements are taken as positive (as defined in Fig. 7.2).

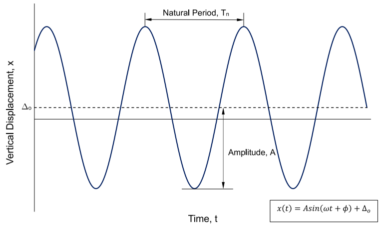

Fig. 7.3 – Displacement of a spring-mass system under free vibration.

Other Methods for Calculating ω_n

The natural frequency f_n is an important parameter as it allows us to determine if a structure is susceptible to time-varying loads. Although Eq. (7.6) can be used to calculate it, determining the stiffness **k** can be difficult if the structure has a complex geometry. A more convenient approach is to instead define the natural frequency in terms of the vertical displacement of the structure under gravity loads. This can be done by re-arranging Eq. (7.11) to express **k** in terms of Δ_o:

Note: The response of structures under time-varying or dynamic loads is discussed in Lecture 19.

$$k = \frac{mg}{\Delta_o} \tag{7.12}$$

Substituting Eq. (7.12) into Eq. (7.6) results in the following expression for f_n:

$$f_n = \frac{1}{2\pi}\sqrt{\frac{mg}{\Delta_o}\cdot\frac{1}{m}} = \frac{1}{2\pi}\sqrt{\frac{g}{\Delta_o}} \tag{7.13}$$

If the acceleration due to gravity is taken as 9,810 mm/s^2 and Δ_o is in units of mm, then f_n can be calculated as:

Note: Eq. (7.14) requires Δ_o to be in units of mm, otherwise the resulting answer will be incorrect.

$$f_n = \frac{1}{2\pi}\sqrt{\frac{9{,}810}{\Delta_o}} \cong \frac{15.76}{\sqrt{\Delta_o}} \tag{7.14}$$

Thus, the natural frequency can be conveniently calculated for a structure if its static displacement, Δ_o is known.

Lecture 8 – Factors of Safety: Dead vs. Live Load, Brittle vs. Tough

Overview

Although previous lectures have introduced the necessary tools to design structures in idealized conditions, uncertainties in the expected loads on the structure and the strength of the materials used must be considered to avoid failure. This lecture describes the concept of working stress design, which employs factors of safety to carry out design safely.

Dead and Live Loads

When designing structures to safely carry loads, it is common to distinguish between the different kinds of loads which can be expected. In CIV102, we will primarily focus on dead loads and live loads.

Dead loads are loads which remain constant over the lifetime of the structure. Examples of dead load include the self-weight of the structure and the self-weight of nonstructural components which are attached to the structure (sometimes referred to as superimposed dead loads).

Live loads are loads which vary over time and are primarily attributed to the use of the structure by people. Examples of live loads include the weight of a crowd of people, the weight of vehicular traffic on a bridge, or the weight of objects which are not permanently attached to the structure such as furniture. The weight of a tightly packed crowd of people is a significant live load, which has traditionally been approximated as 100 lbs per square foot, which converts to a load of about 5 kPa.

Other types of loads which are commonly considered when designing structures include wind loads, snow loads, and earthquake loads.

Structural Failure

Failure occurs when the stresses in the structure caused by the applied loads, σ_{demand}, equals or exceed the strength of the materials, $\sigma_{capacity}$:

$$\sigma_{demand} \geq \sigma_{capacity} \tag{8.1}$$

Although this concept is relatively straightforward, consideration must be made to account for uncertainty in the loads, as well as uncertainty in the strengths of the materials used to build the structure. A dangerous situation may occur if the loads are higher than expected and/or the strength of the materials is lower than specified. This variation in the capacity and demand is illustrated in Fig. 8.1, where the two curves represent the probability distributions of the demand (red) and capacity (blue). The height of the curves represents the likelihood of the capacity or demand being a certain value.

Note: The region where the two curves overlap <u>does not</u> represent the probability of failure.

Fig. 8.1 describes a situation where the expected capacity exceeds the expected demand on average. However, there is substantial overlap between the two curves due to the variability in the both the applied loads and the strength of the materials. The overlap, while not the probability of failure, nonetheless suggests that there is a reasonable chance that Eq. (8.1), our failure condition, may be satisfied. Therefore, simply designing so that the expected strength is on average higher than the expected demand is not a sufficient method to ensure that the resulting structure is safe.

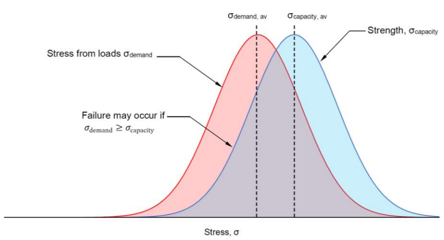

Fig. 8.1 – A comparison of applied stresses vs. the strength of the material. Although the average demand is less than the average capacity, there is substantial overlap between the two curves where failure occurs.

Note: Failure is not a straightforward concept to define, as it depends on the criteria used to determine what constitutes failure. Common metrics used to define failure include when the material begins to experience permanent deformations ($\sigma = \sigma_{yield}$), when the material breaks ($\sigma = \sigma_{ult}$), or when the deformations of a structure exceed an acceptable value ($\Delta \geq \Delta_{max}$).

Factors of Safety

To account for the uncertainty in the loads and strength of the materials, the concept of a ***factor of safety*** (FOS) is used in engineering design. The factor of safety is a measure of the capacity in the system relative to its demand. In structural engineering, the capacity refers to the strength of the materials and the demand refers to the stresses caused by applied loads. If the factor of safety is less than 1.0, then the demand exceeds the capacity and failure occurs.

Note: Values of the factor of safety are chosen in order to limit the probability of failure to be less than an acceptable value. Using working stress design, the factor of safety depends both on the quality of the material and the danger of the failure mode in question. Larger factors of safety are employed against failure mechanisms which are sudden and cause more catastrophic consequences.

$$FOS = \frac{\text{Capacity}}{\text{Demand}} \tag{8.2}$$

In practice, factors are safety are employed to reduce the permissible demand in order to reduce the likelihood of failure occurring to an acceptable level. This is known as ***working stress design***, in which the maximum allowable stress in the structure, σ_{allow}, is calculated as:

$$\sigma_{allow} = \frac{\sigma_{fail}}{FOS} \tag{8.3}$$

In Eq. (8.3), σ_{fail} is the stress which causes the structure to fail. The benefit of using factors of safety is illustrated when comparing Fig. 8.2, shown on the following page, to Fig. 8.1. By employing a factor of safety to limit the stress permitted in the structure to be σ_{allow}, the area where the two curves overlap has been significantly reduced, which reduces the likelihood of a failure taking place.

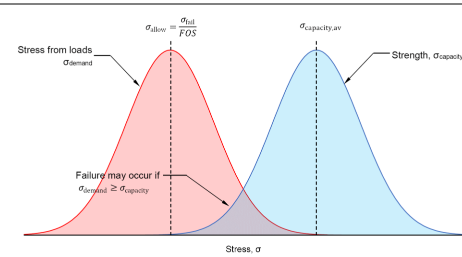

Fig. 8.2 – Reduced likelihood of failure by employing a factor of safety.

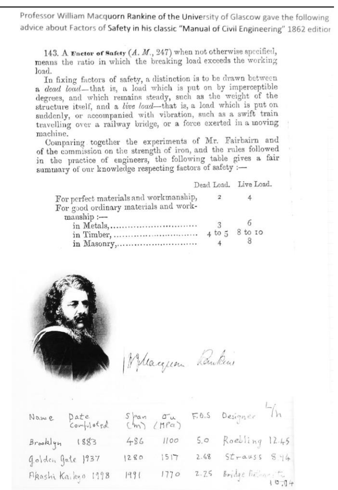
Professor William Macquorn Rankine of the University of Glasgow gave the following advice about Factors of Safety in his classic "Manual of Civil Engineering" 1862 edition

143. A **Factor of Safety** (*A. M.*, 247) when not otherwise specified, means the ratio in which the breaking load exceeds the working load.

In fixing factors of safety, a distinction is to be drawn between a *dead load*—that is, a load which is put on by imperceptible degrees, and which remains steady, such as the weight of the structure itself, and a *live load*—that is, a load which is put on suddenly, or accompanied with vibration, such as a swift train travelling over a railway bridge, or a force exerted in a moving machine.

Comparing together the experiments of Mr. Fairbairn and of the commission on the strength of iron, and the rules followed in the practice of engineers, the following table gives a fair summary of our knowledge respecting factors of safety :—

	Dead Load.	Live Load.
For perfect materials and workmanship,	2	4
For good ordinary materials and workmanship :—		
in Metals,	3	6
in Timber,	4 to 5	8 to 10
in Masonry,	4	8

Name	Date Completed	Span (m)	σ_u (MPa)	F.O.S	Designer	L/h
Brooklyn	1883	486	1100	5.0	Roebling	12.45
Golden Gate	1937	1280	1517	2.68	Strauss	8.94
Akashi Kaikyo	1998	1991	1770	2.25	Bridge [illegible]	10.04

Fig. 8.3 – Suggested values of safety factors and historic values of safety factors used in suspension bridges

Examples of Safety Factors in Engineering Design:

Fig. 8.3 shows some suggested values for factors of safety as recommended by William Rankine, as well as the actual factors of safety used in the Brooklyn Bridge, the Golden Gate Bridge, and more recently the Akashi Kaikyo Bridge. The factors of safety suggested by Rankine are very large (up to 10!) compared to those employed in modern design, which are typically around 2.0. This is due to advances in design/construction practices and improvements in predicting the loads which structures may be subjected to over their lifetime.

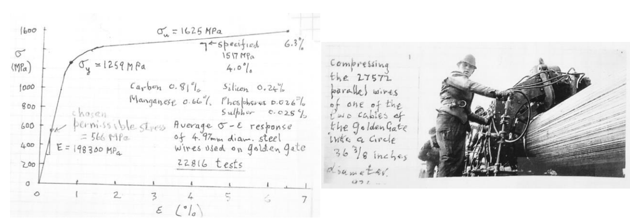

Fig. 8.4 – Stress-strain characteristics of steel used in the main cables of the Golden Gate Bridge.

Lecture 9 – Weight a Moment! What is I?

Overview:
In the previous chapters, we have discussed the basic equations for stress and strain which are sufficient for studying members subjected to direct tension. However, they are inadequate for describing the behaviour of members which bend when carrying bending moments or when buckling under compression forces. In this chapter, the fundamentals of rotational motion are discussed. Although structures rarely experience significant rotations, the concepts used to describe rotational motion are analogous to those needed to explain the behaviour of structures when they bend.

Relating a Moment to the Angular Acceleration of a Point Mass
Consider the system shown in Fig. 9.1, which shows a point mass **m** attached to a pivot point by means of a weightless, rid rod with length **y**. If a pure moment **M** is applied to the system, the mass will spin around the axis of rotation with an angular acceleration of **α** radians per second squared.

*Note: the distance used for rotational motion, taken here as **y**, is often taken as **r** in other courses.*

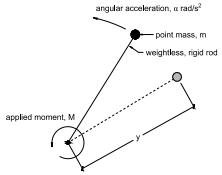

Fig. 9.1 – Point mass rotating as a result of an applied moment.

The relationship between the moment and the angular acceleration can be determined by considering the effective translational force applied to the mass and the corresponding translational acceleration. Recall from Lecture 2 that a moment is the product of a force, **F**, and a perpendicular distance to a reference point, which is referred to here as **y**:

$$M = Fy \tag{9.1}$$

The translational acceleration of the mass, **a**, is related to the angular acceleration, **α**, in the same way that the length of a circular arc is equal to the product of the radius and the angle traversed:

$$a = \alpha y \tag{9.2}$$

Now that the force and acceleration are known, they can be related to each other using Newton's second law of motion, which is F = m×a. This allows Eq. (9.1) and (9.2) to be combined:

$$M = Fy = (m\alpha y)y = m\alpha y^2 \tag{9.3}$$

Grouping the mass and length terms produces the following result:

$$M = (my^2)\alpha \tag{9.4}$$

The term my^2 describes the resistance of the mass to rotation and is analogous to the concept of inertia used in Newton's laws of motion. Rewriting Eq. (9.4) to be applicable to more complex situations than the simple example shown in Fig. (9.1) results in the fundamental equation of rotational motion:

$$M = I_m\alpha \tag{9.5}$$

In Eq. (9.5), $\mathbf{I_m}$ is the ***moment of inertia*** and has dimensions of mass × length squared.

Defining the moment of inertia, $\mathbf{I_m}$
The resistance of a point mass to rotation about an axis is defined as its moment of inertia, $\mathbf{I_m}$. For a small object which has mass $\mathbf{m_i}$ and is located a distance $\mathbf{y_i}$ away from the axis of rotation, its individual moment of inertia $\mathbf{I_{m,i}}$ is defined as:

$$I_{m,i} = m_i y_i^2 \tag{9.6}$$

Although Eq. (9.6) allows us to calculate the moment of inertia for a point mass relative to an axis of rotation, how can we extend it to consider objects whose mass is not distributed at a single point? Consider the body shown in Fig. 9.2 which has been subdivided into many discrete point masses $\Delta\mathbf{m_i}$ which are each located a distance of $\mathbf{y_i}$ relative to the axis of rotation. The moment of inertia of the body is the sum of the moments of inertia of each point mass, $\mathbf{I_{m,i}}$, over the whole body:

$$I_m \cong \sum I_{m,i} = \sum \Delta m_i y_i^2 \tag{9.7}$$

Note: $\sum$ is used to denote the summation of terms (typically over n terms). Eq. (9.3) can be expanded to be:

$$\sum \Delta m_i y_i^2 = \Delta m_1 y_1^2 + \Delta m_2 y_2^2 + \cdots + \Delta m_n y_n^2$$

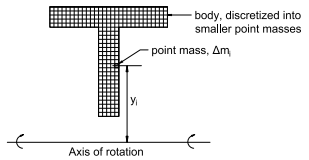

Fig. 9.2 – Calculation of I_m for a two-dimensional body which has been discretized into smaller pieces.

Eq. (9.7) is an approximation for $\mathbf{I_m}$, as the value of $\mathbf{I_m}$ obtained using the equation depends on how finely we have subdivided the original body. The approximation becomes more accurate as we subdivide the body into smaller pieces,

which in turn reduces the size of the individual point masses. If we take the limit as $\Delta\mathbf{m_i}$ approaches zero, then the summation can be instead replaced by an integral and $\mathbf{I_m}$ can be calculated exactly:

$$I_m = \lim_{\Delta m_i \to 0} \sum \Delta m_i y_i^2 = \int_M y^2 dm \tag{9.8}$$

Eq. (9.8) is the definition of the moment of inertia for a finite body, which is the sum of the moments of inertia contributed by the infinitesimally small point masses **dm** over the entire mass **M**.

In the special case where the body under consideration is a two-dimensional object having a uniform density with dimensions of mass per area, then **dm** can be written as the product of the density **ρ** and a differential area **dA**:

$$dm = \rho dA \tag{9.9}$$

Equations (9.8) and (9.9) can hence be combined to produce the following result:

$$I_m = \int_M y^2 dm = \rho \int_A y^2 dA \tag{9.10}$$

Note: Eq (9.10) is only valid if ρ does not vary over the area of the body. If it does, then it must be included inside of the integral.

The moment of inertia is thus the product of the density of the material multiplied by an integral term which consists of purely geometric properties. The integral term is known as the ***second moment of area, I***, which has dimensions of length⁴.

$$I = \int_A y^2 dA \tag{9.11}$$

Physical Interpretation of the Moment of Inertia:
By examining Eq. (9.6) to Eq. (9.8), the following properties can be understood about the moment of inertia, $\mathbf{I_m}$. These properties are also true for the second moment of area, **I**, if the references to mass instead refer to area.

1. $\mathbf{I_m}$ depends on the location and orientation of the axis of rotation, as this affects the term $\mathbf{y_i}$.
2. Masses which are located further away from axis of rotation tend to have a larger contribution to $\mathbf{I_m}$ compared to masses which are located closer to the axis of rotation.

To illustrate these properties, consider the steel I-beam shown in Fig. (9.3). Its designation, W530×92, refers to its nominal height of 530 mm and weight of 92 kilograms per metre of length. The central image in the figure shows the member being rotated about its y-axis, and the image on the left shows the member being rotated about its x-axis. It can be seen that the member has a substantially larger second moment of area taken about its x-axis compared to its y-axis. This is because the majority of its area is distributed far away from the axis of rotation when it is aligned about its x-axis.

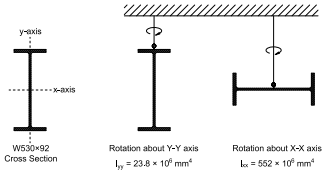

Fig. 9.3 – Sample values of I for a W530×92 I-beam.

Example Calculation of I: Rectangle
A simple example of applying Eq. (9.11) is to find the second moment of area of a rectangle about its own centroid, which is located at its mid-height. We begin the process by expressing a small area of the rectangle, **dA**, as the product of the rectangle's width **b** and a small thickness **dy**, as shown in Fig. 9.4.

$$dA = bdy \tag{9.12}$$

We can now calculate the second moment of area by substituting Eq. (9.12) into the definition of **I** and then integrating over the height of the rectangle, which is from y = -h/2 to y = h/2:

$$I = \int_{-\frac{h}{2}}^{\frac{h}{2}} by^2 dy = \frac{1}{3}by^3\Big|_{-\frac{h}{2}}^{\frac{h}{2}} = \frac{1}{3}b\left(\left(\frac{h}{2}\right)^3 - \left(-\frac{h}{2}\right)^3\right) \tag{9.13}$$

Evaluating Eq. (9.13) results in a simple expression for I of a rectangle which is rotating about an axis at its mid-height:

$$I = \frac{bh^3}{12} \tag{9.14}$$

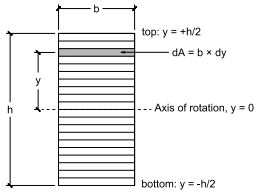

Fig. 9.4 – Derivation of the second moment of area of a rectangle about its centroid. Each "slice" of area has a thickness of dy.

Lecture 10 – Introduction to the Bending of Beams

Overview:
In this lecture, the principles discussed in previous chapters are used to derive equations describing the behaviour of members which bend.

Fundamental Assumption for Bending: Plane Sections Remain Plane
Consider a series of vertical lines on a beam which are drawn a distance $\mathbf{L_o}$ apart. As the beam is bent, it will curve to form the arc of a circle. These lines will remain straight but will rotate so that on one side of the beam, say the top, they are slightly further apart, and on the other side, the bottom, they are slightly closer together. At the centroid of the beam, these lines retain a separation of $\mathbf{L_o}$. This phenomenon was described by Robert Hooke in 1678 using the phrase *"plane sections remain plane"* and is illustrated in Fig. 10.1. One way to quantify how much the beam has bent is to measure the relative angle between two vertical lines, $\boldsymbol{\theta}$, and divide this angle by the original distance between them, which is $\mathbf{L_o}$. The resulting quantity is called the average curvature. In general, the ***curvature*** $\boldsymbol{\phi}$ is more rigorously defined as the change of this angle $\boldsymbol{\theta}$ along the length of the member, **x**.

$$\phi = \frac{d\theta}{dx} \tag{10.1}$$

A property of the curvature is that the quantity $1/\phi$ is equal to radius of the circle formed by the beam after it has been curved. This quantity is known as the ***radius of curvature***.

Bending of the member produces strains in the member because the distance between the vertical lines is no longer equal to the original spacing $\mathbf{L_o}$ except at the centroid. Consider the spacing of points A and B which are drawn on the beam in Fig. 10.1 and located a distance **y** above the centroidal axis. After the beam has been bent with a curvature $\boldsymbol{\phi}$, the change in angle between A and B is equal to $\theta_{AB} = \phi \times L_o$, and the distance between these points and the centre of the circle will be $y + 1/\phi$. Using this information, the distance between points A and B after the beam has been curved, $\mathbf{L_{AB}'}$, can be calculated as:

$$L'_{AB} = (\phi L_o) \cdot \left(y + \frac{1}{\phi}\right) = \phi y L_o + L_o \tag{10.2}$$

Using the deformed length, we can now calculate the strain of the member between points A and B which are located a distance **y** above the centroidal axis:

$$\varepsilon(y) = \frac{\Delta l}{L_o} = \frac{L'_{AB} - L_o}{L_o} \tag{10.3}$$

Substituting Eq. (10.2) into Eq. (10.3) yields the fundamental relationship between the strains in the member, $\boldsymbol{\varepsilon}$, and its curvature, $\boldsymbol{\phi}$:

$$\varepsilon(y) = \phi y \tag{10.4}$$

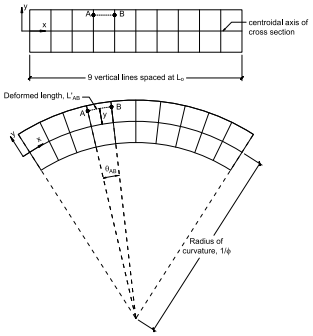

Fig. 10.1 – Figure illustrating Robert Hooke's 1678 hypothesis that when members are subjected to pure bending, "Plane Sections Remain Plane". The vertical lines drawn on the side of the member remain straight when it is curved.

The strains in a member subjected to pure bending are not constant over the cross section as was the case for pure tension. Rather, they vary linearly along the height, from a maximum tensile strain on one side of the member to a maximum compressive strain on the other. The strain at the height of the centroid, which is the axis about which each section rotates, is equal to zero. These observations are summarized in Fig. 10.2.

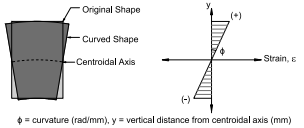

Fig. 10.2 – Strain profiles caused by pure bending. Note that for a beam made of a linear elastic material, $\varepsilon = 0$ at the centroidal axis ($y = 0$).

Flexural Stiffness – Determining the Relationship between Bending Moment and Curvature
When we were studying the behaviour of members subjected to axial force, we were interested in calculating the axial stiffness of the member, **k**, which related the tension in the member to its elongation. For members which bend, we are instead interested in the relationship between the moment carried by a member, **M**, and its curvature, $\boldsymbol{\phi}$. Just like how we used the definitions of stress and strain to derive the axial stiffness of a member, we will do the same to derive the ***flexural stiffness*** based on our assumption that plane sections remain plane.

To begin, we can first determine the stresses in a member which has a curvature $\boldsymbol{\phi}$ if we know the Young's modulus of the material, **E**:

$$\sigma = E\varepsilon \rightarrow \sigma(y) = E\phi y \tag{10.2}$$

Eq. (10.2) states that like the strains $\boldsymbol{\varepsilon}$, the stresses $\boldsymbol{\sigma}$ also vary linearly across the height of the cross section. To understand how the distribution of stresses is related to the bending moment, consider a thin slice of the cross section with area $\mathbf{\Delta A}$. The stresses in this slice of the cross-sectional area act uniformly over $\mathbf{\Delta A}$ if $\mathbf{\Delta A}$ is relatively small, producing a force $\mathbf{\Delta F}$ which can be calculated using our definition of stress:

$$\sigma = \frac{F}{A} \rightarrow \Delta F = \sigma(y)\Delta A \tag{10.3}$$

Because the force $\mathbf{\Delta F}$ does not necessarily pass through the centroidal axis of the member, it will produce a turning effect. The moment $\mathbf{\Delta M}$ caused by $\mathbf{\Delta F}$ acting a distance **y** away from the centroidal axis can be calculated using our definition of a moment:

$$M = F \cdot d \rightarrow \Delta M = \Delta F \cdot y \tag{10.4}$$

Substituting the Eq. (10.2) and (10.3) into (10.4) yields the following expression for $\mathbf{\Delta M}$:

Note: The process of calculating the resulting bending moment from the linearly varying strains is shown in Fig. 10.3. The flexural stresses, shown in the second figure, act over a differential area of the cross section, dA, producing a force dF. These forces, shown in the third figure which shows a slice of the beam from elevation view, produce a moment on the left side which equilibrates the applied bending moment on the right side.

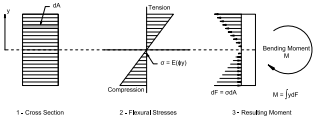

Fig. 10.3 – Summary of how the bending moment carried by a member is determined if the distribution of strains is known from the curvature.

$$\Delta M = \phi E y^2 \Delta A \tag{10.5}$$

We can now find the total moment carried by the member by summing the turning effects caused by each piece of area in the cross section. If we used slices with a nonzero thickness, this will be an approximation of the true moment because the resulting sum will depend on the size of the slides considered. As the thickness of each slice becomes infinitesimally small, $\mathbf{\Delta A}$ approaches zero and the summation sign is instead replaced with an exact integral:

$$M = \lim_{dA \to 0} \sum \phi E y^2 \Delta A = \int_A \phi E y^2 dA \tag{10.6}$$

In Eq. (10.6), we can move $\boldsymbol{\phi}$ out of the integral because the curvature of the member is constant over the cross section and not a function of **A**. If the member is made of the same material over the whole cross section, we can also remove **E** from the integral, which results in the following expression for **M**:

$$M = \phi E \int_A y^2 dA \tag{10.7}$$

By examining Eq. (10.7), we recognize that the integral of y^2 over the area of the cross section is the definition of the second moment of area, **I**, which was introduced in Lecture 9. Substituting this property into the equation yields the final result:

$$M = EI \cdot \phi \tag{10.8}$$

In Eq. (10.8), $\mathbf{EI}$ is the ***flexural stiffness*** of the member. Like the axial stiffness **k**, which was derived in Lecture 5, the flexural stiffness $\mathbf{EI}$ also relates a force-based quantity, the bending moment, to a displacement-based quantity, the curvature. Similarly, it is a function of both the stiffness of the material, **E**, and the geometric stiffness provided by the shape of the cross section, **I**. This comparison is shown in Fig. 10.4.

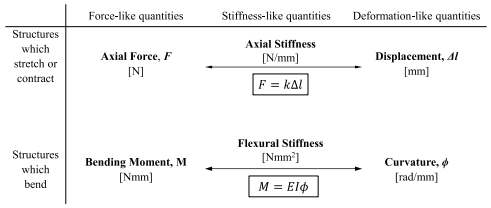

Fig. 10.4 – A comparison of the axial and flexural stiffnesses of a member.

Lecture 11 – Statically Determinate Structures

Overview:
Structural engineering is primarily concerned about determining how structures transfer loads from one location to another. For most civil structures, this involves transmitting vertical loads (i.e. gravity loads) or horizontal loads (i.e. wind loads or earthquake loads) to the ground. In this chapter, the basics of structural analysis are introduced, beginning with the determination of reaction forces for statically determinate structures.

Supports
Supports are the elements which hold up the structure and transmit the forces carried by the structure to the ground below. Examples of supports include bearing pads, foundations, and hinges, which all transmit some degree of force and/or moment to support the structure and prevent it from accelerating. The forces/moments which are supplied by supports to hold up the structure are called ***reaction forces***.

Reaction forces are closely related to the level of restraint which a support can provide. For example, a hinge support which is well-anchored to the ground can prevent an attached structure from moving translationally but will freely swivel. Hence, a hinge can provide reaction forces which resist translational movement but cannot provide any moment to prevent rotation. The key principle is that increasing the amount of restraint provided by the support increases, increases its ability provide a reaction force along that that degree of freedom, and vice-versa.

In structural engineering, we typically define three common types of supports which are called ***rollers***, ***pins*** and ***fixed ends***. Solving any structural engineering problem typically first involves calculating the reaction forces which these supports provide to the structure. Table 11.1 describes each type of support, its permitted degrees of freedom, and the support reactions which can be supplied to the attached structure.

Note: A simple example of a hinge support are the hinges which fasten a door to a door frame. These hinges prevent the door from translating, but do not provide any resistance to the door being swung open.

Note: Real supports cannot perfectly restrain a structure like the idealized pins, rollers and fixed ends described in Table 11.1. Choosing which idealized support best reflects realistic conditions requires engineering judgement and experience.

*Note: The **degrees of freedom**, when used to refer to geometric situations such as 2-D space or 3-D space, are the variables required to describe the position and orientation of a body. Three degrees of freedom are needed to define a non-deformable body in 2-D space. These are:*
1. *Position in the x-direction*
2. *Position in the y-direction*
3. *Rotational orientation in the x-y plane*

A body which deforms may require more degrees of freedom to describe its position, orientation, and deformed shape.

Table 11.1 – Types of supports and their reaction forces

Name	Symbol	Permitted Degrees of Freedom	Restrained Degrees of Freedom	Support Reactions
Roller		$\Delta x, \theta_{xy}$	$\Delta y = 0$	F_y
		$\Delta y, \theta_{xy}$	$\Delta x = 0$	F_x
Pin		θ_{xy}	$\Delta x = \Delta y = 0$	F_x, F_y
Fixed end		None	$\Delta x = \Delta y = \theta_{xy} = 0$	F_x, F_y, M_{xy}

Solving for Reaction Forces – Free Body Diagrams

Solving for the reaction forces requires understanding how the loads carried by the structure are distributed to the supports on which it sits. Consider the structure shown in Fig. 11.1, which is a beam supported by a pin and roller and carrying three masses, m_1, m_2 and m_3:

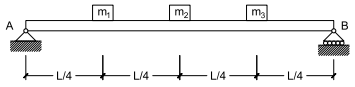

Fig. 11.1 – Simply supported beam carrying three weights.

A complete understanding how the structure transmits the weight of the three masses to the ground below can be obtained by drawing a series of free body diagrams. Five free body diagrams can be drawn which each describes the interaction between an applied load or support and the structure. The sixth free body diagram is of the structure itself being subjected to the various applied loads and reaction forces caused by the supports and weights. These free body diagrams are shown below in Fig. 11.2:

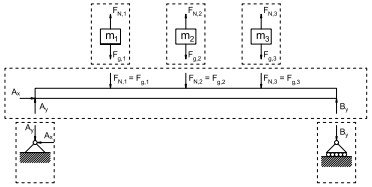

Fig. 11.2 – Free body diagrams demonstrating how the weight of the three loads is transferred to the ground.

In Fig. 11.2, **F**N is the normal force supplied by the beam to hold up the masses, **F**g is the force of gravity acting on each mass and **A**x, **A**y and **B**y are the reaction forces. The self-weight of the beam is ignored. When drawing these free body diagrams, the following two rules have been used:

1. According to Newton`s third law of motion, the force applied to the structure by an applied load or support is equal and opposite to the force applied by the structure to the applied load or support.
2. When drawing in a force which is unknown, like an undetermined reaction force, any assumed direction will suffice. The assumed direction will not affect the solution as long as the equilibrium equations are consistent with the drawn free body diagram.

Note: If the assumed direction is incorrect, then the resulting value obtained by solving the equations of equilibrium will be a negative number.

Because the system as a whole is in equilibrium, each subsystem will also be in equilibrium, and hence the equilibrium equations must be satisfied for each free body diagram. As noted in Lecture 3, these equations are:

$$\sum F_x = 0 \tag{11.1}$$

$$\sum F_y = 0 \tag{11.2}$$

$$\sum M = 0 \tag{11.3}$$

These equations can then be used to determine the unknown reaction forces, **A**x, **A**y and **B**y once the appropriate free body diagrams have been drawn. Typically, the most useful free body diagram to consider is the free body of the structure itself being subjected to the applied loads and reaction forces.

Statically Determinate Structures

Structures whose reaction forces can be directly solved using the three equations of equilibrium are called ***statically determinate***. Statically determinate structures have the property where the reaction forces are purely a function of the size, quantity, location, and direction of the applied loads, and are unrelated to the stiffness of the structure. This occurs if the number of unknown reaction forces is equal to the number of equilibrium equations. Most simple 2-D structures are statically determinate if their supports provide a total of three reaction forces.

Structures which have fewer reaction forces than the number of equilibrium equations are called ***mechanisms***. This is because they are unstable and can accelerate when subjected to an applied load.

Structures which have more reaction forces than the number of equilibrium equations are ***statically indeterminate***. The reaction forces cannot be directly solved using the equilibrium equations alone, and hence must consider other factors such as the stiffness of the structure and positioning of the applied loads. The degree of indeterminacy is a measure of how statically indeterminate a structure is and is equal to the number of reaction forces minus the number of equilibrium equations.

Examples of the three situations can be found in Fig. 11.3.

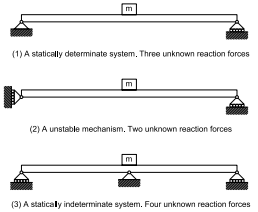

Fig. 11.3 – Examples of a statically determinate structure, a mechanism, and a statically indeterminate structure.

Note: Many building structures are statically indeterminate. Solving for their reaction forces and internal stresses requires more advanced analysis methods than those covered in CIV102.

Example: Structures with an Internal Hinge

Some structures are built with an internal hinge which connects two substructures together. Because a hinge freely rotates and is unable to resist moment, it has the effect of reducing the indeterminacy of the structure by one for each internal hinge. The following example illustrates how to account for hinges in a structure when solving for the reaction forces.

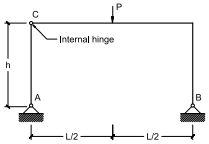

Fig. 11.4 – Example of a frame structure containing an internal hinge.

Consider the frame shown above in Fig. 11.4 which is carrying a point load, P, acting downwards on the top beam. The frame is supported on two pins, resulting in 2 × 2 = 4 unknown reaction forces. Although this might suggest that the structure is statically indeterminate, we can take advantage of the internal hinge to solve for these unknown forces. To do this, two free body diagrams which cut through the hinge are drawn, which reveals the two internal hinge forces. Because each free body diagram is in equilibrium, we have a total of six equilibrium equations (three from each free body diagram) which we can use to solve for the four reaction forces and two internal hinge forces. These free body diagrams are shown below in Fig. 11.5.

Note: When the frame is cut and separated at the internal hinge, the hinge forces must be drawn in opposite directions on the two free body diagrams. This is to ensure that the forces cancel out when the frame is "put back together".

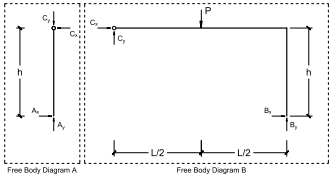

Fig. 11.5 – Free body diagrams of the frame after it has been separated at the hinge.

The three equilibrium equations which correspond to Free Body Diagram A are shown below. Note that the moment equation is taken about point A, the left support.

$$\sum F_x = 0 \rightarrow A_x - C_x = 0 \tag{11.4}$$

$$\sum F_y = 0 \rightarrow A_y - C_y = 0 \tag{11.5}$$

$$\sum M_A = 0 \rightarrow C_x \times h = 0 \tag{11.6}$$

The three equilibrium equations corresponding to Free Body Diagram B are shown below, with the moment equation being taken about point B, the right support.

$$\sum F_x = 0 \rightarrow B_x + C_x = 0 \tag{11.7}$$

$$\sum F_y = 0 \rightarrow B_y + C_y - P = 0 \tag{11.8}$$

$$\sum M_B = 0 \rightarrow C_x \times h + C_y \times L - P \times \frac{L}{2} = 0 \tag{11.9}$$

Because we have six equations (Eqs. (11.4) to (11.9)) and six unknowns (A_x, A_y, B_x, B_y, C_x and C_y), we can solve for each force and hence the system is statically determinate.

Lecture 12 – A Bridge Over Troubled Waters

Overview:
In this chapter, truss bridge systems are discussed. Trusses, which are assemblies of steel or timber members connected to form lattice-like structures, resist loads by having their members carry axial tension and axial compression forces. The design process for truss bridges is introduced.

Truss Bridges and their Historical Development
Truss bridges were originally used by the Romans, who built them by connecting wooden members to cross distances which could not be achieved using bridges built using post-and-beam construction. None of these early bridges survived after the downfall of the empire, which led to this style of bridge construction being lost. During the Renaissance era, the Italian architect Andrea Palladio became the first to revive the use of wooden truss bridges and documented his designs in his *Four Books of Architecture*, which were published in 1570. An example of one of his designs, the Bridge of Cismone, is shown below in Fig. 12.2, and described in the excerpt shown in Fig. 12.3.

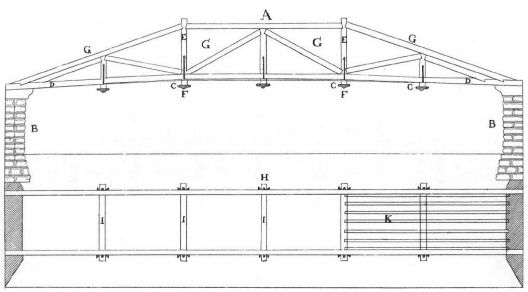

Fig. 12.2 – Elevation (top) and plan (bottom) views of Palladio's Cismone truss bridge.

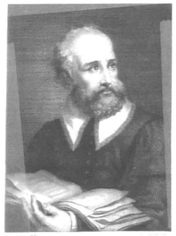

Fig. 12.1 – Portrait of Andrea Palladio, the Italian architect who produced the first written documentation of wooden truss bridges.

Palladio built his truss bridges by connecting wooden pieces together with iron clamps. Wooden truss bridges based on Palladio's original designs continued to be in use until the early 20th century, when variants built out of cast iron or steel members bolted or riveted together became more common. Modern truss bridges are commonly built using steel members, often hollow tubes, which are bolted or welded together, and are primarily used for pedestrian or railway traffic.

CIV102H1F CIV102 Course Notes September 2021

Trusses are an economical structural system for crossing moderate spans because the material is used efficiently, and they can be analyzed by a design engineer with relative ease. A fundamental assumption used in analysis is that the member connections are rotationally flexible, which allows them to be modelled as pins. A consequence of this assumption is that all of the members in the truss will either be in pure tension or pure compression.

Note: Efficiency refers to the high strength and stiffness of truss structures relative to its cost and volume of material required to build them.

Design Process
The process of designing a truss bridge is a straightforward but iterative task. At a high level, the design begins by first determining a suitable arrangement of the members which make up the bridge. An estimate of the loads applied to the bridge is then made, and these loads are used to calculate the forces which each member must safely carry. The members are then sized to carry these loads with an appropriate factor of safety. The bridge must then be checked to ensure that it is adequately stiff under service loads and can resist dynamic effects caused by vibrating or moving loads. The initial estimates of the loads must then be verified to ensure that they are do not underestimate the actual demand. Finally, the cost of the structure is estimated to determine the feasibility of the project. Iteration is often needed to resolve issues which may be encountered during any stage of the design process.

The aforementioned process is explained in more detail below:

1. Define the truss geometry. During this stage of the design process, the span, height, deck width, and configuration of the members must be determined. Increasing the height of the truss at the midspan has the advantage of reducing the magnitude of the forces in the ***top*** and ***bottom chords***, but the increased amount of material needed may make this option uneconomical. Two examples of possible truss geometries are shown in Fig. 12.4 below.

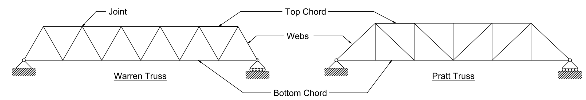

Fig. 12.4 – Examples of common truss designs: Warren truss (left) and Pratt truss (right).

2. **Estimate the joint loads.** Once the geometry has been determined, the loads which the truss will carry must be obtained. Calculating these loads, which are represented as point loads applied to the truss where the deck meets the structure, is broken down into two processes: (a) estimating the weight carried by the deck due to dead and live loads, which are typically expressed as area loads, and (b) converting these area loads into discrete loads applied to the joints.

The area load applied to the deck due to gravity, $\mathbf{w_{total}}$, is the sum of the deck weight, $\mathbf{w_{deck}}$, the weight of the structural members, $\mathbf{w_{struct}}$, and the live load of a large crowd of people, $\mathbf{w_{live}}$:

$$w_{total} = w_{deck} + w_{struct} + w_{live} \tag{12.1}$$

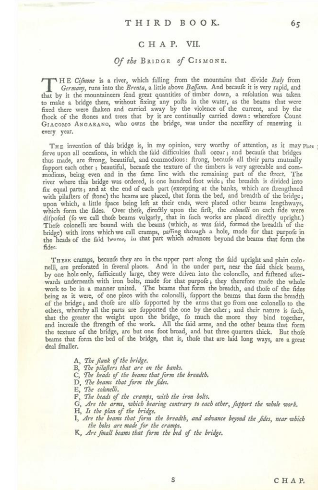

THIRD BOOK. 65

CHAP. VII.

Of the BRIDGE *of* CISMONE.

THE *Ciſmone* is a river, which falling from the mountains that divide *Italy* from *Germany*, runs into the *Brenta*, a little above *Baſſano*. And becauſe it is very rapid, and that by it the mountaineers ſend great quantities of timber down, a reſolution was taken to make a bridge there, without fixing any poſts in the water, as the beams that were fixed there were ſhaken and carried away by the violence of the current, and by the ſhock of the ſtones and trees that by it are continually carried down: wherefore Count GIACOMO ANGARANO, who owns the bridge, was under the neceſſity of renewing it every year.

THE invention of this bridge is, in my opinion, very worthy of attention, as it may ſerve upon all occaſions, in which the ſaid difficulties ſhall occur; and becauſe that bridges thus made, are ſtrong, beautiful, and commodious: ſtrong, becauſe all their parts mutually ſupport each other; beautiful, becauſe the texture of the timbers is very agreeable and commodious, being even and in the ſame line with the remaining part of the ſtreet. The river where this bridge was ordered, is one hundred foot wide; the breadth is divided into ſix equal parts; and at the end of each part (excepting at the banks, which are ſtrengthned with pilaſters of ſtone) the beams are placed, that form the bed, and breadth of the bridge; upon which, a little ſpace being left at their ends, were placed other beams lengthways, which form the ſides. Over theſe, directly upon the firſt, the *colonelli* on each ſide were diſpoſed (ſo we call thoſe beams vulgarly, that in ſuch works are placed directly upright.) Theſe colonelli are bound with the beams (which, as was ſaid, formed the breadth of the bridge) with irons which we call cramps, paſſing through a hole, made for that purpoſe in the heads of the ſaid beams, in that part which advances beyond the beams that form the ſides. Plate 3.

THESE cramps, becauſe they are in the upper part along the ſaid upright and plain colonelli, are preforated in ſeveral places. And in the under part, near the ſaid thick beams, by one hole only, ſufficiently large, they were driven into the colonello, and faſtened afterwards underneath with iron bolts, made for that purpoſe; they therefore made the whole work to be in a manner united. The beams that form the breadth, and thoſe of the ſides being as it were, of one piece with the colonelli, ſupport the beams that form the breadth of the bridge; and thoſe are alſo ſupported by the arms that go from one colonello to the others, whereby all the parts are ſupported the one by the other; and their nature is ſuch, that the greater the weight upon the bridge, ſo much the more they bind together, and increaſe the ſtrength of the work. All the ſaid arms, and the other beams that form the texture of the bridge, are but one foot broad, and but three quarters thick. But thoſe beams that form the bed of the bridge, that is, thoſe that are laid long ways, are a great deal ſmaller.

A, *The flank of the bridge.*
B, *The pilaſters that are on the banks.*
C, *The heads of the beams that form the breadth.*
D, *The beams that form the ſides.*
E, *The colonelli.*
F, *The heads of the cramps, with the iron bolts.*
G, *Are the arms, which bearing contrary to each other, ſupport the whole work.*
H, *Is the plan of the bridge.*
I, *Are the beams that form the breadth, and advance beyond the ſides, near which the holes are made for the cramps.*
K, *Are ſmall beams that form the bed of the bridge.*

S CHAP.

Fig. 12.3 – An excerpt from Palladio's work "*I quattro libri dell'architettura*" (Four Books of Architecture), describing the design of a wooden truss bridge.

CIV102H1F CIV102 Course Notes September 2021

When calculating $\mathbf{w_{total}}$, the live load, $\mathbf{w_{live}}$, should be taken as 5.0 kPa, which is approximately equal to 100 lbs/ft^2. A reasonable estimate of the deck load, $\mathbf{w_{deck}}$, if it is made from wood is 1.0 kPa, and the weight of the structural members is typically between $\mathbf{w_{struct}}$ = 0.5 - 1.0 kPa when using hollow steel members to span distances of up to 100 m.

Note: The values listed here are just suggestions. The actual loads are typically provided by a building standard, or regulatory body, or by a product supplier.

The loads applied to each of the joints, $\mathbf{P_i}$, are obtained by multiplying the area load, $\mathbf{w_{total}}$, by the ***tributary area*** of the deck, $\mathbf{A_{trib}}$, which is the portion of the deck that the joint is responsible for supporting. This is shown below in Eq. (12.2):

$$P_i = w_{total} A_{trib} \tag{12.2}$$

The tributary area is obtained using the heuristic that each joint is responsible for carrying a deck area which extends halfway towards each of its neighbours. This can be seen in Fig. 12.5, which shows the view of the deck from above:

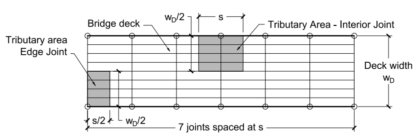

Fig. 12.5 – Plan view of the deck, showing the tributary areas for an interior (middle) and edge (bottom right) joint.

3. Solve for the reaction forces and analyze all of the forces in the members. This step is done using the tools described in Lecture 11 for obtaining the reaction forces, and the analysis methods discussed in Lecture 13.

4. Size the members so that they can safely resist the loads. The method used to proportion the members to resist tension and compression loads is discussed in Lecture 15.

5. Repeat steps 1-4 to design bracing to provide resistance against wind loads and instability effects. In addition to the vertical loads caused by gravity, structures must also resist horizontal loads due to high winds. The cross bracing used to resist the wind loads must also provide adequate support for long members in compression to avoid instability due to buckling. The process of designing braces to fulfill these functions is discussed in Lectures 16 and 17.

6. Calculate the stiffness of the bridge by estimating its deflection at the midspan. A structure must be able to safely carry the applied loads while minimizing the accompanying deformations. A procedure to calculate the deflection of a truss structure called the ***Method of Virtual Work*** and is described in Lecture 18.

CIV102H1F CIV102 Course Notes September 2021

7. Design against dynamic loads. In addition to being able to support a very large, slowly moving crowd of people, a truss bridge must be able to carry a smaller crowd of people walking over the bridge at a brisk pace. In this second situation, the bridge will be subjected to significant dynamic loading which can lead to large displacements and forces due to ***resonance***. Lecture 19 presents a simple method to account for these dynamic effects.

8. Check if the initial estimate of $\mathbf{w_{struct}}$ is greater than the actual weight of the bridge. At the beginning of the design process, an estimate of $\mathbf{w_{struct}}$ was needed to proceed with the design. During this stage of the design process, the true weight of the structural components is compared with the initial estimate, and if the initial estimate of $\mathbf{w_{struct}}$ is lower than the actual weight, then the design process must be repeated. This requirement is mathematically represented as:

$$w_{struct,actual} = \frac{\sum_{i=1}^{n} l_i w_i}{L \times w_{deck}} \leq w_{struct,estimate} \tag{12.3}$$

In Eq. (12.3), **n** is the total number of members in the bridge, $\mathbf{l_i}$ and $\mathbf{w_i}$ are the length and weight per unit length of each member, **L** is the span of the bridge and $\mathbf{w_{deck}}$ is the width of the deck.

If Eq. (12.3) is not satisfied, the design must begin again from step 2 using a more conservative estimate of $\mathbf{w_{struct}}$.

Lecture 13 – Truss Analysis: Method of Joints, Method of Sections

Overview

In this chapter, two methods used for the analysis of forces in truss bridges are discussed. The Method of Joints, which uses the two translational equations of equilibrium, is best suited for performing a complete analysis of the forces in a truss structure. On the other hand, the Method of Sections uses all three equations of equilibrium and is a useful technique for checking the forces in the structure at a particular location of interest.

Pre-Analysis Steps

Each of the methods presented herein are used to calculate the forces in the members caused by external loads at the joints. Joint forces, which are point loads applied to the structure at the joints, can be determined from distributed area loads by using the tributary area concept discussed in Lecture 12. This is process is illustrated in Fig. 13.2

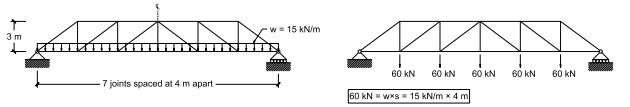

Fig. 13.2 – Truss bridge with distributed loads (left) and equivalent joint loads (right).

Once the joint loads have been determined, the reaction forces can be calculated using the three equations of equilibrium. For a simply supported structure supported by a pin and roller on its two ends and carrying a uniform load, the vertical reactions are each equal to half of the total load due to symmetry. More complicated cases involving non-symmetric load patterns require using the full set of equilibrium equations to get the reaction forces.

Fig. 13.3 shows a truss structure whose loads have been converted to joint loads and has had its reaction forces determined. The structure is now ready to have its member forces determined using either the Method of Joints or Method of Sections.

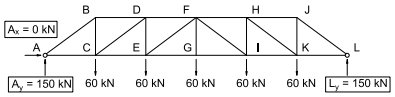

Fig. 13.3 – Truss structure with joint loads and solved reaction forces.

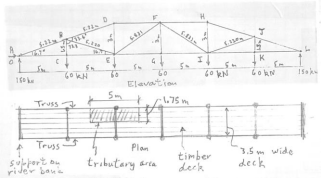

Fig. 13.1 – Summary of truss analysis for Palladio's truss bridge over the Cismone River.

Method of Joints

Conceptually, the Method of Joints involves evaluating the state of equilibrium in the structure one joint at a time. At each joint, the two translational equations of equilibrium are used to solve for the unknown forces carried in the members framing into the joint. Finding all of the forces in the structure is done joint-by-joint, two forces at a time.

To illustrate how the Method of Joints works, we will apply it to the truss structure shown in Fig. 13.3 which has 12 joints and 21 member forces. Due to symmetry, the number of unknown member forces can be reduced to 11, which is solvable by examining 6 joints. We will begin the analysis at joint A which has only two unknown members forces; with the exception of joint L, the other joints cannot be used as a starting point because they each contain three or more unknown member forces, which is greater than the two equations of equilibrium we have at our disposal.

When drawing a free body diagram at a joint, both the external forces applied to the joint (due to the reaction loads or applied loads) and the internal forces in the attached members must be considered. To illustrate this, Fig. 13.4 shows a free body diagram of joint A. Also shown are the two unknown member forces, AB and AC, as well as the reaction forces, A_x and A_y (note that $A_x = 0$).

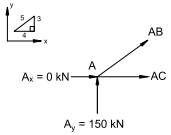

Fig. 13.4 – Free Body Diagram of joint A.

The corresponding equations of equilibrium are:

$$\sum F_x = 0 \rightarrow A_x + AB_x + AC_x = 0 \tag{13.1}$$

$$\sum F_y = 0 \rightarrow A_y + AB_y = 0 \tag{13.2}$$

Substituting A_y = 150 kN into Eq. (13.2) and solving for AB results in the following:

$$AB_y = -150 \rightarrow AB = \frac{5}{3} \times (-150) = -250 \text{ kN} \tag{13.3}$$

Once the force in member AB is known, the force in member AC can be determined using Eq. (13.1):

$$AC = AC_x = -AB_x \rightarrow AC = -\frac{4}{5} \times (-250) = +200 \text{ kN} \tag{13.4}$$

Note: Recall that for a member carrying an axial force F, its x- and y- components F_x and F_y are related to F by the inclination of the member:

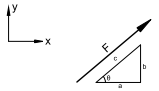

$$F_x = F\cos\theta = \frac{a}{c}F$$

$$F_y = F\sin\theta = \frac{b}{c}F$$

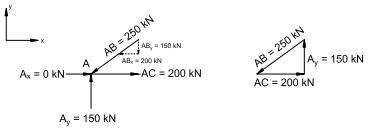

Fig. 13.5 – Summary of member forces framing into joint A.

After solving for the unknown forces, it is helpful to summarize them in a diagram like the one shown on the left free body diagram in Fig. 13.5. Because we found that the force in member AB was a negative number using our initial sign convention in Fig. 13.4, the direction has been reversed in Fig. 13.5. The x- and y- components of AB are also shown, which allows the state of equilibrium at joint A to be easily checked. Furthermore, it is clear that member AB is in compression as it pushes into joint A, and member AC is in tension because it pulls away from joint A.

The force vector diagram in Fig. 13.5 graphically illustrates equilibrium of the joint by rearranging the forces in the free body diagram so that the tails and tips of each force are connected. Equilibrium is satisfied because the rearranged force vectors are able to form a closed path.

Once the forces in member AB and AC have been solved by analyzing joint A, the process is repeated at an adjacent joint to solve for more unknown member forces. Joints B and C are possible candidates; however, joint C has three unknown member forces and hence cannot be solved yet. Therefore, we will move to joint B which only has two unknown forces to solve.

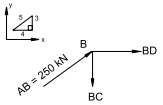

Fig. 13.6 – Free Body Diagram of joint B.

A free body diagram of joint B is shown in Fig. 13.6, which contains two unknown member forces, BC and BD, and force AB which we solved at joint A. Note the sign convention used to define the direction of the three forces: BC and BD are assumed to be in tension and pull away from the joint. AB, which was determined to be in compression from our analysis of joint A, is directed to push into joint B with a magnitude of 250 kN. The resulting equations of equilibrium are the following:

Note: It is very easy to make errors with the sign convention and accidentally identify tension members as compression members and vice versa. Note the following rules:

- *If a force is assumed to pull away from the joint but is calculated to be negative using the corresponding equilibrium equations, then the member is in compression.*
- *If a force is assumed to push into a joint but is calculated to be negative using the corresponding equilibrium equations, then the member is in tension.*

Extra care must be taken when carrying over the results from one joint to solve for the forces in an adjacent joint.

Note: Although it is not immediately obvious how to determine if a member is in tension or compression based on a free body diagram of a joint, it is helpful to think of Newton's third law:

- *If a member is in tension, the joints apply forces to the members which pull away from the member. To resist these forces, the member applies forces to the joints which pulls them together.*
- *If a member is in compression, the joints apply forces to the member which push into the member. To resist these forces the member applies forces to the joints to push them apart.*

These principles are illustrated in Fig. 13.7 below:

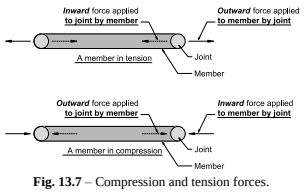

Fig. 13.7 – Compression and tension forces.

$$\sum F_x = 0 \rightarrow AB_x + BD = 0 \tag{13.5}$$

$$\sum F_y = 0 \rightarrow AB_y - BC = 0 \tag{13.6}$$

Solving for BC and BD can then be done by substituting the magnitude of the compression force in AC, 250 kN, into Eq. (13.5) and (13.6), which results in:

$$BD = -AB_x = -\frac{4}{5} \times (250) = -200 \text{ kN} \tag{13.7}$$

$$BC = AB_y = \frac{3}{5} \times (250) = +150 \text{ kN} \tag{13.8}$$

Summarizing these forces into the free body diagram shown below in Fig. 13.8 shows that member BD, like member AB, is in compression as it applies a force which pushes into joint B. Member BC on the other hand is in tension, applying a force which pulls away from joint B. The force vector diagram also shown in Fig. 13.8 also demonstrates that the joint is in equilibrium.

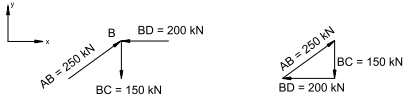

Fig. 13.8 – Summary of member forces framing into joint B.

With these results, the process continues at joint C, and repeats until all of the member forces have been found. The results of the complete analysis are shown below in Fig. 13.8, with tension forces indicated as positive and compression forces indicated as negative.

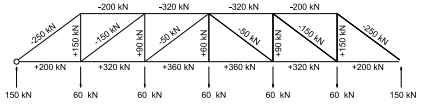

Fig. 13.9 – Summary diagram showing the solved member forces in the truss bridge.

Note: When interpreting a free body diagram of the joint, remember that the drawn forces are the forces applied by the member to the joint.

Note: When presenting your solutions on assignments, quizzes and on the final exam, follow the same sign convention: members in tension are positive, and members in compression are negative.

Method of Sections

Although the Method of Joints is a robust tool for solving for all of the forces in a truss structure, solving for member forces which are located far away from the starting point, like the ones close to the midspan in Fig. 13.9, is a tedious process because they can only found after the forces closer to the supports are known. A faster way to obtain these forces, which is suitable for checking the correctness of the results or performing a preliminary design, is to instead use the Method of Sections.

The Method of Sections uses the three equations of equilibrium to solve for up to three unknown member forces which pass through a "section" of the truss structure. Using the method involves first cutting the structure apart with a line passing through the three members of interest. The equations of equilibrium are then applied to either of the resulting two substructures to solve for the unknown internal forces which were revealed by the section cut.

To illustrate how to apply the Method of Sections, we will solve for the forces in members DF, EF and EG from our previous example. Figure 13.10 shows two free body diagrams, one for the left substructure and one for the right substructure, after the original structure was cut through these members. Because the original structure was in equilibrium, each substructure must also be in equilibrium and hence the forces of interest can be determined by examining either of the free body diagrams.

Note: Defining the initial directions of the unknown forces is very important when using the Method of Sections. If the unknown forces are assumed to pull away from the joints, then positive values will correspond to tension and negative values will correspond to compression.

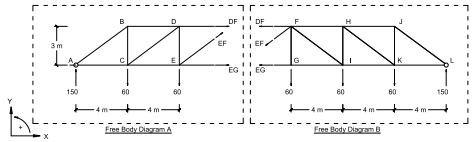

Fig. 13.10 – Free body diagrams used in the Method of Sections to solve DF, EF and EG.

In Free Body Diagram A, the translational equilibrium equations can be written as:

Note: The resulting equations of equilibrium should only include the reaction force at a support, the joint loads applied to the substructure, and the three unknown internal forces which were revealed by the cut.

$$\sum F_x = 0 \rightarrow DF + EF_x + EG = 0 \tag{13.9}$$

$$\sum F_y = 0 \rightarrow 150 + EF_y - 60 - 60 = 0 \tag{13.10}$$

When considering rotational equilibrium, the number of unknown forces which appears in the equation depends on the choice of reference point. A good choice of reference point in this example is joint E, which has two unknown forces, EF and EG, passing through it. This means that the resulting equation will only contain one unknown force, DF, allowing it to be easily solved. In general, it is a good idea to select a point which is common to two of the forces which need to be solved. The resulting equation is shown below:

$$\sum M_E = 0 \rightarrow 60 \times 4 - 150 \times 8 - DF \times 3 = 0 \tag{13.11}$$

Eqs. (13.9) to (13.11) are a system of three equations with three unknowns (DF, EF, and EG), which when solved results in DF = -320 kN, EF = - 50 kN and EG = +360 kN. These results are consistent with our full solution shown in Fig. 13.9.

Note that examining equilibrium of Free Body Diagram B in Fig. 13.10 would result in the same values of DF, EF and EG.

Lecture 14 – Euler Buckling of Struts

Overview

Slender members in compression can fail suddenly due to buckling. This chapter presents the derivation of Euler's equation for predicting the load at which buckling takes place.

Members in Compression

Consider the prismatic member shown in Fig. 14.2. If the two ends of the member are subjected to tensile forces, **T**, the only way for the ends of the member to move apart is if the member elongates. The strains experienced by the member as it stretches can be calculated using the equation $\varepsilon = \Delta l / L_o$, and the member will fail when the stress in the member, $\sigma = T/A$, is equal to the ultimate tensile strength of the material.

Consider now the members subjected to compression forces in Fig. 14.3. Under the compressive forces, the two ends of the member are forced to come together. However, unlike the member in tension, there are two possible ways for the member to deform to allow this to happen. The first way is for the member to simply shorten, which is the opposite of what would happen if it was instead in tension. The second way is if the member, instead of changing length, curves to bring the two ends together. These two actions are shown on the central and right figures in Fig. 14.3 respectively.

Failure due to the first mode of deformation, which typically occurs for short, stocky members, is called ***crushing***, and the force which causes crushing is sometimes referred to as the ***squash load***. The second mode of failure, which commonly occurs in long, slender members, is called ***buckling***. How a member fails depends on the relative amount of force required to cause crushing or buckling; whichever is easier will be the determining cause of failure.

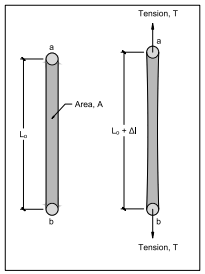

Fig. 14.2 – Members in tension.

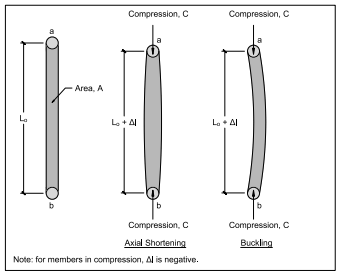

Fig. 14.3 – Members in compression.

Fig. 14.1 – Soviet-era stamp celebrating the 250th birthday of the famous mathematician Leonard Euler.

Calculating the squash load of a member, $\mathbf{P_{crush}}$, is straightforward if the cross-sectional area **A** and the ultimate compressive stress, $\boldsymbol{\sigma_{crush}}$, are known:

$$P_{\text{crush}} = \sigma_{\text{crush}} A \tag{14.1}$$

Calculating the load which causes buckling to take place is more challenging because failure involves the member bending. The solution to the buckling problem was eventually solved by Leonhard Euler in 1757, leading to his celebrated equation for the Euler load, or the load causing buckling, $\mathbf{P_e}$:

$$P_e = \frac{\pi^2 EI}{L^2} \tag{14.2}$$

Derivation of the Euler Load for Elastic Buckling

Euler's derivation of the buckling equation begins with the following assumptions on the member, shown in Fig. 14.4, which has a length of **L** and is being subjected to a compression force **P** which causes the member to curve as it buckles:

i. The material is homogenous and linear elastic, having a uniform Young's modulus, **E**, and second moment of area, **I**.
ii. The top and bottom ends of the member are free to rotate. Furthermore, the top of the member is free to move vertically, and the bottom of the member is translationally fixed in place.
iii. The member is initially perfectly straight and either end is free to translate horizontally.

Note: Recall that the product EI is the flexural stiffness of a member.

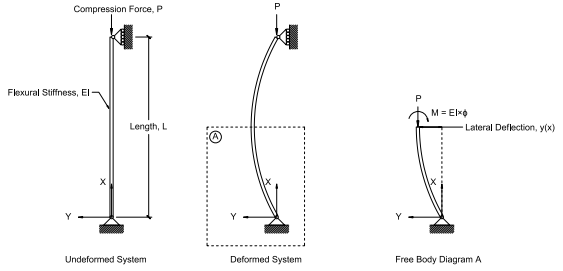

Fig. 14.4 – Derivation of Euler's critical buckling load.

To investigate the how the member resists the load while in its curved position, a free body diagram can be drawn which cuts through the member a distance **x** away from the pin support. At the cut, the member is transmitting the compressive force **P**, which forms a counterclockwise couple with the reaction force at the base. To resist this couple, the bent member must also carry an internal moment **M** at the location of the cut, which rotates clockwise satisfy rotational equilibrium. Taking the sum of moments to equal to zero results in the following equation:

$$P \times y = M \tag{14.3}$$

In Eq. (14.3), **y** is the lateral displacement of the member relative to its original position. Recall that the moment carried by the member is related to its curvature, **ϕ**, by the flexural stiffness **EI**:

$$M = EI\phi \tag{14.4}$$

Substituting Eq. (14.4) into Eq. (14.3) the results in the following equation:

$$Py = EI\phi \tag{14.5}$$

Recall that the curvature is defined as the change in slope along the length of the member, and the slope is the change in lateral displacement. Therefore, the curvature is the second derivative of the lateral displacement; noting that the member has displaced in the positive y direction but is concave down, **ϕ** and **y** have the following relationship:

$$\phi = -\frac{d^2y}{dx^2} \tag{14.6}$$

Substituting Eq. (14.6) into Eq. (14.5) and then dividing both sides by **EI** results in the following differential equation:

$$\frac{P}{EI}y = -\frac{d^2y}{dx^2} \tag{14.7}$$

We can solve Eq. (14.7) in the same way that we solved the differential equation for free vibrations in Lecture 7, which was by assuming a function for **y**, and then checking to see that it satisfies the equation. Because Eq. (14.7) resembles the differential equation that we saw in Lecture 7, we will assume that **y** has the form:

$$y = A\sin(\omega x + B) \tag{14.8}$$

Taking the second derivative of Eq. (14.8) and then substituting everything into Eq. (14.7) results in the following requirement for **ω**:

$$\omega = \sqrt{\frac{P}{EI}} \tag{14.9}$$

We can learn more about the shape of the buckled member if we make use of the fact that the member is prevented from having any lateral displacements at its ends. These are summarized in the following ***boundary conditions***:

$$y(x = 0) = 0;\ y(x = L) = 0 \tag{14.10}$$

Substituting the first boundary condition into Eq. (14.8) results in the requirement that **B** = 0:

$$0 = A\sin(\omega \times 0 + B) \rightarrow B = 0 \tag{14.11}$$

Using this new information and then substituting the second boundary equation into Eq. (14.8) results in the requirement that **ωL** be an integer multiple of pi (i.e., **n** = 0, 1, 2, 3, etc.):

$$0 = A\sin(\omega L) \rightarrow \omega L = n\pi \tag{14.12}$$

Combining Eq. (14.9) with Eq. (14.12) and isolating for the load carried by the buckled member, **P**, results in the following equation:

$$P = \frac{n^2\pi^2 EI}{L^2} \tag{14.13}$$

The smallest nonzero value of **P** requires using n = 1. This corresponds to the Euler load in Eq. (14.2), which is reproduced below as Eq. (14.14):

$$P_e = \frac{\pi^2 EI}{L^2} \tag{14.14}$$

Higher Modes of Buckling

Note that in our equation for **P**, the compressive force carried by the buckled member, there were numerous values of **n** which were possible. Values of **n** which are greater than n = 1 correspond to higher modes of buckling, which occur when the member buckles into more complex shapes. For the simple member used in this example, **n** corresponds to the number of half cycles that the sinusoidally-shaped member assumes. The shapes corresponding to various values of **n** are shown in Fig. 14.5.

Stability of Members under Compression Loads

Buckling is an unstable form of equilibrium. Unlike tension for example, where pulling on a member produces a restoring force which helps to return the member back to its original shape, a member which is buckling will continuously weaken and curve more and more as it is loaded.

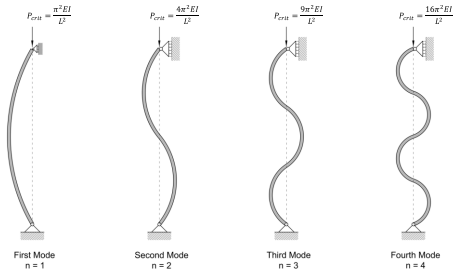

Fig. 14.5 – Higher modes of buckling and associated critical buckling loads.

Under ideal conditions, members are perfectly straight and will theoretically remain so before suddenly buckling once the critical buckling load is reached. Real members however are not perfect and will have a nonzero initial lateral deflection at their midspan, Δ_o because they are not straight. This initial deflection means that they will visibly bend before the Euler load is reached. The relationship derived by the British mathematician Richard Southwell suggests that that lateral deflection of an imperfect member, Δ_{lat}, when subjected to a compression force **P** is:

$$\Delta_{lat} = \frac{\Delta_o}{1 - \frac{P}{P_{crit}}} \tag{14.15}$$

In Eq. (14.15), $\mathbf{P_{crit}}$ is the critical buckling load, which is equal to the Euler load for members which satisfy the support conditions used to derive $\mathbf{P_e}$. The behaviour predicted by Eq. (14.15) is compared with ideal buckling behaviour in Fig. 14.6.

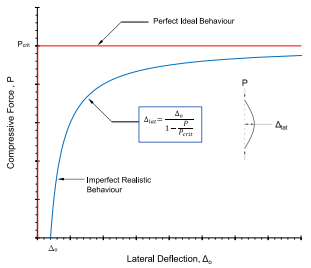

Fig. 14.6 – Comparison of compression response for perfect (red) and imperfect (blue) members.

Note: The response of ideal members which remain perfectly straight before buckling at the Euler load is an example of ***bifurcation behaviour.***

Note: A graphical representation of Southwell's method can be used to determine the critical buckling load of an as-built member without subjecting it to forces which approach its failure load. This is useful for evaluating the safety of structures which are in service and cannot be loaded to failure.

Lecture 15 – Truss Bridge Design Continued

Overview

In this chapter, the process of selecting appropriate members in a steel truss using working stress design is discussed. The properties of hollow structural sections (HSS) are described in detail. Although the design of truss members using steel HSS are covered in this chapter, the basic concepts are also applicable to the design of trusses using other materials (i.e., wood) or alternative types of steel sections.

Design of Members in Tension

As discussed in Lecture 6, steel behaves in a linear elastic manner for relatively small stresses. Once the stress in the material reaches the yield stress, it will yield and elongate substantially, with most of these deformations being non-recoverable. The steel will be able to resist a higher stress than the yield stress, the ultimate stress, due to the effects of strain hardening, before failing shortly after.

Although designing structures using the ultimate strength can lead to material savings, structures must prioritize safety over economy. This is because the consequences of exceeding the ultimate stress, which include structural failure and a potentially catastrophic loss of life, are not worth the relatively minor savings in the cost of construction. It is for this reason that the yield strength is instead used as the design strength of the materials involved. Furthermore, large factors of safety are also employed to reduce the likelihood of failure, as discussed in Lecture 8, and guarantee that the structure remains in a linear elastic state during its service life.

Note: Another reason why the yield strength is used instead of the ultimate strength is because the significant permanent deformations due to yielding are not desirable. Although structures which have yielded may still be strong enough to carry substantial forces, they will appear unsafe and may not be able to fulfill their other non-structural functions.

The stress, **σ**, in a member with a cross sectional area **A** when it is carrying a tension force **F** is:

$$\sigma = \frac{F}{A} \tag{15.1}$$

In design, the maximum allowable stress which may be carried by a member in tension is the yield stress, $\boldsymbol{\sigma_y}$, divided by a factor of safety; an appropriate factor of safety for yielding is $\mathbf{FOS_{yield}}$ **= 2.0**. Substituting this into Eq. (15.1) results in the following requirement on the cross-sectional area of a member which must carry a tensile force **F**:

$$A \geq FOS_{yield}\frac{F}{\sigma_y} = 2.0\frac{F}{\sigma_y} \tag{15.2}$$

A common value of the yield strength of structural steel products made in Canada is $\boldsymbol{\sigma_y}$ **= 350 MPa**.

Design of Members in Compression

Members in compression can fail by either crushing or buckling. Crushing failures, which occur in stocky members which do not buckle, occur when the stresses reach the compressive strength of the material. For steel, the stress which causes yielding in compression is the same as the yield stress in tension, which is 350 MPa. Therefore, Eq. (15.2), using a factor of safety of 2.0 for yielding in compression, can also be used to determine the required cross-sectional area for members in compression.

Buckling occurs when the load carried by the member reaches its critical buckling load, $\mathbf{P_e}$. Recall that for a member with Young's Modulus **E**, second moment of area **I** and length **L**, the buckling load is equal to:

$$P_e = \frac{\pi^2 EI}{L^2} \tag{15.3}$$

Buckling is a more dangerous mode of failure than yielding. Some reasons for this are because it generally occurs more suddenly than yielding and is associated with instability and a loss of strength once it takes place. Therefore, the factor of safety associated with buckling is $\mathbf{FOS_{buckling} = 3.0}$, which is larger than the corresponding factor of safety for yielding due to the above reasons. Reducing the allowable compressive force by taking $\mathbf{P_e}$ and dividing it by the factor of safety results in the following requirement on the second moment area of a member which must carry a compression force **F**:

$$I \geq FOS_{buckling}\frac{FL^2}{\pi^2 E} = 3.0\frac{FL^2}{\pi^2 E} \tag{15.4}$$

As noted in earlier chapters, the Young's modulus of steel is **E = 200,000 MPa**.

The stress causing failure of a member subjected to compression forces is the smaller of the failure stresses associated with yielding and buckling. The yield stress is a property of the material and is independent of its size. On the other hand, the Euler buckling stress $\boldsymbol{\sigma_e}$, which is calculated by taking the buckling load $\mathbf{P_e}$ and dividing by the cross-sectional area **A**, depends on the length of the member, **L**:

$$\sigma_e = \frac{P_e}{A} = \frac{\pi^2 EI}{AL^2} \tag{15.5}$$

We can simplify Eq. (15.5) by introducing a new term **r**, which is called the ***radius of gyration***:

Note: The radius of gyration is not a directly measurable property and is not equal to the radius of a circle. Its physical meaning can be deduced by considering that I is the geometric property of a cross section which affects its flexural stiffness, and A is the geometry property which affects its axial stiffness. The radius of gyration is hence a ratio of a member's flexural stiffness to its axial stiffness.

$$r = \sqrt{\frac{I}{A}} \tag{15.6}$$

Substituting the definition of **r** into Eq. (15.5) results in the following representation of the buckling stress:

$$\sigma_e = \frac{\pi^2 E}{\left(L/r\right)^2} \tag{15.7}$$

In Eq. (15.7), **L/r** is called the ***slenderness ratio***, a nondimensional term which describes the tendency of a member to buckle. Members with a large slenderness ratio tend to fail due to buckling, and those with a small slenderness ratio tend to fail by crushing.

Fig. 15.1 plots the failure stress of members in compression as a function of the slenderness ratio of the member. For short members with low slenderness ratios, the buckling stress approaches infinite and hence these members instead fail at the yield stress of the material. However, as the slenderness ratio increases, the buckling stress decreases rapidly which causes very slender members to fail at a fraction of the yield stress of the material. The red curve, which is obtained by taking the smaller of the yield stress and the buckling stress, represents the failure stress of the member and is often referred to as a ***failure envelope***. The blue curve is obtained in a similar manner as the failure envelope but considers the minimum of the allowable yield stress and the allowable buckling stress. This curve is suitable for design because it incorporates appropriate factors of safety for the two modes of failure.

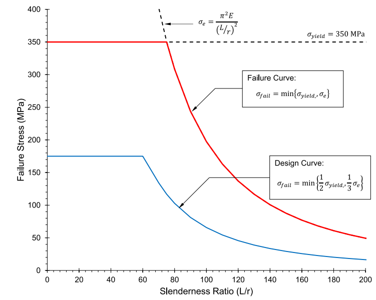

Fig. 15.1 – Influence of slenderness ratio on the strength of compression members. Values plotted are for steel with σ_y = 350 MPa and E = 200,000 MPa.

Summary of Design Requirements
When designing the individual members used in a structure, the primary task required of an engineer is to proportion the sizes of the members so that they are able to safely resist the applied loads. Once the minimum required values of the cross-sectional properties, such as the cross-sectional area **A**, second moment of area **I**, and radius of gyration **r**, have been obtained, the structural member is specified from a catalogue of available products.

Eq. (15.2) is appropriate for selecting the required **A** for both tension and compression members. The minimum required **I** for compression members can be determined by using Eq. (15.4); this check is not required for tension members which cannot buckle. Furthermore, modern design codes also limit the slenderness ratio of a member to discourage the use of very slender members which are vulnerable to unexpected changes in loading. This requirement is shown in Eq. (15.8):

Table 15.1 – Design Equations for Tension and Compression Members

Member Type	Cross-Sectional Area, **A**	Second Moment of Area, **I**	Radius of Gyration, **r**
Tension Members	$A \geq 2.0\frac{F}{\sigma_y}$	N/A	$r \geq \frac{L}{200}$
Compression Members		$I \geq 3.0\frac{FL^2}{\pi^2 E}$	

$$\frac{L}{r} \leq 200 \tag{15.8}$$

A summary of equations used to design tension and members used in truss structures is shown in Table 15.1

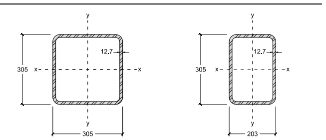

Fig. 15.2 – HSS 305x305x13 (left) and HSS 305x203x13 (right). All dimensions in mm.

Steel Truss Design using Hollow Structural Sections
Steel is a common building material used in civil construction, and a particularly common family of steel members used in steel truss bridges are ***hollow structural sections*** (HSS). HSS are hollow steel tubes which are formed by rolling sheets of steel to form members which are square, rectangular or circular in cross section. Being hollow, HSS members are relatively light, and being made of steel, can be both strong and stiff. HSS are sold by many steel fabricators in commonly produced sizes, some of which are shown in Table 15.2 which is reproduced in Appendix B.

Fig. 15.2 shows the cross sections of a square (left) and rectangular (right) HSS, which have the height, width and thickness as key geometric properties. Many types of HSS which have the same outside dimensions can be ordered in various thicknesses. HSS are typically specified in engineering drawings and specifications using their nominal dimensions. For example, an HSS 305x203x13 is a rectangular HSS which is nominally 305 mm tall, 203 mm wide and has a nominal wall thickness of 13 mm.

*Note that the **designation** of an HSS, which refer to the nominal dimension of the section, is different than the **size** of the HSS, which refer to the actual dimensions. In reality, an HSS 305x203x13 will have a wall thickness of 12.7 mm, not 13 mm.*

Typically, when designing with HSS, it is common to use one continuous member size for the entire bottom chord of a bridge, and one continuous member size for the entire top chord. The web members, which should be smaller than the chords to facilitate the process of connecting the members together, can be individually sized to match the anticipated forces that they must carry. However, it is advisable to only choose one or two members for the webs to reduce the likelihood of errors during construction.

Table 15.2 – Table of Standard HSS Properties

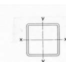

STEEL
SQUARE Hollow Structural Sections — METRIC Dimensions and Properties

Designation	Size	Mass	Dead Load	Area	I	S	r	Z	Torsion J	Surface Area	Shear C_{rt}
mm x mm x mm	mm x mm x mm	kg/m	kN/m	mm²	10⁶ mm⁴	10³ mm³	mm	10³ mm³	10³ mm⁴	m²/m	mm²
HSS 305x305x13	HSS 305x305x12.7	113	1.110	14 400	202	1 330	118	1 560	324 000	1.18	6 450
x 11	x 11.1	100	0.982	12 800	181	1 190	119	1 390	288 000	1.18	5 790
x 9.5	x 9.53	86.5	0.848	11 000	158	1 040	120	1 210	250 000	1.19	5 080
x 8.0	x 7.95	72.8	0.714	9 280	135	886	121	1 030	211 000	1.19	4 340
x 6.4	x 6.35	58.7	0.576	7 480	110	723	121	833	171 000	1.20	3 550
HSS 254x254x13	HSS 254x254x12.7	93.0	0.912	11 800	113	888	97.6	1 060	183 000	0.972	5 160
x 11	x 11.1	82.4	0.808	10 500	102	799	98.4	945	163 000	0.978	4 660
x 9.5	x 9.53	71.3	0.699	9 090	89.3	703	99.1	825	142 000	0.983	4 110
x 8.0	x 7.95	60.1	0.590	7 660	76.5	602	99.9	702	121 000	0.989	3 530
x 6.4	x 6.35	48.6	0.476	6 190	62.7	494	101	571	97 900	0.994	2 900
HSS 203x203x13	HSS 203x203x12.7	72.7	0.713	9 260	54.7	538	76.8	650	90 700	0.769	3 870
x 11	x 11.1	64.6	0.634	8 230	49.6	488	77.6	584	81 200	0.775	3 530
x 9.5	x 9.53	56.1	0.550	7 150	43.9	432	78.4	513	71 000	0.780	3 150
x 8.0	x 7.95	47.5	0.465	6 050	37.9	373	79.2	438	60 500	0.786	2 730
x 6.4	x 6.35	38.4	0.377	4 900	31.3	308	79.9	359	49 300	0.791	2 260
HSS 178x178x13	HSS 178x178x12.7	62.6	0.614	7 970	35.2	396	66.4	484	59 200	0.668	3 230
x 11	x 11.1	55.7	0.547	7 100	32.1	361	67.2	436	53 200	0.673	2 970
x 9.5	x 9.53	48.5	0.476	6 180	28.6	322	68.0	385	46 700	0.678	2 660
x 8.0	x 7.95	41.1	0.403	5 240	24.8	279	68.8	330	39 900	0.684	2 320
x 6.4	x 6.35	33.4	0.327	4 250	20.6	231	69.6	271	32 700	0.689	1 940
x 4.8	x 4.78	25.5	0.250	3 250	16.1	181	70.3	209	25 200	0.695	1 520
HSS 152x152x13	HSS 152x152x12.7	52.4	0.514	6 680	21.0	275	56.0	341	36 000	0.566	2 580
x 11	x 11.1	46.9	0.460	5 970	19.3	253	56.8	310	32 500	0.571	2 400
x 9.5	x 9.53	40.9	0.401	5 210	17.3	227	57.6	275	28 700	0.577	2 180
x 8.0	x 7.95	34.8	0.341	4 430	15.1	198	58.4	237	24 600	0.582	1 920
x 6.4	x 6.35	28.3	0.278	3 610	12.6	166	59.2	195	20 300	0.588	1 610
x 4.8	x 4.78	21.7	0.213	2 760	9.93	130	59.9	152	15 700	0.593	1 270
HSS 127x127x11	HSS 127x127x11.1	38.0	0.373	4 840	10.4	164	46.4	205	18 000	0.470	1 840
x 9.5	x 9.53	33.3	0.327	4 240	9.47	149	47.2	183	16 000	0.475	1 690
x 8.0	x 7.95	28.4	0.279	3 620	8.35	132	48.0	159	13 900	0.481	1 510
x 6.4	x 6.35	23.2	0.228	2 960	7.05	111	48.8	132	11 500	0.486	1 290
x 4.8	x 4.78	17.9	0.175	2 280	5.60	88.1	49.6	103	8 920	0.492	1 030
HSS 102x102x9.5	HSS 102x102x9.53	25.7	0.252	3 280	4.44	87.4	36.8	110	7 740	0.374	1210
x 8.0	x 7.95	22.1	0.217	2 820	3.98	78.4	37.6	96.6	6 780	0.379	1110
x 6.4	x 6.35	18.2	0.178	2 320	3.42	67.3	38.4	81.3	5 670	0.385	968
x 4.8	x 4.78	14.1	0.138	1 790	2.75	54.2	39.2	64.3	4 450	0.390	789
HSS 89x89x9.5	HSS 88.9x88.9x9.53	21.9	0.215	2 790	2.79	62.7	31.6	80.2	4 970	0.323	968
x 8.0	x 7.95	18.9	0.186	2 410	2.53	57.0	32.4	71.2	4 390	0.328	908
x 6.4	x 6.35	15.6	0.153	1 990	2.20	49.5	33.2	60.5	3 700	0.334	806
x 4.8	x 4.78	12.2	0.119	1 550	1.79	40.3	34.0	48.2	2 930	0.339	667
HSS 76x76x8.0	HSS 76.2x76.2x7.95	15.8	0.155	2 010	1.49	39.0	27.2	49.7	2 630	0.278	706
x 6.4	x 6.35	13.1	0.129	1 670	1.31	34.4	28.0	42.7	2 250	0.283	645
x 4.8	x 4.78	10.3	0.101	1 310	1.08	28.5	28.8	34.4	1 800	0.288	546
HSS 64x64x6.4	HSS 63.5x63.5x6.35	10.6	0.104	1 350	0.701	22.1	22.8	28.0	1 230	0.232	484
x 4.8	x 4.78	8.35	0.082	1 060	0.593	18.7	23.6	22.9	1 000	0.238	424
x 3.8	x 3.81	6.85	0.067	872	0.506	15.9	24.1	19.2	836	0.241	368
x 3.2	x 3.18	5.82	0.057	741	0.441	13.9	24.4	16.5	717	0.243	323
HSS 51x51x6.4	HSS 50.8x50.8x6.35	8.05	0.079	1 030	0.317	12.5	17.6	16.3	580	0.181	323
x 4.8	x 4.78	6.45	0.063	821	0.278	10.9	18.4	13.8	485	0.187	303
x 3.8	x 3.81	5.33	0.052	679	0.242	9.54	18.9	11.7	410	0.190	271
x 3.2	x 3.18	4.55	0.045	580	0.214	8.42	19.2	10.2	355	0.192	242
x 2.8	x 2.79	4.05	0.040	516	0.194	7.64	19.4	9.15	318	0.194	221
HSS 38x38x4.8	HSS 38.1x38.1x4.78	4.54	0.044	578	0.100	5.27	13.2	6.91	184	0.136	181
x 3.8	x 3.81	3.81	0.037	485	0.091	4.77	13.7	6.04	160	0.139	174
x 3.2	x 3.18	3.28	0.032	418	0.082	4.31	14.0	5.34	141	0.141	161
x 2.5	x 2.54	2.71	0.026	345	0.071	3.71	14.3	4.51	118	0.144	142
HSS 32x32x3.8	HSS 31.8x31.8x3.81	3.06	0.030	389	0.048	3.01	11.1	3.92	87.0	0.114	126
x 3.2	x 3.18	2.65	0.026	338	0.044	2.77	11.4	3.51	77.6	0.116	121
x 2.5	x 2.54	2.20	0.022	281	0.039	2.44	11.7	3.01	66.1	0.118	110
HSS 25x25x3.2	HSS 25.4x25.4x3.18	2.01	0.020	257	0.020	1.56	8.79	2.05	36.3	0.091	80.6
x 2.5	x 2.54	1.69	0.017	216	0.018	1.41	9.12	1.79	31.6	0.093	77.4

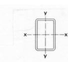

STEEL
RECTANGULAR Hollow Structural Sections — METRIC Dimensions and Properties

Designation	Size	Mass	Dead Load	Area	I_x	S_x	r_x	Z_x	I_y	S_y	r_y	Z_y	Torsion J	Shear C_{rt}
mm x mm x mm	mm x mm x mm	kg/m	kN/m	mm²	10⁶ mm⁴	10³ mm³	mm	10³ mm³	10⁶ mm⁴	10³ mm³	mm	10³ mm³	10³ mm⁴	mm²
HSS 305x203x13	HSS 305x203x12.7	93.0	0.912	11 800	147	964	111	1 190	78.1	769	81.2	896	167 000	6 450
x 11	x 11.1	82.4	0.808	10 500	132	867	112	1 060	70.5	693	81.9	802	149 000	5 790
x 9.5	x 9.53	71.3	0.699	9 090	116	762	113	925	62.1	611	82.7	701	130 000	5 080
x 8.0	x 7.95	60.1	0.590	7 660	99.4	652	114	787	53.3	524	83.4	596	111 000	4 340
x 6.4	x 6.35	48.6	0.476	6 190	81.5	535	115	640	43.8	431	84.1	486	89 800	3 550
HSS254x152x13	HSS254x152x12.7	72.7	0.713	9 260	75.2	592	90.1	746	33.6	441	60.2	522	78 200	5 160
x 11	x 11.1	64.6	0.634	8 230	68.2	537	91.0	671	30.6	401	61.0	470	70 200	4 660
x 9.5	x 9.53	56.1	0.550	7 150	60.3	475	91.9	589	27.2	357	61.7	413	61 600	4 110
x 8.0	x 7.95	47.5	0.465	6 050	52.0	409	92.7	503	23.5	309	62.4	353	52 600	3 530
x 6.4	x 6.35	38.4	0.377	4 900	42.9	338	93.6	411	19.5	256	63.1	290	43 000	2 900
HSS 203x152x13	HSS 203x152x12.7	62.6	0.614	7 970	43.0	123	73.4	528	27.3	358	58.5	432	56 400	3 870
x 11	x 11.1	55.7	0.547	7 100	39.1	385	74.2	476	24.9	327	59.3	390	50 800	3 530
x 9.5	x 9.53	48.5	0.476	6 180	34.8	343	75.1	419	22.3	292	60.0	344	44 600	3 150
x 8.0	x 7.95	41.1	0.403	5 240	30.2	297	75.9	360	19.3	254	60.7	295	38 200	2 730
x 6.4	x 6.35	33.4	0.327	4 250	25.0	246	76.7	295	16.1	211	61.5	243	31 200	2 260
x 4.8	x 4.78	25.5	0.250	3 250	19.5	192	77.5	228	12.6	165	62.2	188	24 100	1 760
HSS 203x102x13	HSS 203x102x12.7	52.4	0.514	6 680	31.2	307	68.4	405	10.2	201	39.1	246	27 000	3 870
x 11	x 11.1	46.9	0.460	5 970	28.7	282	69.3	367	9.46	186	39.8	224	24 600	3 530
x 9.5	x 9.53	40.9	0.401	5 210	25.8	253	70.3	325	8.56	168	40.5	199	21 900	3 150
x 8.0	x 7.95	34.8	0.341	4 430	22.5	221	71.2	281	7.54	148	41.2	172	18 900	2 730
x 6.4	x 6.35	28.3	0.278	3 610	18.8	185	72.2	232	6.35	125	42.0	143	15 600	2 260
x 4.8	x 4.78	21.7	0.213	2 760	14.7	145	73.1	180	5.03	99.0	42.7	111	12 200	1 760
HSS 178x127x13	HSS 178x127x12.7	52.4	0.514	6 680	26.4	297	62.8	377	15.5	243	48.1	298	33 600	3 230
x 11	x 11.1	46.9	0.460	5 970	24.2	272	63.7	342	14.2	224	48.8	270	30 400	2 970
x 9.5	x 9.53	40.9	0.401	5 210	21.7	244	64.6	303	12.8	202	49.6	240	26 900	2 660
x 8.0	x 7.95	34.8	0.341	4 430	18.9	213	65.4	261	11.2	177	50.3	207	23 100	2 320
x 6.4	x 6.35	28.3	0.278	3 610	15.8	178	66.2	216	9.40	148	51.1	171	19 000	1 940
x 4.8	x 4.78	21.7	0.213	2 760	12.4	140	67.1	167	7.41	117	51.8	133	14 700	1 520
HSS 152x102x11	HSS 152x102x11.1	38.0	0.373	4 840	13.6	179	53.1	230	7.13	140	38.4	172	16 300	2 400
x 9.5	x 9.53	33.3	0.327	4 240	12.4	162	54.0	205	6.50	128	39.1	154	14 500	2 180
x 8.0	x 7.95	28.4	0.279	3 620	10.9	143	54.8	178	5.76	113	39.9	134	12 600	1 920
x 6.4	x 6.35	23.2	0.228	2 960	9.18	121	55.7	148	4.88	96.1	40.6	112	10 500	1 610
x 4.8	x 4.78	17.9	0.175	2 280	7.28	95.6	56.5	116	3.89	76.6	41.3	87.8	8 160	1 270
HSS 127x76x9.5	HSS 127x76.2x9.53	25.7	0.252	3 280	6.12	96.4	43.2	126	2.69	70.5	28.6	87.5	6 600	1 690
x 8.0	x 7.95	22.1	0.217	2 820	5.49	86.4	44.1	111	2.43	63.8	29.4	77.2	5 810	1 510
x 6.4	x 6.35	18.2	0.178	2 320	4.70	74.0	45.1	93.3	2.10	55.1	30.1	65.2	4 890	1 290
x 4.8	x 4.78	14.1	0.138	1 790	3.78	59.5	45.9	73.8	1.70	44.7	30.8	51.7	3 860	1 030
HSS 127x64x9.5	HSS 127x63.5x9.53	23.8	0.234	3 030	5.28	83.2	41.7	112	1.70	53.6	23.7	67.4	4 640	1 690
x 8.0	x 7.95	20.5	0.201	2 610	4.77	75.1	42.7	98.9	1.56	49.1	24.4	60.0	4 130	1 510
x 6.4	x 6.35	16.9	0.166	2 150	4.11	64.8	43.7	83.6	1.36	42.9	25.1	51.0	3 510	1 290
x 4.8	x 4.78	13.1	0.129	1 670	3.33	52.4	44.6	66.3	1.12	35.2	25.9	40.7	2 800	1 030
HSS 127x51x9.5	HSS 127x50.8x9.53	21.9	0.215	2 790	4.45	70.0	39.9	97.7	0.961	37.8	18.6	48.9	2 930	1 690
x 8.0	x 7.95	18.9	0.186	2 410	4.05	63.8	41.0	86.9	0.897	35.3	19.3	44.0	2 650	1 510
x 6.4	x 6.35	15.6	0.153	1 990	3.53	55.5	42.1	73.8	0.798	31.4	20.0	37.9	2 290	1 290
x 4.8	x 4.78	12.2	0.119	1 550	2.87	45.3	43.1	58.9	0.665	26.2	20.7	30.5	1 850	1 030
HSS 102x76x9.5	HSS 102x76.2x9.53	21.9	0.215	2 790	3.41	67.2	35.0	87.6	2.15	56.3	27.7	71.3	4 710	1 210
x 8.0	x 7.95	18.9	0.186	2 410	3.10	61.0	35.8	77.7	1.96	51.4	28.5	63.5	4 170	1 110
x 6.4	x 6.35	15.6	0.153	1 990	2.68	52.8	36.7	65.9	1.71	44.8	29.3	54.0	3 530	968
x 4.8	x 4.78	12.2	0.119	1 550	2.18	43.0	37.5	52.5	1.39	36.6	30.0	43.1	2 800	789
HSS 102x51x8.0	HSS 102x50.8x7.95	15.8	0.155	2 010	2.21	43.5	33.2	58.8	0.709	27.9	18.8	35.4	1 950	1 110
x 6.4	x 6.35	13.1	0.129	1 670	1.95	38.4	34.2	50.6	0.638	25.1	19.5	30.7	1 690	968
x 4.8	x 4.78	10.3	0.101	1 310	1.61	31.8	35.1	40.8	0.536	21.1	20.3	24.9	1 370	789
x 3.8	x 3.81	8.37	0.082	1 070	1.36	26.8	35.7	33.9	0.456	18.0	20.7	20.8	1 140	658
x 3.2	x 3.18	7.09	0.069	903	1.17	23.1	36.1	29.0	0.397	15.6	21.0	17.9	979	565
HSS 89x64x8.0	HSS 88.9x63.5x7.95	15.8	0.155	2 010	1.87	42.1	30.5	54.9	1.09	34.3	23.3	43.2	2 450	908
x 6.4	x 6.35	13.1	0.129	1 670	1.65	37.1	31.4	47.1	0.966	30.4	24.0	37.2	2 100	806
x 4.8	x 4.78	10.3	0.101	1 310	1.36	30.6	32.3	38.0	0.803	25.3	24.8	30.1	1 690	667
x 3.8	x 3.81	8.37	0.082	1 070	1.15	25.8	32.8	31.5	0.679	21.4	25.2	25.0	1 400	561
x 3.2	x 3.18	7.09	0.069	903	0.990	22.3	33.1	27.0	0.588	18.5	25.5	21.4	1 190	485
HSS 76x51x8.0	HSS 76.2x50.8x7.95	12.6	0.123	1 600	1.01	26.6	25.1	35.9	0.522	20.5	18.0	26.7	1 270	706
x 6.4	x 6.35	10.6	0.104	1 350	0.917	24.1	26.1	31.4	0.477	18.8	18.8	23.5	1 110	645
x 4.8	x 4.78	8.35	0.082	1 060	0.774	20.3	27.0	25.7	0.407	16.0	19.6	19.3	911	546
x 3.8	x 3.81	6.85	0.067	872	0.660	17.3	27.5	21.6	0.349	13.8	20.0	16.3	762	465
HSS 51x25x3.2	HSS 50.8x25.4x3.18	3.28	0.032	418	0.122	4.81	17.1	6.33	0.040	3.14	9.77	3.84	106	242
x 2.5	x 2.54	2.71	0.026	345	0.105	4.15	17.5	5.35	0.035	2.75	10.1	3.27	89.8	206

Lecture 16 – Blowing in the Wind

Overview

In addition to loads caused by gravity, which generally act downwards, structures must be designed to resist wind loads which typically act laterally. This chapter presents a simple method for determining the loads caused by severe windstorms and outlines a procedure for designing cross bracing to safely resist them.

Wind Loads

A strong wind is capable of producing forces that are large enough to cause structures to collapse, like the trees shown in Fig. 16.1 and the bridge over the Firth of Tay shown in Fig. 16.2. The bridge collapsed in 1879 when a train attempted to cross over it during winds blowing at speeds of up to 117 km/h, killing all 75 passengers on board. In regions of low seismicity, wind loads are usually the most important lateral load which structural engineers must consider when designing structures.

When a wind is blowing onto a surface of a body, it applies a force, $\mathbf{F_{wind}}$, which can be calculated using Newton's drag equation:

$$F_{wind} = \frac{1}{2}\rho v^2 c_D A \tag{16.1}$$

In Eq. (16.1), $\boldsymbol{\rho}$ is the density of the fluid, $\mathbf{v}$ is its velocity, $\mathbf{A}$ is the frontal area on which the wind acts, and $\mathbf{c_D}$ is a drag coefficient which describes the ability of the wind to travel around the body. $\mathbf{c_D}$ may take on a range of values, being 0.2 for a well-designed sports car, 0.75 for a sphere or cylinder, and 1.5 for boxy objects like a cube or a wall.

A simple design value of the wind pressure, $\mathbf{w_{wind}}$, can be obtained by using the density of air, $\boldsymbol{\rho}$ = 1.2 kg/m^3, and assuming appropriately conservative values for $\mathbf{v}$ and $\mathbf{c_D}$, If the maximum wind speed is assumed to be 170 km/h and c_D is taken as 1.5, the wind pressure is equal to:

$$w_{wind} = \frac{F_{wind}}{A} = 2.0 \text{ kPa} \tag{16.2}$$

Therefore, an appropriate value for design is w_{wind} = 2.0 kPa of force, acting horizontally on the structure.

Design of Cross Bracing to Resist Wind Loads

To prevent the main trusses of a bridge from collapsing due to the force of the wind, cross bracing must be provided to connect the top chords and bottom chords together. With this bracing, the bridge will then be able to transfer the applied wind forces to the supports on the ends, in a similar way that the main trusses support the gravity loads applied to the deck and transfer them to the supports. A typical arrangement for the top and bottom braces is shown in Fig. 16.3.

Fig. 16.1 – Pine trees broken by a windstorm

Fig. 16.2 – Firth of Tay Bridge, 29 December 1879. The engineer, Sir Thomas Bouch, was unable to produce the wind calculations during the subsequent investigation.

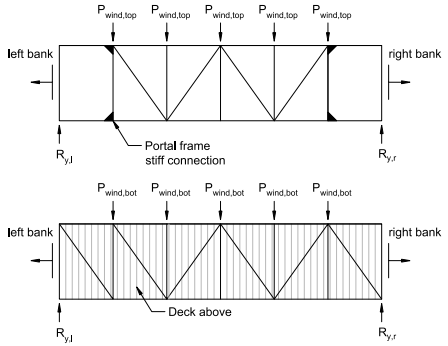

Fig. 16.3 – Arrangement of cross bracing on the top (above) and bottom (below) of a truss bridge. The bridge has the same geometry as the one analyzed in Lecture 13.

In each of the schematics shown in Fig. 16.3, $\mathbf{P_{wind}}$ is the joint load caused by the wind blowing onto the side of the bridge. Because the direction of the wind is not fixed, the cross bracing must be designed to resist loads acting on either side. Furthermore, the loads can push towards the bridge, or pull away due to suction effects. This results in four possible combinations of loading which must be considered when designing the members.

Determining the forces in the bottom cross bracing follows the same process as the analysis of the main truss for gravity loads. First, the reaction forces $\mathbf{R_{y,l}}$ and $\mathbf{R_{y,r}}$ must be determined based on the applied loads. After these loads have been determined, the forces in the braces can be obtained by using the Method of Joints or Method of Sections.

Analyzing the top cross bracing using a truss analysis method like the Method of Joints is not immediately possible due to the lack of diagonal members which connect the supports to the rest of the braces. These members are omitted to allow entry and egress of the bridge. In lieu of these members, the connection is typically stiffened to allow the forces in the cross bracing to be transferred to the ground.

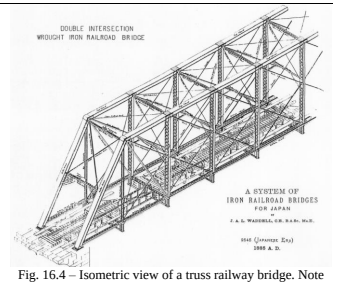

Fig. 16.4 – Isometric view of a truss railway bridge. Note the use of stiff connections at the front to eliminate the need for a brace crossing over this region. The open entryway stiffened at the corners is called a ***Portal Frame***.

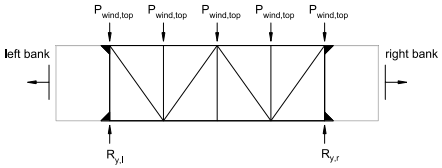

Fig. 16.5 – Analysis of the forces in the top braces.

Fig. 16.5 shows a simplified approach to solving for the forces in the top braces. In this schematic, we have assumed that the reaction forces provided at the supports can be transferred along the outside members to meet the braces. With this assumption, the brace forces can now be determined using the Method of Joints.

Calculating Joint Loads using the Tributary Area

Although calculating the brace forces once the wind loads have been determined is a straightforward task, obtaining the joint loads caused by the wind requires a series of intricate calculations to be done. The joint load $\mathbf{P_{wind}}$ is calculated in a similar way as the joint loads caused by gravity, but instead the loads act on the frontal area of the bridge, $\mathbf{A_{frontal}}$, instead of on the deck:

$$P_{\text{wind}} = w_{\text{wind}} A_{\text{frontal}} \tag{16.3}$$

In Eq. (16.3), $\mathbf{w_{wind}}$ is typically taken as 2.0 kPa.

When determining the frontal area, the tributary area concept is used in the same way it was used for obtaining the gravity loads, meaning that a joint is responsible for carrying the loads applied to the surfaces halfway to each of its surrounding neighbours. The frontal area used in Eq. (16.3) is hence the solid area within this tributary zone.

Fig. 16.6 show the elevation view of a truss bridge and illustrates how the wind pressure is distributed to produce discrete loads applied to the joints. The frontal area associated with joint A is all of the solid area within Zone A, and likewise for joint B. Due to the presence of the handrail in Zone B, the force applied to joint B will greatly exceed what joint A must carry.

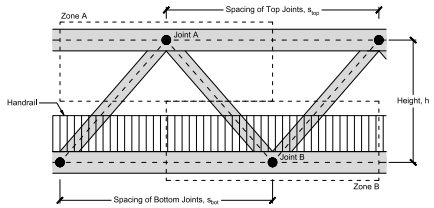

Fig. 16.6 – Elevation view of a truss bridge. Joint A is responsible for carrying the loads applied to the solid surfaces within Zone A, and joint B is responsible for carrying the loads applied to the solid surfaces in Zone B.

Fig. 16.7 shows the details of Zone A and B in more detail. Each zone has a height of h/2, and a width of s_{top} and s_{bot} respectively. The frontal area in Zone A can be approximated using the following equation:

$$A_{frontal} \cong \sum_{i=1}^{n} b_i l_i = b_1 l_1 + b_2 l_2 + b_3 l_3 + b_4 l_4 \tag{16.4}$$

In Eq. (16.4), $\mathbf{n}$ is the number of members within the zone, $\mathbf{b_i}$ is the outside dimension of the cross section facing the wind, and $\mathbf{l_i}$ is the length of the member within the zone.

For situations involve a handrail, like in Zone B in Fig. 16.7, the frontal area of the handrail is much larger than the frontal area of the HSS, which can hence be neglected for simplicity. Although the handrail may consist of closely spaced vertical members with gaps in between, the resulting turbulence as the air flows through these narrow spaces will increase the drag force applied to the railing. Therefore, the handrail may be approximated as a solid surface, resulting in a frontal area of:

$$A_{frontal} \cong h_{rail} s_{bot} \tag{16.5}$$

Note that Eq. (16.4) and (16.5) should be modified when used in situations where the horizontal or vertical spacing of the joints is irregular. The governing principle when making these modifications is that each joint is responsible for the zone halfway to each of its neighbours.

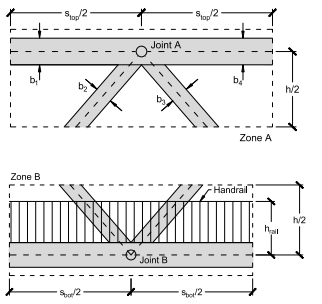

Fig. 16.7 – Schematics for determining the tributary areas in Zone A and Zone B.

Note: Moving the reaction force from the support to the top bracing requires a carefully designed connection. The design of these connections is outside of the scope of CIV102 but can pose a serious design challenge in real-life engineering practice.

Lecture 17 – A Bracing Lecture

Overview

In this chapter, the process of designing cross braces to laterally support members in compression is presented. Compression members typically tend to deform because of imperfect alignment, which can reduce their buckling strength if their joints are not adequately restrained from moving. A simple analysis technique is derived to ensure that the lateral movements at any joint does not exceed 1% of the attached member's length.

Stability and Misalignment of Compression Members

Consider the truss bridge shown in Fig. 17.1, whose top chord is in compression as it supports a substantial gravity load applied to the deck. When designing the chord, it was assumed that the member and its joints were perfectly aligned so that the compression member buckled between the joints with an effective buckling length equal to the spacing between the joints (i.e., L = the joint spacing) when evaluating the buckling force $\mathbf{P_{crit.}}$

Recall: Gravity loads are applied to the deck, and include the weight of the deck itself, the weight of the structural components, and the weight of a large crowd of people.

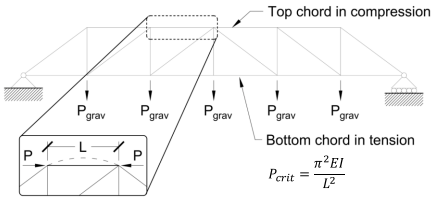

Fig. 17.1 – Design of top chords against buckling using the joint spacing, L.

In reality, these assumptions are generally not true: the members will be slightly misaligned due to the imperfect nature of construction, and the stability of the joints will depend on the stiffness of the braces used to connect the chords of the truss together. In extreme cases, like truss bridge in Fig. 17.2 which does not contain any diagonal braces connecting its top chords together, the compression chords can buckle over the entire length of the bridge at a much lower load than originally anticipated.

The bridge shown on the right in Fig. 17.2, which contains diagonal braces and rigid connections at the portal frame, avoids this issue by preventing the joints from deforming in the out-of-plane direction. Having this bracing system provides stability to the structure and allows us to design the compression members using our original assumption that the effective buckling length is the joint spacing. The braces which connect these compression members must therefore be sized so that they can provide an adequate restraining force to prevent the chord from buckling at its joints.

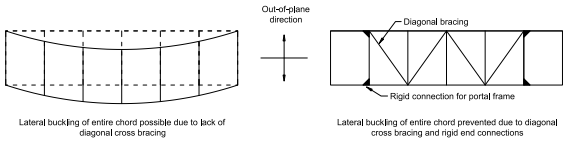

Fig. 17.2 – View of a truss bridge from above, showing how cross bracing can restrain the chords from buckling over the entire span.

Design Check for Stability

Fig. 17.3 shows two schematics of a compression member with a length of **2L** and subjected to a compression force of **P**. Because the joint at the midspan is not restrained, it buckles and displaces laterally at its midspan by a distance **Δ**. To prevent the system from deforming further, a restraining force, **R**, is required to pull the displaced joint back to its original position; this is shown in the second drawing in the figure.

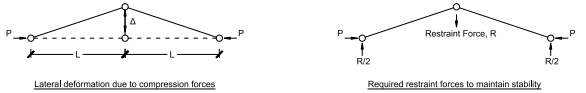

Fig. 17.3 – Analysis of a compression member as the joint moves out of plane.

The required restraint force to restore the joint back into its original position depends on how much it has displaced, i.e., as the deformation **Δ** increases, **R** must increase as well. In design, an appropriate value of **Δ** to use is **Δ = 0.01L** (1% of L). This misalignment, equal to 1% of the of the length of the individual members, is a reasonable upper bound of what can be expected given modern construction practices.

Fig. 17.4 shows a free body diagram of half of the situation shown in Fig. 17.3. Because the system is in equilibrium, taking moments about the bottom left joint results in the following equation:

$$P \times \Delta = \frac{R}{2} \times L \tag{17.1}$$

Substituting the requirement that Δ = **0.01L** results in the following requirement for the restraint force:

$$R = 0.02P \tag{17.2}$$

Therefore, to ensure that the compression member is adequately braced for stability, there must be braces attached to each of its joints which are able to provide a local restraining force of R = 0.02P.

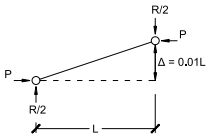

Fig. 17.4 – Free body diagram used to determine the required restraining force, R, if Δ = 0.01L.

Fig. 17.5 shows how the diagonal braces provide the required restraining force as the intermediate joint moves laterally. As the joint displaces outwards, the two diagonal braces come into tension and pull the joint back to its original position. To maintain vertical equilibrium at the bottom joints, the vertical members must go into compression, which in turn stabilizes the top joints by providing the reaction forces shown in Fig. 17.3. The opposite occurs if the intermediate joint was to instead displace inwards.

Just like when designing for wind, the braces supporting compression members must also be designed for four possible situations because either of the compression chords may buckle towards or away from the centre of the bridge. These four situations are illustrated in Fig. 17.6, which shows a portion of the braces connecting the top chords from plan view.

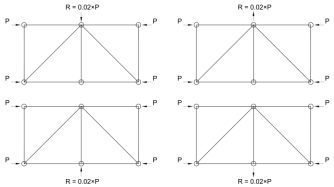

Fig. 17.6 – Summary of design cases when designing braces for stability.

It should be emphasized that the stability design described above is a **local** check to ensure that each joint is adequately supported by the braces. This contrasts with a **global** analysis, which is done when designing for wind for example, which involves obtaining the reaction forces and complete member forces for the entire bridge.

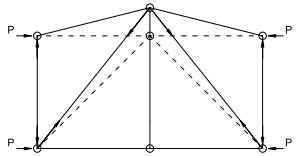

Fig. 17.5 – Mechanism by which cross bracing restrains joints from buckling outwards.

Design Process for Cross Bracing

The design of the braces on the top and bottom of the bridge to resist wind loads and instability effects can be done together once the main trusses have been designed to resist the gravity loads. The braces which connect the bottom chord will typically only need to be designed for wind loads because the gravity loads cause them to go into tension. This contrasts with the design of the braces on the top of the bridge, which must both resist wind loads and provide stability when the gravity loads cause the top chords to carry significant amounts of compression.

To design the top braces, the following steps should be followed:

1. Calculate the wind loads and determine the brace forces. This is a global analysis which involves solving for the reaction forces and then obtaining the brace forces by using the Method of Joints or Method of Sections.

2. Calculate the forces in the braces which are required to stabilize the compression chords under gravity loads. Using the forces in the chords as obtained under gravity loads, calculate the required restraint force needed to support the joints along the top chord from displacing laterally. This is done by performing a series of local analyses, like the ones shown in Fig. 17.6, with the goal of calculating the forces in the members directly attached to the displaced joint.

*Note: The compression force in the top chord varies along its length. If you find when drawing a schematic like those in Fig. 17.6 that the forces in the chords on the two sides are not equal, use the larger value to find **R** to be conservative.*

3. Select appropriate HSS sections which can carry the larger of the forces obtained in steps 1 and 2. The braces should be designed for both tension and compression because the wind or instability can act in any direction. Typically, only one or two HSS sizes are used for the braces to avoid errors during construction and avoid potential supply issues.

Note: The braces need to be designed for the more severe case of wind or instability, but not both at the same time. This is because the loads will not occur at the same time. For example, during the event of a severe windstorm, it is highly unlikely for a large crowd of people to occupying the bridge at the same time. High wind loads will generally occur in the absence of high gravity loads, and vice-versa.

The design process for the bottom braces is identical but omits step 2 because the bottom chords will not buckle under the tension forces caused by gravity loads.

Lecture 18 – Method of Virtual Work

Overview

Although determining the forces in a truss bridge structure is a straightforward task, determining the deflection of a loaded structure can be an arduous challenge. In this chapter, the Method of Virtual Work is presented, which transforms the task of solving displacements from a complex geometric problem to a simple statics problem.

Introduction

In structural engineering, it is equally important for a structure to have adequate strength and stiffness. The importance of strength, which is the ability of a structure to safely carry the expected loads, has been discussed extensively in previous chapters. Stiffness on the other hand is a measure of how well a structure can limit its deformations under service loads. Excessive deformations can disrupt other functions of the structure and are generally unpleasant if they are large enough to be observed by users of the structure.

Note: Service loads refer to the loads which the structure must carry under normal circumstances. This is different from extreme loads which arise from severe windstorms, earthquakes, or large crowds.

Determining the deformations of a truss structure when loaded can be done by solving for the forces in the members, calculating the corresponding changes in length of all of the members, and then determining the displaced shape using these new member lengths. Although this is a feasible procedure to determine the deflections of very simple structures, it quickly becomes impractical as the number of members which need to be considered increases.

An alternative means of solving for the displacements uses energy methods. According to the theorem of conservation of energy, the work done by the externally applied loads **F** acting over the external displacements Δ, W_{ext}, must equal to the work done by the internal members changing length, Δ**l**, while carrying internal forces **P**, $\mathbf{W_{int}}$. In the case where **m** loads are applied to a truss structure with **n** members, this can be expressed as:

$$W_{\text{ext}} = W_{\text{int}} \tag{18.1}$$

The work terms in Eq. (18.1) can be expanded further, which results in the following:

$$\sum_{i=1}^{m} \int F_i d\Delta_i = \sum_{j=1}^{n} \int P_j d\Delta l_j \tag{18.2}$$

Note: The integrals in Eq. (18.2), which represent the work done by the forces acting over displacements, are a mathematical representation of the area under a force-displacement curve. Refer to Lecture 6 for more information.

The equivalence of the external work and internal work is the basis of the ***Method of Virtual Work***.

The Method of Virtual Work: Derivation

To introduce the Method of Virtual work, consider the simple two-member truss which is shown in Fig. 18.1. There is a force **F** applied to the structure which causes joint B to translate horizontally and vertically by ΔB_x and ΔB_y respectively. The two members, member AB and BC, will resist the applied force by carrying internal member forces, $\mathbf{P_{AB}}$ and $\mathbf{P_{BC}}$ respectively, and will stretch or contract by $\Delta\mathbf{l_{AB}}$ and $\Delta\mathbf{l_{BC}}$ as a result. The quantity which we would like to solve is the vertical displacement of point B, $\Delta\mathbf{B_y}$.

Note: The derivation of the method of virtual work is included here for completeness but will not be assessed during the course. You will be assessed based on how well you are able to apply the method to solve problems.

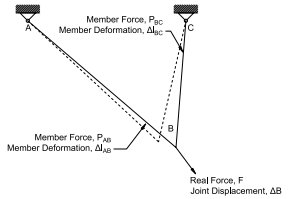

Fig. 18.1 – Real system of forces and displacements.

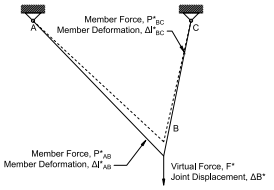

Fig. 18.2 – Virtual system of forces and displacements.

Consider the equivalence of the external work done by the force **F** as it acts over the displacements at joint B and the internal work done by the members as they deformed in response to the applied load. If it is assumed that all of the members are linear elastic, then Eq. (18.2) can be rewritten as:

$$\sum_{i=1}^{m} \frac{1}{2} F_i \Delta_i = \sum_{j=1}^{n} \frac{1}{2} P_j \Delta l_j \tag{18.3}$$

Expanding Eq. (18.3) for our simple system and breaking up **F** into its x- and y- components yields:

$$\frac{1}{2}F_x\Delta B_x + \frac{1}{2}F_y\Delta B_y = \frac{1}{2}P_{AB}\Delta l_{AB} + \frac{1}{2}P_{BC}\Delta l_{BC} \tag{18.4}$$

The terms on the right side of Eq. (18.4), which contain the internal forces and the changes in lengths of the members, can be solved using tools discussed in the previous chapters. However, the left side of our equation contains two unknown displacements, ΔB_x and ΔB_y, which cannot be solved because we only have one equation.

To overcome this issue, we will introduce a ***virtual system***, shown in Fig. 18.2, which is geometrically identical as the original system, but only contains a single ***virtual force***, **F***, which acts in the same position and direction of our displacement of interest, ΔB_y. The virtual force causes the system to have virtual member forces, $\mathbf{P^*_{AB}}$ and $\mathbf{P^*_{BC}}$ which result in virtual member deformations, $\Delta\mathbf{l^*_{AB}}$ and $\Delta\mathbf{l^*_{BC}}$, and virtual displacements at joint B, ΔB^*_x and ΔB^*_y. Writing the work equation for this system, noting that the x-component of **F*** is equal to zero, results in:

$$\frac{1}{2}F^*\Delta B^*_y = \frac{1}{2}P^*_{AB}\Delta l^*_{AB} + \frac{1}{2}P^*_{BC}\Delta l^*_{BC} \tag{18.5}$$

Note: The virtual force F has an arbitrary magnitude and is usually taken as F* = 1 kN. The key concept when specifying F* is that* ***F* has the same location and orientation as the displacement of interest.*** *F* is sometimes called a dummy load.*

Eq. (18.5) contains the products of virtual forces and virtual displacements, which are unrelated to the real forces and real displacements which we are interested in. If we take advantage of the fact that the structure is linear elastic, then we can combine our virtual system with our real system, resulting in a hybrid system which has both real and virtual forces and real and virtual displacements. This is shown in Fig. 18.3.

Note: The net forces, stresses and strains resulting from the real load F and virtual force F acting together is simply the sum of the effects caused by each individual force. This is called the* ***Superposition Property*** *(sometimes referred to as the* ***Superposition Principle)*** *and is applicable to any linear elastic system.*

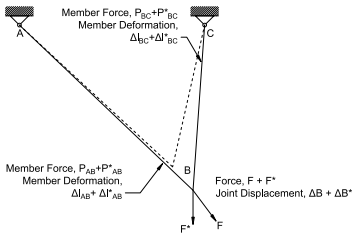

Fig. 18.3 – Hybrid system containing both real and virtual quantities.

Fig. 18.4 contains four plots which show the force-displacement relationships of the structure and its members due to the application of both the real and virtual forces. The top two plots show the relationships between the externally applied forces and the displacements of joint B, and the bottom two plots show the relationships between the internal member forces and their member deformations. The area underneath the curves represents the work done; the red areas correspond to work done by the real forces acting over the real displacements, and the blue areas represent the work done by the virtual forces acting over the virtual displacements.

By using the principle of equivalent internal and external work in Eq. (18.1), the total area underneath the top two graphs, the external work, must be equal to the total area underneath the bottom two graphs. Furthermore, the red areas in the top graphs must equal the red areas in the bottom graphs, due to Eq. (18.4), and the blue areas in the top graphs must also equal to the blue areas in the bottom graphs, due to Eq. (18.5).

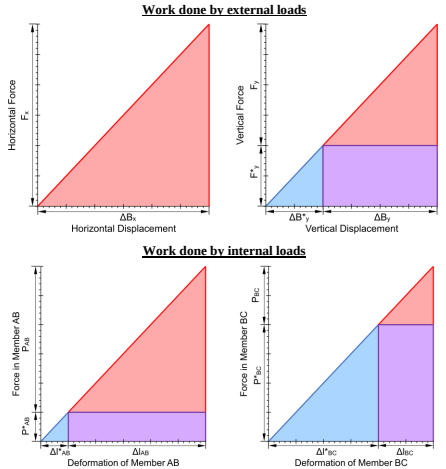

Fig. 18.4 – Load-displacement plots for the structure (top) and individual members (bottom) when subjected to a real load F and a virtual load F*. The area underneath each curve is equal to the work done.

Because the total areas, as well as the red and blue areas, must equal, it can also be concluded that the area of the purple regions, which are the product of a virtual force and a real displacement, must equal as well. These areas represent the ***virtual work*** done by the virtual forces, $\mathbf{P^*_{AB}}$ and $\mathbf{P^*_{CB}}$ acting over the real displacements, $\Delta\mathbf{B_y}$, $\Delta\mathbf{l_{AB}}$ and $\Delta\mathbf{l_{BC}}$. Expressing this equivalence mathematically results in the following equation:

$$F^*\Delta B_y = P^*_{AB}\Delta l_{AB} + P^*_{BC}\Delta l_{BC} \tag{18.5}$$

Note: The terms in Eq. (18.5) do not have a coefficient of ½ because they represent the rectangular areas under the load-displacement relationships.

In Eq. (18.5), there is now only one unknown displacement, $\Delta \mathbf{B}_y$, which can be solved once the other terms are found from statics and Hooke's law. The advantage of using the Method of Virtual work is that by using a virtual system which contains one load, we are always able to obtain single equation with one unknown displacement, regardless of the size of the structure and complexity of the real loads. Therefore, Eq. (18.5) can be generalized for a system of arbitrary complexity to be:

$$F^* \Delta = \sum_{i=1}^{n} P_i^* \Delta l_i \qquad (18.6)$$

Where the variables in Eq. (18.6) are defined as follows:

- $\mathbf{\Delta}$ is a real joint displacement of interest.
- $\mathbf{F^*}$ is a virtual load of arbitrary value (usually taken as 1 kN) applied to the structure which has the same location and direction as $\mathbf{\Delta}$.
- $\mathbf{P^*_i}$ are the virtual member forces resulting from the virtual force $\mathbf{F^*}$.
- $\mathbf{\Delta l_i}$ **are** the real member deformations caused by the real forces in the system.
- $\mathbf{n}$ is the total number of members in the truss structure.

The Method of Virtual Work: Summary and Example

The basic procedure to use the method of virtual work is shown below:

1. Solve for all of the member forces, $\mathbf{P_i}$, due to the real loads using any analysis method.
2. Using the member properties and the real member forces, calculate the real member deformations $\mathbf{\Delta l_i}$.
3. Identify the displacement of interest, $\mathbf{\Delta}$.
4. Create a separate virtual system with a single virtual load, $\mathbf{F^*}$, which has the same location and direction as $\mathbf{\Delta}$.
5. Solve for the virtual member forces, $\mathbf{P^*_i}$.
6. Use Eq. (18.6) and solve for $\mathbf{\Delta}$.

To illustrate this process, consider the truss bridge shown below in Fig. 18.5 whose member forces are the result of the real applied loads.

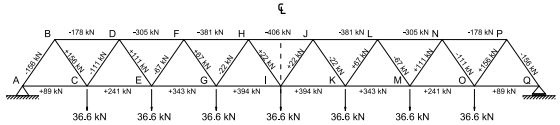

Fig. 18.5 – Real member forces. Note that each horizontal member is 3.75 m long and each diagonal member is 3.29 m long.

Note: When using Eq. (18.6), the product of a force and displacement will be in Joules if the force is in kN and the displacement is in mm. Furthermore, the sign of the virtual work is important, as a compressive force acting over a tensile deformation produces negative work as does an upwards external force acting over a downwards displacement (and vice versa).

If the deflection of the bridge at the midspan is required, a separate virtual system consisting of a single point load applied downwards at the centre of the bridge will be used. This virtual system, including the resulting virtual member forces, is shown in Fig. 18.6.

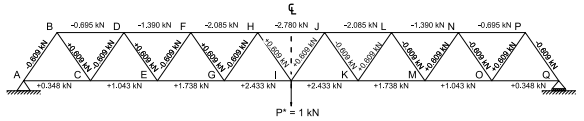

Fig. 18.6 – Virtual system of forces caused by a 1 kN load at the midspan.

Performing the calculations when applying Eq. (18.6) to a large system is commonly done using a large table, like the one shown in Fig. 18.7. The column on the far right, which contains the virtual work, is the product of the calculated member deformations, Δ, and the virtual member forces $\mathbf{P^*}$. By summing over the sixteen members in the table and multiplying by two (to account for the work done by the sixteen members on the other side of the bridge), the total internal work done was found to be 68.7 J. Equating this value to the external work and dividing by the 1 kN virtual load results in a calculated deflection of 68.7 mm downwards.

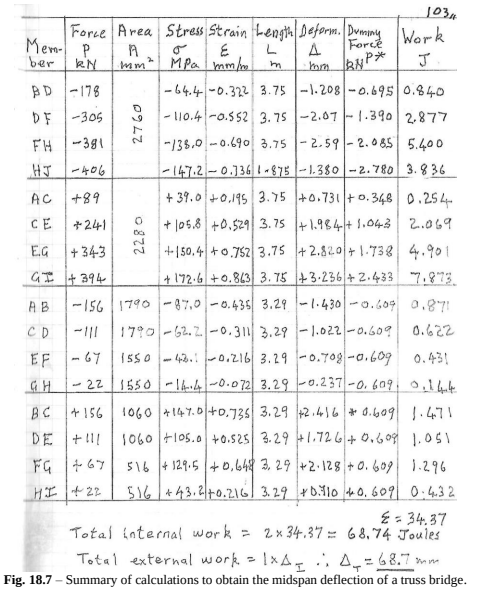

Member	Force P kN	Area A mm²	Stress σ MPa	Strain ε mm/m	Length L m	Deform. Δ mm	Dummy Force P* kN	Work J
BD	−178		−64.4	−0.332	3.75	−1.208	−0.695	0.840
DF	−305	2760	−110.4	−0.552	3.75	−2.07	−1.390	2.877
FH	−381		−138.0	−0.690	3.75	−2.59	−2.085	5.400
HJ	−406		−147.2	−0.736	1.875	−1.380	−2.780	3.836
AC	+89		+39.0	+0.195	3.75	+0.731	+0.348	0.254
CE	+241	2280	+105.8	+0.529	3.75	+1.984	+1.043	2.069
EG	+343		+150.4	+0.752	3.75	+2.820	+1.738	4.901
GI	+394		+172.6	+0.863	3.75	+3.236	+2.433	7.873
AB	−156	1790	−87.0	−0.435	3.29	−1.430	−0.609	0.871
CD	−111	1790	−62.2	−0.311	3.29	−1.022	−0.609	0.622
EF	−67	1550	−43.1	−0.216	3.29	−0.708	−0.609	0.431
GH	−22	1550	−14.4	−0.072	3.29	−0.237	−0.609	0.144
BC	+156	1060	+147.0	+0.735	3.29	+2.416	+0.609	1.471
DE	+111	1060	+105.0	+0.525	3.29	+1.726	+0.609	1.051
FG	+67	516	+129.5	+0.648	3.29	+2.128	+0.609	1.296
HI	+22	516	+43.2	+0.216	3.29	+0.710	+0.609	0.432

103ₙ

Σ = 34.37

Total internal work = 2 × 34.37 = 68.74 Joules

Total external work = 1 × Δ_T ∴ Δ_T = 68.7 mm

Fig. 18.7 – Summary of calculations to obtain the midspan deflection of a truss bridge.

Lecture 19 – Where Have All the Soldiers Gone?

Overview

Several types of loading, such as a moving crowd of people, a windstorm, or an earthquake, apply dynamic loads to structures. Dynamic loads, unlike static loads, vary in time, and may produce resonant effects which can magnify the stresses and deflections experienced by the structure. In this chapter, a simple method to consider dynamic effects in linear elastic structures is introduced.

Free Vibration

As noted in Lecture 7, the behaviour of a simple spring-mass system is governed by the following differential equation:

$$m\frac{d^2x(t)}{dt^2} + kx(t) = 0 \qquad (19.1)$$

Where $\mathbf{x(t)}$ is a time-varying function describing the displacement of the mass, $\mathbf{m}$ is the mass, and $\mathbf{k}$ is the axial stiffness of the spring. Solving Eq. (19.1) for a system which vibrates vertically results in a sinusoidal function with amplitude $\mathbf{A}$, natural frequency $\boldsymbol{\omega_n}$ and phase shift $\boldsymbol{\phi}$ which oscillates around the static displacement of the mass under the force of gravity, $\mathbf{\Delta_o}$:

$$x(t) = A\sin(\omega_n t + \phi) + \Delta_o \qquad (19.2)$$

The response described by Eq. (19.2) is shown in Fig. (19.1). Note that in this idealized system, there is no loss of energy, and the mass will continue to oscillate until it is interrupted by an external action.

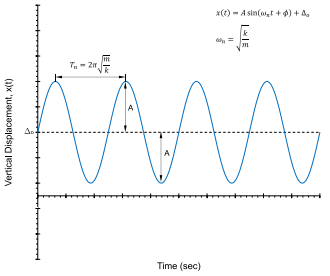

Fig. 19.1 – Undamped free vibration.

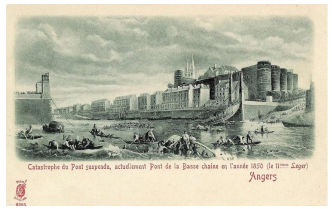

Fig. 19.1 – Collapse of the Angers Bridge in France in 1850. The bridge collapsed as a battalion of soldiers was marching across, leading to 226 deaths.

Note: A system undergoing free vibration is sometimes referred to as a ***Simple Harmonic Oscillator.***

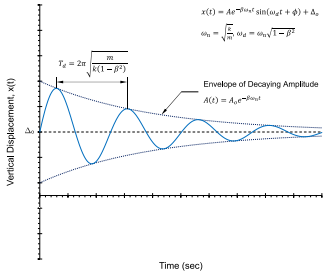

Fig. 19.2 – Damped free vibration.

Damped Free Vibrations

In reality, vibrating systems will eventually come to a rest due to energy being dissipated by friction or other effects. This gradual loss of energy in a vibrating system is caused by ***damping***, which can be an engineered feature or an inherent property of the system. The damping in a system is quantified by the ***damping ratio***, **β**, which is the ratio between the provided damping properties of the system and the minimum amount of damping needed to prevent the system from oscillating.

The differential equation for freely vibrating systems which have damping is a slightly modified version of Eq. (19.1):

$$m\frac{d^2x(t)}{dt^2} + 2\beta\sqrt{mk}\frac{dx(t)}{dt} + kx(t) = 0 \qquad (19.3)$$

The solution to this differential equation is a sinusoidal function like the solution to Eq. (19.3), but has an amplitude which decays to zero exponentially:

$$x(t) = Ae^{-\beta\omega_n t}\sin(\omega_d t + \phi) + \Delta_o \qquad (19.4)$$

In Eq. (19.4), **ωd** is the damped frequency which has units of rad/s. It is related to the natural frequency, **ωn**, by the following equation:

$$\omega_d = \omega_n\sqrt{1-\beta^2} \qquad (19.5)$$

Note: In civil structures, typical values of β range from 0 to 0.05 (5%). Mechanical systems, like vehicles or other equipment, may have damping ratios which are 1.0 or greater.

Note: The derivation of the differential equation and its solution are beyond the scope of CIV102. This material will be covered in future physics and dynamics courses.

In civil structures, the value of β is usually very low, resulting in **ωd** being essentially the same as **ωn**. The response described by Eq. (19.4) is shown in Fig. (19.2), where it can be seen that the amplitude of vibration gradually dies out and the mass eventually settles at x = Δ_o.

Forced Oscillation

In the previous scenarios, the spring-mass system was freely vibrating without the influence of an externally applied dynamic load. In reality, structures may be subjected to dynamic loading due to the movement of people crossing over a bridge or the vibrations caused by an earthquake. The simplest form of dynamic loading is when the system is subjected to harmonic or sinusoidal load with amplitude **F$_o$** and loading frequency **ω** in rad/sec (or ***f*** in cycles per second):

$$F(t) = F_o\sin\omega t \qquad (19.6)$$

Substituting this loading into the dynamic equilibrium equation for a damped oscillator results in the following differential equation:

$$m\frac{d^2x(t)}{dt^2} + 2\beta\sqrt{mk}\frac{dx(t)}{dt} + kx(t) = F_o\sin\omega t \qquad (19.7)$$

The complete solution to Eq. (19.7) is complex and beyond the scope of CIV102. It is composed of two parts: a ***transient*** component, which describes the behaviour shortly after the loading is first applied, and a ***steady state*** component, which describes the response of the system after it has settled into a rhythmic pattern. The steady state solution, which is particularly relevant for design, is shown below:

$$x(t) = DAF \times \frac{F_o}{k}\sin(\omega t + \phi) + \Delta_o \qquad (19.8)$$

In Eq. (19.8), the **DAF** is a ***Dynamic Amplification Factor***, which is calculated as:

$$DAF = \frac{1}{\sqrt{\left(1-\left(\frac{f}{f_n}\right)^2\right)^2 + \left(\frac{2\beta f}{f_n}\right)^2}} \qquad (19.9)$$

The response of a vibrating system when subjected to time-varying loads is strongly influenced by the ratio of the driving frequency, ***f***, and the natural frequency of the system, ***f$_n$***, as it influences both the frequency of the resulting displacement and the amplitude of the response through the DAF. To illustrate this, Fig. 19.3 shows the response of a system when subjected to the same load but at different frequencies. The plot on the left shows a minor reduction in amplitude for a driving frequency which is much higher than the natural frequency, while the plot on the right shows a major increase in amplitude when the driving frequency is about half of the natural frequency.

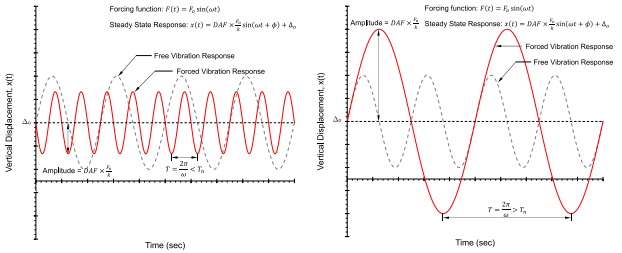

Fig. 19.3 – Forced oscillation for *f*/*f$_n$* = 2.5 (left) and *f*/*f$_n$* = 0.5 (right). Note the influence of the driving frequency on the amplitude of vibration.

A plot showing the influence of *f*/*f$_n$* on the Dynamic Amplification Factor is shown in Fig. 19.4. The first thing which should be noted is that the highest value of the DAF is when the driving frequency is approximately equal to the natural frequency – this is commonly noted as ***resonance.*** The second observation is that increasing the amount of damping in the system tends to reduce the amplification, especially the peak value at resonance. Finally, the DAF is equal to 1 when *f*/*f$_n$* is equal to zero, and gradually becomes 0 when the ratio *f*/*f$_n$* becomes large.

Designing for Dynamic Effects

Although calculating the complete response of a structure under dynamic loads is necessary in certain situations, in most cases it is sufficient to only check the if maximum stresses which result do not cause the structure to fail due to buckling or yielding. This can be done by calculating the effective static loading which produces the same effect on the structure as the dynamic loads.

Consider a set of dynamic loads, **w$_{total}$**, which has the following form:

$$w_{\text{total}} = w_{\text{stationary}} + w_o\sin(\omega t) \qquad (19.10)$$

In Eq. (19.10), **w$_{stationary}$** refers to the component of the loading which does not vary in time, like the dead load of the structure and the weight of the people as they stand on the structure. The amplitude of the loading is **w$_o$**, which could represent the impact loading on the bridge due to the crowd of people walking around, and the frequency of the impact loading is **ω** rad/sec (or ***f*** = ω/2π cycles/sec). Sample values of these terms for a single person as they walk are shown in Fig. 19.5.

Note: w may be an area loading in kPa, a line load in kN/m, or a collection of joint loads in kN.

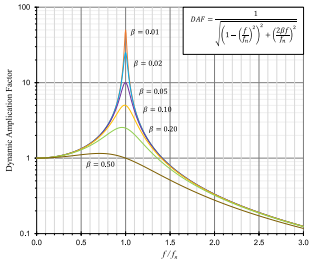

Fig. 19.4 – Influence of *f*/*f$_n$* on the DAF for various values of β.

Using Eq. (19.8), the equivalent static load, **w$_{eq}$**, is equal to the stationary component of the loading plus an amplified dynamic component. The amplified dynamic component is obtained by taking the amplitude of loading, **w$_o$**, and multiplying it by the Dynamic Amplification Factor to consider the interaction between the frequency of loading and the natural frequency, which results in the following:

$$w_{eq} = w_{\text{stationary}} + DAF \times w_o \qquad (19.11)$$

Evaluating the DAF is a straightforward process once the damping, **β**, and the natural frequency of the structure, ***f$_n$*** are known. Two simple equations for calculating the natural frequency for truss or beam structures are shown below in Table 19.1. Once the equivalent static load has been obtained, then the member forces and stresses can be checked.

Table 19.1 – Simple expressions for calculating f_n for truss or beam structures

	Point Load at Midspan	**Uniformly Distributed Load**
Schematic	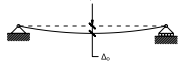	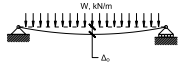
Natural Frequency (Hz)	$f_n = \frac{15.76}{\sqrt{\Delta_o}}$	$f_n = \frac{17.76}{\sqrt{\Delta_o}}$

** Δ_o is the midspan deflection under $w_{stationary}$ in mm.

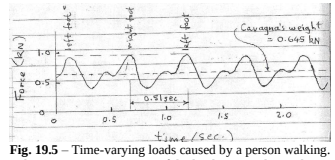

Fig. 19.5 – Time-varying loads caused by a person walking. The stationary component of the load is 0.645 kN with an amplitude of approximately 0.25 kN, occurring at a frequency of approximately 2 hz.

*Note: When designing a pedestrian bridge, **the frequency of loading caused by people walking is typically assumed to be 2 Hz**. Therefore, unless the bridge contains components which can provide significant amounts of damping, having a natural frequency which is close to 2 Hz will lead to large amounts of amplification and may cause the bridge to collapse.*

Lecture 20 – Bending of Beams – Navier's Equation – 1826

Overview

In this chapter, the derivation of Navier's equation for calculating bending stresses in a beam is presented. Relevant section properties are discussed, and the table of standard steel wide flange sections is explained.

Derivation of Navier's Equation

As previously discussed in Lecture 10, when a member is subjected to pure bending by applying a moment to its two ends, it curves to form the arc of a circle. If vertical lines were drawn on the member which are perpendicular to its longitudinal axis, these lines would remain straight as the member curves and point towards a common point. The assumption that those vertical lines – also referred to as plane sections – stay straight is known as the ***plane sections remain plane*** assumption. In Lecture 10, we concluded that this assumption results in the following equation for the longitudinal strain in the member, **ε**, which varies linearly over the height of the member:

$$\varepsilon(y) = \phi y \tag{20.1}$$

In Eq. (20.1), **ϕ** is the curvature in rad/mm and **y** is the vertical distance from the location of interest and the neutral axis of the member. The curvature is a measure of how curved a member is, being defined as the change in the member's slope per unit length, and the neutral axis is the location on the beam which does not experience any change in length as the member bends. These terms are defined in Fig. 20.2.

For a beam made from a linear elastic material, the stress will be related to the strain by the Young's modulus, **E**. Applying Hooke's law to Eq. (20.1) results in the following equation for the stress, which also varies linearly over the height:

$$\sigma(y) = E\phi y \tag{20.2}$$

Consider a differentially small area of the cross section, dA, which is located a distance **y** away from the neutral axis. The stress which it is carrying, **σ(y)**, will result in a differential force **dF(y)** acting through its centroid, which is calculated as:

$$dF(y) = \sigma(y)dA \tag{20.3}$$

This force will also produce a moment about the neutral axis, **dM(y)**:

$$dM(y) = ydF(y) = y\sigma(y)dA \tag{20.4}$$

Eq. (20.3) and (20.4) can be written in terms of the curvature and Young's modulus by using Eq. (20.2), which results in the following:

$$dF(y) = E\phi ydA \tag{20.5}$$

$$dM(y) = E\phi y^2 dA \tag{20.6}$$

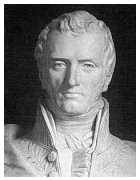

Fig. 20.1 – Bust of Claude-Louis Navier, who made many important contributions to the fields of elasticity and structural mechanics.

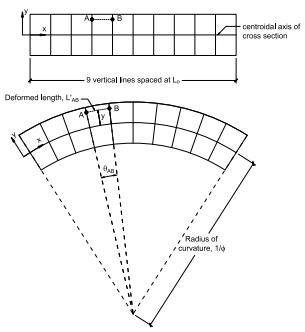

Fig. 20.2 – Figure illustrating Robert Hooke's 1678 hypothesis that when members are subjected to pure bending, "Plane Sections Remain Plane". Reproduced from Fig. 10.1.

Integrating **dF** over the cross-sectional area produces the axial force, **N**, which is carried by the member. When subjected to pure bending, the axial force will be equal to zero, which results in the following equation:

$$N = \int_A E\phi ydA = 0 \tag{20.7}$$

In Eq. (20.7), the **ϕ** is a property of the member and **E** is a constant related to the material; if the member is homogeneous, neither of these quantities will vary over the cross section, and hence they can be removed from the integral. The resulting equation governs the location of the neutral axis when the member is subjected to pure bending, requiring that the ***first moment of area*** taken about the neutral, or centroidal, axis of the member equals zero.

$$0 = \int_A ydA \tag{20.8}$$

If we integrate **dM** in Eq. (20.6) over the cross-sectional area, we will obtain the bending moment which is carried by the member, **M**:

$$M = \int_A E\phi y^2 dA \tag{20.9}$$

We can evaluate Eq. (20.9) by first removing **E** and **ϕ** from the equation like we did to obtain Eq. (20.8). The resulting equation, which we derived in Lecture 10, contains an integral term, the ***second moment of area*** of the cross section, which is abbreviated as **I**:

$$M = E\phi \int_A y^2 dA = EI\phi \tag{20.10}$$

Eq. (20.10) illustrates the fundamental relationship between the bending moment carried by a member, **M**, and the curvature, **ϕ**. Combining Eq. (20.10) with Eq. (20.2) results in another important equation, which is the relationship between the moment and the flexural stresses in the member:

$$\sigma(y) = \frac{My}{I} \tag{20.11}$$

Eq. (20.11) is called ***Navier's Equation***, which allows the flexural stresses in a member with second moment of area, **I**, and carrying a bending moment, **M**, to be calculated. The resulting distribution of flexural stresses caused by bending moments is shown in Fig. 20.3, and a summary of the derivation is shown in Fig. 20.4.

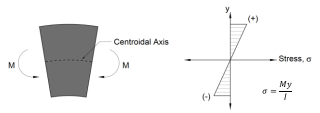

Fig. 20.3 – Distribution of flexural stresses caused by bending moments.

Note: The relationship $M = EI\phi$ was previously derived in Lecture 10.

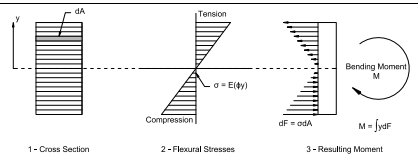

Fig. 20.4 – Summary of how the bending moment carried by a member is determined if the distribution of strains is known from the curvature. Reproduced from Fig. 10.3.

Steel Wide Flange Members

A common type of member used in beams and columns in structures is called a ***wide flange section.*** Wide flange sections are commonly used in members which bend, like in beams, because their shape allows them to carry bending moments very efficiently. The reason for this is because most of their area is concentrated in the flanges, which are located far away from the centroidal axis, which is located at mid-height. Because the second moment of area is calculated by multiplying the area by the square of the distance from the centroidal axis, moving the area away from the neutral axis allows their contribution to **I** to be maximized.

Navier's equation states that the bending stresses vary linearly over the height of the member and are equal to zero at the location of the neutral axis. Because the maximum tensile and compressive stresses occur at the extremities of the member, it is often convenient to simply calculate the stresses on the top and bottom of the beam only. If we define $\mathbf{y_{top}}$ and $\mathbf{y_{bot}}$ as the vertical distance from the neutral axis to the top and bottom of the member respectively, then the largest flexural stresses can be found using the following equations:

$$\sigma_{max,top} = \frac{My_{top}}{I} = \frac{M}{S_{top}} \tag{20.12}$$

$$\sigma_{max,bot} = \frac{My_{bot}}{I} = \frac{M}{S_{bot}} \tag{20.13}$$

In Eq. (20.12) and (20.13), **S** is called the ***section modulus*** and allows the largest flexural stresses at the top and bottom of the member to be calculated in a concise manner. For members having a horizontal axis of symmetry, $\mathbf{S_{top}}$ and $\mathbf{S_{bot}}$ are the same.

Tables 20.1 and 20.2 show the section properties for common types of steel wide-flange sections and sawn timber sections respectively. The relevant properties for bending, **I**, **S** and the radius of gyration **r**, are specified for both the strong axis (x-x) and weak axis (y-y). The strong axis of bending, which refers to the orientation when the flanges of an I-beam are parallel to the centroidal axis, or when the taller dimension for a timber section is the height, typically has substantially higher values of **I**, **S** and **r** compared to when the member is oriented along its weak axis.

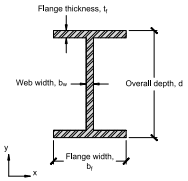

Fig. 20.5 – Steel wide flange beam cross section

Note: Wide-flange sections are often called I-beams when used as beams in buildings and bridges. When inserted into the ground to support structures built above, they are sometimes called H-piles.

Note: Recall that the radius of gyration is defined as:

$$r = \sqrt{\frac{I}{A}}$$

Table 20.1 – Steel Wide Flange Beam Table

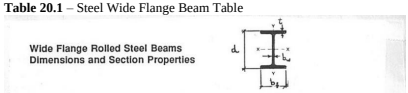

Designation	Dimensions				Dead Load	Area	Strong Axis x-x			Weak Axis y-y			Torsion Constant	Shear Depth
	d	b_f	t	b_w			I_x	S_x	r_x	I_y	S_y	r_y	J	I_x/Q
mm × kg/m	mm	mm	mm	mm	kN/m	mm²	10^6 mm⁴	10^3 mm³	mm	10^6 mm⁴	10^3 mm³	mm	10^3 mm⁴	mm
W920 × 446	933	423	43	24.0	4.38	57000	8470	18200	385	540	2550	97.3	26800	822
× 365	916	419	34	20.3	3.57	46400	6710	14600	380	421	2010	95.3	14400	813
× 313	932	309	34	21.1	3.06	39800	5480	11800	371	170	1100	65.4	11600	806
× 238	915	305	26	16.5	2.33	30400	4060	8880	365	123	806	63.6	5140	796
W840 × 329	862	401	32	19.7	3.23	42000	5350	12400	357	349	1740	91.2	11500	764
× 210	846	293	24	15.4	2.06	26800	3110	7340	341	103	700	62.0	4050	738
× 176	835	292	19	14.0	1.72	22400	2460	5900	331	78.2	536	59.1	2220	722
W760 × 257	773	381	27	16.6	2.52	32800	3420	8840	323	250	1310	87.3	6380	689
× 173	762	267	22	14.4	1.70	22100	2060	5400	305	68.7	515	55.8	2690	663
× 147	753	265	17	13.2	1.44	18700	1660	4410	298	52.9	399	53.2	1560	651
W690 × 217	695	355	25	15.4	2.13	27700	2340	6740	291	185	1040	81.7	4560	618
× 152	688	254	21	13.1	1.49	19400	1510	4380	279	57.8	455	54.6	2200	604
× 125	678	253	16	11.7	1.23	16000	1190	3500	273	44.1	349	52.5	1180	594
W610 × 195	622	327	24	15.4	1.91	24900	1680	5400	260	142	871	75.5	3970	554
× 155	611	324	19	12.7	1.51	19700	1290	4220	256	108	666	74.0	1950	545
× 125	612	229	20	11.9	1.22	15900	985	3220	249	39.3	343	49.7	1540	537
× 101	603	228	15	10.5	0.99	13000	764	2530	242	29.5	259	47.6	781	527
W530 × 182	551	315	24	15.2	1.78	23100	1240	4480	232	127	808	74.1	3740	492
× 150	543	312	20	12.7	1.47	19200	1010	3710	229	103	659	73.2	2160	487
× 109	539	211	19	11.6	1.06	13900	667	2480	219	29.5	280	46.1	1260	471
× 82	528	209	13	9.5	0.81	10500	479	1810	214	20.3	194	44.0	530	463
W460 × 144	472	283	22	13.6	1.41	18400	726	3080	199	83.6	591	67.4	2440	421
× 97	466	193	19	11.4	0.95	12300	445	1910	190	22.8	237	43.1	1130	408
× 82	460	191	16	9.9	0.80	10400	370	1610	189	18.6	195	42.3	691	404
× 61	450	189	11	8.1	0.60	7760	259	1150	183	12.2	129	39.7	289	395
W410 × 114	420	261	19	11.6	1.12	14600	462	2200	178	57.2	439	62.6	1490	376
× 74	413	180	16	9.7	0.73	9550	275	1330	170	15.6	173	40.4	637	364
× 60	407	178	13	7.7	0.58	7580	216	1060	169	12.0	135	39.8	328	363
× 39	399	140	9	6.4	0.38	4990	127	634	160	4.0	57.7	28.5	111	348
W360 × 314	399	401	40	24.9	3.07	39900	1100	5530	166	426	2120	103	18500	345
× 122	363	257	22	13.0	1.19	15500	365	2010	153	61.5	478	63.0	2100	322
× 79	354	205	17	9.4	0.78	10100	227	1280	150	24.2	236	48.9	814	317
× 64	347	203	14	7.7	0.63	8140	176	1030	148	18.8	186	48.1	438	312
× 45	352	171	10	6.9	0.44	5730	122	691	146	8.18	95.7	37.8	160	313
× 33	349	127	8	5.8	0.32	4170	82.7	474	141	2.91	45.8	26.4	85.9	305
W310 × 253	356	319	40	24.4	2.48	32200	682	3830	146	215	1350	81.7	14800	304
× 118	314	307	19	11.9	1.15	15000	275	1750	135	90.2	588	77.5	1600	282
× 79	306	254	15	8.8	0.77	10100	177	1160	132	39.9	314	62.9	657	277
× 60	303	203	13	7.5	0.59	7590	129	849	130	18.3	180	49.1	397	274
× 39	310	165	10	5.8	0.38	4940	85.1	549	131	7.27	88.1	38.4	126	279
× 21	303	101	6	5.1	0.21	2690	37.0	244	117	0.983	19.5	19.1	29.4	258
W250 × 115	269	259	22	13.5	1.12	14600	189	1410	114	64.1	495	66.3	2130	236
× 49	247	202	11	7.4	0.48	6250	70.6	572	106	15.1	150	49.2	241	223
× 33	258	146	9	6.1	0.32	4170	48.9	379	108	4.73	64.7	33.7	98.5	231
W200 × 59	210	205	14	9.1	0.58	7560	61.1	582	89.9	20.4	199	51.9	465	187
× 36	201	165	10	6.2	0.35	4580	34.4	342	86.7	7.64	92.6	40.8	146	181
× 27	207	133	8	5.8	0.26	3390	25.8	249	87.2	3.30	49.6	31.2	71.3	185
W150 × 30	157	153	9	6.6	0.29	3790	17.2	219	67.4	5.56	72.6	38.3	101	141
× 14	150	100	6	4.3	0.13	1730	6.87	91.5	63.0	0.92	18.4	23.0	17.0	133

Note: The Torsion Constant will not be used in CIV102. The Shear Depth will be discussed when shear stresses are introduced in Lecture 25.

Table 20.2 – Sawn Timber Section Table

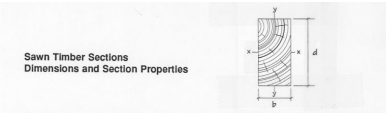

Size and Designation $b \times d$	Nominal Dimensions	Dead Load	Area	Strong Axis x-x			Weak Axis y-y			Torsion Constant
				I_x	S_x	r_x	I_y	S_y	r_y	J
mm	in.	kN/m	mm^2	$10^6\ mm^4$	$10^3\ mm^3$	mm	$10^6\ mm^4$	$10^3\ mm^3$	mm	$10^6\ mm^4$
292 × 495	12 × 20	0.907	145000	2950	11900	143	1030	7030	84.3	2570
× 445	× 18	0.816	130000	2140	9640	129	923	6320	84.3	2190
× 394	× 16	0.722	115000	1490	7550	114	817	5600	84.3	1760
× 343	× 14	0.629	100000	982	5730	99.0	712	4870	84.3	1370
× 292	× 12	0.535	85300	606	4150	84.3	606	4150	84.3	1030
241 × 495	10 × 20	0.749	119000	2440	9840	143	577	4790	69.9	1600
× 445	× 18	0.673	107000	1770	7950	129	519	4310	69.6	1360
× 394	× 16	0.596	95000	1230	6240	114	460	3810	69.6	1130
× 343	× 14	0.519	82700	810	4730	99.0	400	3320	69.6	900
× 292	× 12	0.442	70400	500	3420	84.3	341	2830	69.6	671
× 241	× 10	0.365	58100	281	2330	69.6	281	2330	69.6	476
191 × 495	8 × 20	0.594	94600	1930	7800	143	287	3010	55.1	868
× 445	× 18	0.534	85000	1400	6300	129	258	2710	55.1	751
× 394	× 16	0.472	75300	974	4940	114	229	2400	55.1	636
× 343	× 14	0.411	65500	642	3750	99.0	199	2090	55.1	515
× 292	× 12	0.350	55800	396	2710	84.3	170	1780	55.1	403
× 241	× 10	0.289	46000	223	1850	69.6	140	1470	55.1	285
× 191	× 8	0.229	36500	111	1160	55.1	111	1160	55.1	188
140 × 445	6 × 18	0.391	62300	1030	4620	129	102	1450	40.4	325
× 394	× 16	0.346	55200	714	3620	114	90.1	1290	40.4	279
× 343	× 14	0.301	48000	471	2750	99.0	78.4	1120	40.4	232
× 292	× 12	0.257	40900	290	1990	84.3	66.8	954	40.4	186
× 241	× 10	0.212	33700	163	1360	69.6	55.1	787	40.4	139
× 191	× 8	0.168	26700	81.3	851	55.1	43.7	624	40.4	94.9
× 140	× 6	0.123	19600	32.0	457	40.4	32.0	457	40.4	54.2
89 × 387	4 × 16	0.216	34400	430	2220	112	22.7	511	25.7	77.5
× 337	× 14	0.188	30000	284	1680	97.3	19.8	445	25.7	65.9
× 286	× 12	0.160	25500	174	1210	82.6	16.8	378	25.7	53.8
× 235	× 10	0.131	20900	96.3	819	67.8	13.8	310	25.7	41.9
× 184	× 8	0.103	16400	46.2	502	53.1	10.8	243	25.7	30.1
× 140	× 6	0.078	12500	20.4	291	40.4	8.22	185	25.7	19.8
× 114	× 5	0.064	10200	11.0	193	32.9	6.70	151	25.7	13.8
× 89	× 4	0.050	7920	5.23	118	25.7	5.23	117	25.7	8.85
64 × 337	3 × 14	0.135	21600	204	1210	97.3	7.36	230	18.5	25.8
× 286	× 12	0.115	18300	125	872	82.6	6.25	195	18.5	21.4
× 235	× 10	0.094	15000	69.2	589	67.8	5.13	160	18.5	17.0
× 184	× 8	0.074	11800	33.2	361	53.1	4.02	126	18.5	12.5
× 140	× 6	0.056	8960	14.6	209	40.4	3.06	95.6	18.5	8.68
× 114	× 5	0.046	7300	7.90	139	32.9	2.49	77.8	18.5	6.41
× 89	× 4	0.036	5700	3.76	84.5	25.7	1.94	60.8	18.5	4.29
38 × 337	2 × 14	0.071	12800	121	719	97.3	1.54	81.1	11.0	5.72
× 286	× 12	0.060	10900	74.1	518	82.6	1.31	68.8	11.0	4.79
× 235	× 10	0.049	8930	41.1	350	67.8	1.07	56.6	11.0	3.87
× 184	× 8	0.038	6990	19.7	214	53.1	0.84	44.3	11.0	2.91
× 140	× 6	0.029	5320	8.69	124	40.4	0.64	33.7	11.0	2.11
× 114	× 5	0.024	4330	4.69	82.3	32.9	0.52	27.4	11.0	1.65
× 89	× 4	0.019	3380	2.23	50.2	25.7	0.41	21.4	11.0	1.19
× 64	× 3	0.013	2430	0.83	25.9	18.5	0.29	15.4	11.0	0.73
× 38	× 2	0.008	1440	0.17	9.15	11.0	0.17	9.15	11.0	0.29

Lecture 21 – Calculation of Flexural Stresses

Overview

In this chapter, methods used to analyze the bending behaviour of more complex shapes are introduced. For these members, Navier's equation is still capable of determining the flexural stresses, but the location of the centroid and the second moment of area must be determined first.

Calculation of the Centroidal Axis

The centroidal axis, or neutral axis, is a key geometric property of a member when subjected to bending moments because other properties, like the second moment of area **I**, or the section modulus **S**, are calculated based on its location. For this reason, locating the centroidal axis is typically the first task done when approaching a bending problem. Recall from Lecture 20 that if the variable **y** is defined as the vertical distance between a point on the cross section and the neutral axis, then the following is true for members subjected to pure bending and no axial force:

$$0 = \int_A y dA \tag{21.1}$$

When performing calculations, we typically do not evaluate this integral analytically. A more convenient procedure is to instead break up the cross section into various simple shapes, and replace the integral with an algebraic sum:

$$0 = \int_A y dA = \sum_{i=1}^{n} y_i A_i \tag{21.2}$$

In Eq. (21.2), the cross section has been broken up into **n** discrete area components, $\mathbf{A_i}$, and $\mathbf{y_i}$ is the vertical distance from the local centroid of the area component and the centroidal axis of the overall cross section. This is shown in Fig. 21.1.

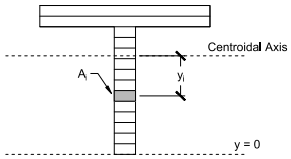

Fig. 21.1 – Definitions of A_i and y_i for evaluating the first moment of area using Eq. (21.2).

Note: If $\mathbf{y_i}$ is the distance from the centroid of the area component $\mathbf{A_i}$ to the centroidal axis of the whole cross section, then the summation term is an exact representation of the integral equation in Eq. (21.1).

Although Eq. (21.2) can be used to verify if the location of the centroidal axis has been correctly determined, it is less useful for actually determining where that axis is. The equation can be repurposed to solve for the location of the centroidal axis relative to the base of the cross section, $\bar{\mathbf{y}}$, using the following coordinate transformation:

$$y_i = \bar{y} - y_{i,b} \tag{21.3}$$

In Eq. (21.3), $\mathbf{y_{i,b}}$ is the vertical distance between the base of the cross section and the centroid of the area of interest. These various definitions of **y** are shown in Fig. 21.2. Substituting Eq. (21.3) into Eq. (21.2) results in the following:

$$0 = \sum_{i=1}^{n} (\bar{y} - y_{i,b}) A_i \tag{21.4}$$

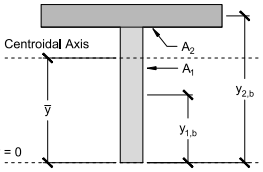

Fig. 21.2 – Definitions of terms used to calculate the location of the centroidal axis using Eq. (21.6).

Expanding the term in brackets and rearranging produces the following result:

$$\sum_{i=1}^{n} \bar{y} A_i = \sum_{i=1}^{n} y_{i,b} A_i \tag{21.5}$$

Finally, by recognizing that $\bar{\mathbf{y}}$ is a constant, we can remove it from the summation term on the left-hand side of the equation, giving us a direct equation to obtain the location of the centroidal axis:

$$\bar{y} = \frac{\sum_{i=1}^{n} y_{i,b} A_i}{\sum_{i=1}^{n} A_i} = \frac{1}{A} \sum_{i=1}^{n} y_{i,b} A_i \tag{21.6}$$

In Eq. (21.6), **A** is the total area of the cross section. An example of using Eq. (21.6) to obtain the centroidal axis of the shape shown in Fig. 21.2 is shown below:

$$\bar{y} = \frac{y_{1,b} A_1 + y_{2,b} A_2}{A_1 + A_2} \tag{21.7}$$

Calculating I for Complex Shapes: Parallel Axis Theorem

The second moment of area, **I**, is defined by Eq. (21.8) shown below, where **y** is the vertical distance measured from the centroidal axis of the cross section, and **A** is the area of the cross section:

$$I = \int_A y^2 dA \tag{21.8}$$

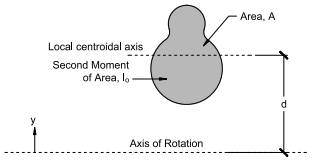

Fig. 21.3 – Schematic of a body rotating around an axis which is not its own local centroidal axis.

When calculating **I** for simple shapes, such as a rectangle or circle, Eq. (21.8) can be explicitly evaluated, resulting in the simple equations shown in Table 21.1. However, structural members often assume more complex shapes whose values of **I** cannot be easily determined by using Eq. (21.8) directly.

A convenient way of calculating **I** for more complex geometries is to first break up the cross section into **n** smaller components and determine their inertia about the global centroidal axis, $\mathbf{I_i}$. The value of **I** of the cross section is then the sum of these individual components:

$$I = \sum_{i=1}^{n} I_i \tag{21.9}$$

When evaluating Eq. (21.9), the equations for $\mathbf{I_o}$ of rectangles and circles in Table 21.1 cannot be used directly because they are the second moments of area about the *local* centroidal axes of the shapes. This is different from $\mathbf{I_i}$, which are the second moments of area about the *global* centroidal axis of the cross section. If the local centroid of the subcomponent area, $\mathbf{A_i}$ is a distance $\mathbf{d_i}$ from the axis of rotation like in the situation shown in Fig. 21.3, then Eq. (21.8) can be re-written as:

$$I_i = \int_{A_i} (y + d_i)^2 dA \tag{21.10}$$

Expanding the terms in brackets results in the following:

$$I_i = \int_{A_i} y^2 + 2 d_i y + d_i^2 dA = \int_{A_i} y^2 dA + \int_{A_i} 2 d_i y dA + \int_{A_i} d^2 dA \tag{21.11}$$

In Eq. (21.11), the first integral term is the second moment of area of the component if interest about its local centroidal axis, which we will define as $\mathbf{I_{o,i}}$. For the second and third integrals, the distance $\mathbf{d_i}$ is not a function of the area and

Table 21.1 – Equations for I_o for simple shapes

	Rectangle	Circle
Shape	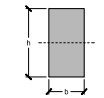	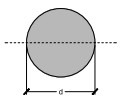
I_o	$I_o = \frac{bh^3}{12}$	$I_o = \frac{\pi d^4}{64}$

can hence be moved outside of the integrals. The second term will then equal to zero, due to Eq. (21.1), which results in the following equation:

$$I_i = I_{o,1} + A_i d_i^2 \tag{21.12}$$

Eq. (21.12) is called the ***Parallel Axis Theorem*** and allows the second moment of area of a shape to be calculated about an axis of rotation which is parallel to its local centroidal axis. If the Parallel Axis Theorem is applied to each of the **n** subcomponents of the cross section, the second moment of area of the whole section can be calculated as:

$$I = \sum_{i=1}^{n} I_i = \sum_{i=1}^{n} (I_{o,i} + A_i d_i^2) \tag{21.13}$$

Fig. 21.4 shows an area as it rotates about an axis which is not aligned with its local centroidal axis. The total movement involves (1) its translation around the axis of rotation along a circular path, and (2) its rotation about its own centroid. Its total inertia is therefore the sum of its inertia against local rotation, $\mathbf{I_{o,i}}$, and its resistance to being translated around the global axis, which is represented by the $\mathbf{A_i d_i^2}$ term.

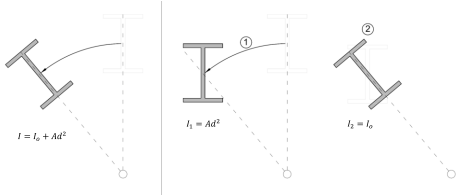

Fig. 21.4 – Illustration of the various displacements associated with the terms in the Parallel Axis Theorem.

Calculating I for Members with a Horizontal Axis of Symmetry

Many common structural shapes, like the hollow tube and I-beam shown in Fig. 21.5, have a horizontal axis of symmetry. This can be used to calculate **I** in a more convenient manner than using Eq. (21.13) by taking advantage of the fact that the $\mathbf{I_i}$ terms in Eq. (21.9) may be positive or negative. This is illustrated for the hollow tube in Fig. 21.5, where **I** is equal to second moment area of a solid rectangle defined by its outside dimensions minus the second moment of area of a solid rectangle defined by its inside dimensions. Likewise, for the I-beam, **I** can be easily found by subtracting the second moment of area of the inner rectangles from the second moment of area of a solid rectangle defined by the overall height and flange width.

Note: Directly adding and subtracting components is only possible if they share a common centroidal axis. If a component which is being added or subtracted has a different centroidal axis, the Parallel Axis Theorem must be applied.

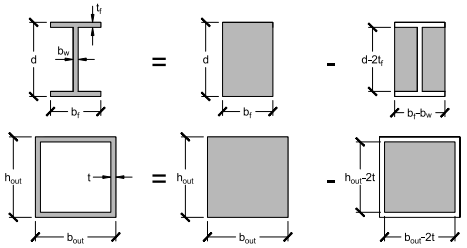

$$I = I_{out} - I_{in}$$

Shape	I_{out}	I_{in}
I beam	$I_{out} = \frac{b_f d^3}{12}$	$I_{in} = \frac{(b_f - b_w)(d - 2t_f)^3}{12}$
Hollow tube	$I_{out} = \frac{b_{out} h_{out}^3}{12}$	$I_{in} = \frac{(b_{out} - 2t)(h_{out} - 2t)^3}{12}$

Fig. 21.5 – Calculation of I for I beams and hollow sections by using horizontal symmetry.

Summary

When approaching a problem involving flexure, the location of the centroidal axis, $\bar{y}$, and the second moment of area, I, must be determined in order to calculate other relevant parameters like the stresses, strains and curvature. The suggested procedure is as follows:

i. Break up the cross section in to simple shapes with area $\mathbf{A_i}$ and whose local centroids are a distance $\mathbf{y_{i,b}}$ from the bottom of the member.
ii. Determine the location of the centroidal axis relative to the bottom of the member, $\bar{y}$, using Eq. (21.6), which is reproduced below:

$$\bar{y} = \frac{1}{A}\sum_{i=1}^{n} y_{i,b} A_i$$

iii. Calculate the distances between the local centroids of the component areas, and the centroidal axis of the global cross section, $\mathbf{d_i}$.
iv. Using the Parallel Axis Theorem, calculate the second moment of area, **I**, using Eq. (21.13), which is reproduced below:

$$I = \sum_{i=1}^{n} I_{o,i} + A_i d_i^2$$

Lecture 22 – Shear Force Diagrams and Bending Moment Diagrams

Overview:

Having introduced the equations which allow the flexural stresses to be calculated if the bending moment carried by the section is known, the concept of stress resultants is presented in this chapter. The relevant methods for calculating the axial load, shear force, and bending moment diagrams for loaded members is presented.

Stress Resultants

Consider the simply supported beam shown in Fig. 22.1 which is carrying a variety of horizontal and vertical loads and transmitting them to the supports. As we saw earlier in the course where a wire transmitted a tension force by carrying internal stresses, this member will also be carrying substantial internal forces. These internal forces, which are called ***stress resultants***, can be found by drawing a free body diagram which cuts the member through a point of interest.

Note: The procedure of cutting through the member to determine the stress resultants is analogous to using the Method of Sections to determine the member forces in a truss.

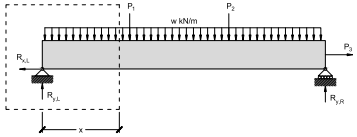

Fig. 22.1 – Simply supported beam subjected to arbitrary loading conditions.

Fig. 22.2 shows a free body diagram of a portion of the larger beam which has been cut at a distance **x** away from the left support. In order to satisfy horizontal, vertical, and rotational equilibrium, it must carry internal horizontal and vertical forces, as well as a moment at the location of the cut. The horizontal force which is parallel to its longitudinal axis is called the ***axial load***, **N**, the vertical force which is perpendicular to the longitudinal axis is called the ***shear force***, **V**, and the moment is called the ***bending moment***, **M**.

Note: The shear force is obtained by integrating the shear stresses carried by the member. Shear stresses will be discussed in more detail in Lecture 25.

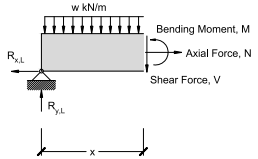

Fig. 22.2 – Section cut of member, revealing stress resultants N, V and M.

Applying the equilibrium equations to the free body diagrams allows these stress resultants to be directly calculated in terms of the applied loads and the reaction forces. If the free body diagram in Fig. 22.2 is valid from x = 0 until just before the first downwards point load from the left, then the stress resultants can be calculated to be:

$$\sum F_x = 0 \rightarrow N = R_{x,L} \tag{22.1}$$

$$\sum F_y = 0 \rightarrow V = R_{y,L} - wx \tag{22.2}$$

$$\sum M_o = 0 \rightarrow M = R_{y,L}x - (wx)\left(\frac{1}{2}x\right) \tag{22.3}$$

As seen from Eqs. (22.1) to (22.3), the stress resultants generally change along the length of the member, based on the loading. In structural engineering, we typically use diagrams to show the change in the axial load, shear force and bending moment along the member instead of using mathematical representations like in the equations above.

As noted in earlier lectures, the stresses carried by the material are related to the stress resultants; knowing how the values of **N**, **V** and **M** vary along the entire member is necessary to determine when it will fail or to design it to safely carry the applied loads.

Shear Force Diagrams

The shear force diagram represents the net vertical force which is carried by a horizontal member at a given location and can be obtained once the reaction forces are known. The shear force is related to the vertical loads applied to the structure, **w(x)** by the following relationship:

$$w(x) = \frac{d}{dx}V(x) \tag{22.4}$$

Note: The sign convention for Eq. (22.4) and (22.5) is that loads which act upwards will cause the shear force to become more positive and loads which act downwards will cause the shear force to become more negative.

According to Eq. (22.4), the change in the shear force at a given location is equal to the loading which is applied at to the member to that section. From this we can conclude that a uniformly distributed load would cause the shear force to vary linearly over the length, and a concentrated point load would cause a sudden change in the shear force diagram. Using the Fundamental Theorem of Calculus, the change in the shear force between two points along the member which are subjected to the loading **w(x)** can be calculated as:

$$\Delta V_{AB} = V_B - V_A = \int_A^B w(x)dx \tag{22.5}$$

Eq. (22.5) provides a means to calculate the shear force at any point along the member based on the given loading. Taking point A as the left side of the member where x = 0 and choosing point B as an arbitrary location which is x away from point A, then Eq. (22.5) can be used to find the shear force at any location along the member using the following heuristic:

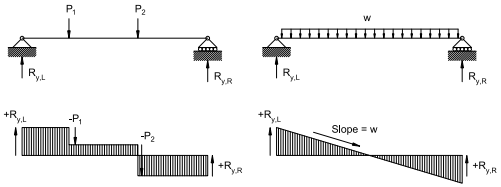

Fig. 22.3 – Examples of obtaining the shear force diagram using the reaction forces and applied loads.

The shear force in the member at a given location is the cumulative sum of the vertical forces applied to the member from the left end of the member to the location of interest.

Note: this heuristic can also be applied by using the right side of the member as the starting point instead of the left side.

Fig. 22.3 illustrates the application of Eq. (22.4) and (22.5) to draw the shear force diagrams for two simple structures. As a consequence of Eq. (22.4), the shear force has sudden jumps at locations where there is a concentrated reaction force or load, as seen in the left example. In the right example, the beam is carrying a uniformly distributed load, which results in the shear force decreasing linearly along the length of the beam. For both examples, the shear force diagram returns to zero at the right-hand side, indicating that the sum of the vertical forces over the entire member equals zero and the member is in vertical equilibrium.

Bending Moment Diagrams

The bending moment diagram is related to the shear force diagram by the following relationship:

$$V(x) = \frac{d}{dx}M(x) \tag{22.6}$$

Note: According to this definition, regions of high shear correspond to "steep" portions on the bending moment diagram, where the moment changes quickly. Regions of low shear correspond to comparatively "flat" portions on the bending moment diagram, where the moment stays approximately the same.

Eq. (22.6) states that the change in moment at a given section is equal to the shear force carried by the member at that location. In regions where there are large shear forces, the moment will change rapidly. Because the shear force is the derivative of the bending moment, a constant shear of V = 0 will cause the moment diagram to be constant, a constant nonzero shear force will cause the bending moment diagram to vary linearly, and a linearly varying shear force will cause the bending moments to vary quadratically. Using the Fundamental Theorem of Calculus, the change in moment, **ΔM**, between two points can then be related to the shear force, **V(x)**, according to the following equation:

$$\Delta M_{AB} = M_B - M_A = \int_A^B V(x)dx \tag{22.7}$$

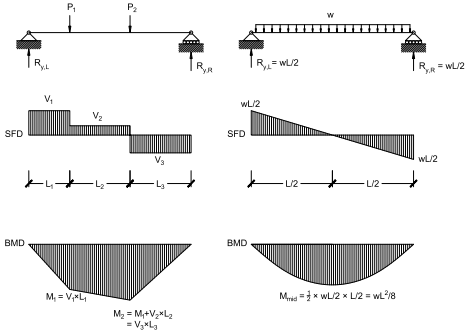

Fig. 22.4 – Examples of obtaining bending moment diagram using the shear force diagram.

Eq. (22.7) states that the change in moment between two points, A and B, is equal to the area underneath the shear force diagram between these locations. Therefore, if the moment is known at the ends of the member, then the moment at any location can be computed using Eq. (22.7) once the shear force diagram has been drawn.

Fig. 22.4 shows the same structures analyzed in Fig. 22.3 and the corresponding shear force diagrams and bending moment diagrams. For the structure on the left, the bending moment diagram is a series of connected lines because the shear force is constant between the applied loads. The change in moment between points is also equal to the area under the shear force diagram between them. For the uniformly distributed beam on the right, the bending moment diagram follows the shape of a parabola because the shear for diagram is linearly varying. Near the supports where the shear force is high, the slope of the bending moment diagram is also high, and at the midspan, where the shear force is equal to zero, the slope of the moment diagram is equal to zero, indicating that it has reached its maximum value. For both structures, the bending moment diagram begins at zero on the left-hand side and returns to zero at the right-hand side, indicating that the sum of moments over the member equals to zero, and the member is in rotational equilibrium.

Note: This condition where the moment equals zero over a support is only true if the ends of the structure are supported by a pin or roller. In general, the moment will not equal to zero over a pin or roller support if the support is located at an intermediate location.

Note: The bending moment at the location of an internal hinge is equal to zero because the hinge will freely rotate if it tries to carry a moment.

Sign Convention

Determining the sign of the shear force diagram and the bending moment diagram can be non-intuitive at first. Fig. 22.5 shows the sign convention for shear force; a general heuristic is that upwards-acting forces induce positive shear forces into the member, while downwards-acting forces induce negative shear forces into the member.

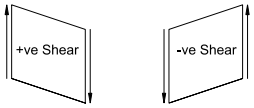

Fig. 22.5 – Sign convention for shear force.

The sign convention for bending moments is shown in Fig. 22.6. Positive moment (which is unintuitively drawn below the axis on a bending moment diagram) corresponds to regions where the bottom of the member is in tension, and negative moment (drawn above the axis) corresponds to regions where the top of the member is in tension. When determining the bending moment diagram from the shear force diagram, a useful heuristic is to note that positive shear results in positive moment (which goes downwards on the bending moment diagram), whereas negative shear results in negative moment (which goes upwards on the bending moment diagram).

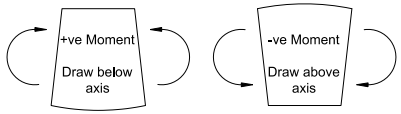

Fig. 22.6 – Sign convention for bending moments.

Lecture 23 – Deflection of Beams: Moment Area Theorems

Overview

Like trusses, obtaining the deformed geometry of a member which is bending can require very complex calculations. In this chapter, the Moment Area Theorems, which permit the deflection of beams to be obtained in a relatively straightforward manner, are presented.

Curvature Diagram

When working on a problem involving beams, the reaction forces, shear force diagram, and bending moment diagram are typically obtained first. Using these diagrams, the flexural stresses can then be calculated once the relevant section properties, like the location of the centroidal axis and the second moment of area, are known. All of this information is necessary to begin calculating qualities relating the deformed shape of the member, like its displacement and slope, at key points of interest.

The curvature of a member, $\boldsymbol{\phi}$, is related to the bending moment, **M**, and the flexural stiffness, **EI**, at any given point by the following equation:

$$\phi = \frac{M}{EI} \tag{23.1}$$

The curvature at every point can be calculated using the bending moment diagram and the flexural stiffness, producing a corresponding ***curvature diagram***.

Moment Area Theorem #1

Recall that the curvature of a member is a measure of how bent it is, and is defined as the change in slope, **θ**, per unit length along the member:

$$\phi = \frac{d\theta}{dx} \tag{23.2}$$

Using the Fundamental Theorem of Calculus, the change in slope between two points, $\boldsymbol{\Delta\theta_{AB}}$, is therefore defined as the integral of the curvature between points A and B. This is mathematically defined in Eq. (23.3) below and represents the area underneath the curvature diagram between the two points.

$$\Delta\theta_{AB} = \theta_B - \theta_A = \int_A^B \phi(x)dx \tag{23.3}$$

Eq. (23.3) is the first Moment Area Theorem, which states:

> ***The change in slope between any two sections of a deflected beam is equal to the area under the curvature diagram between those two sections.***

The first Moment Area Theorem allows us to obtain the slope at any location using the curvature diagram if the slope is already known at some point along the member. This is illustrated in Fig. 23.1.

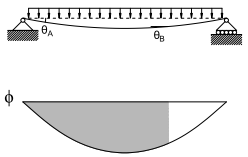

Fig. 23.1 – Summary of Moment Area Theorem #1

Moment Area Theorem #2

Careful integration of the curvature diagram can also be useful for calculating the displaced shape of a member. Consider the curved member shown in Fig. 23.2 which has two points, D and T, defined. Points D and T are located at arbitrary distances x_D and x_T from the origin respectively in the horizontal direction.

Note: Displacements can be obtained by drawing a slope diagram using Eq. (23.3) and then integrating it to find a complete profile of the displaced shape of the member. However, this process is difficult to do analytically except for very simple geometries and loading conditions.

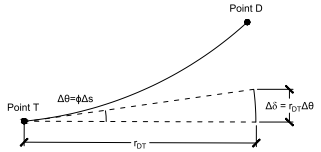

Fig. 23.2 – Curved member used to derive Moment Area Theorem #2.

Consider a small length of the beam, **Δs**, which is located at point T. The curvature at this location is equal to $\phi(x_T)$. If **Δs** is a short distance, then the change in slope of the beam between x = x_T and x = x_T - ds is approximately equal to the following:

$$\Delta\theta(x = x_T) \cong \phi(x_T)\Delta s \tag{12.4}$$

Fig. 23.2 shows this change in angle at point T. If we define the distance $\mathbf{r_{DT}}$ as the distance between point T and a location directly below point D which is measured along the tangent to point T, then the arc length swept by this tangent, **Δδ**, over the angle **Δθ** is equal to:

$$\Delta\delta = r_{DT}\Delta\theta(x = x_T) \cong r_{DT}\phi(x_T)\Delta s \tag{12.5}$$

In structural engineering, members tend to have relatively small curvatures and associated displacements. This allows us to approximate the distance along the member, **Δs**, as a distance in the horizontal direction, **Δx**. Furthermore, the distance along the tangent, $\mathbf{r_{DT}}$, is now the horizontal distance between points D and T, $\mathbf{x_{DT}}$, and **Δδ** becomes a vertical distance **Δy**. These approximations allow Eq. (12.5) to be rewritten as:

$$\Delta y_{DT} = x_{DT}\phi(x_{DT})\Delta x \tag{12.6}$$

Eq. (12.6) represents the vertical distance between a tangent drawn at point T towards point D as the tangent traverses over a small angle **dθ**. The total vertical distance between a tangent drawn at point T and point D for the curved beam, $\boldsymbol{\delta_{DT}}$, can be obtained if we repeat the process for the entire length of the beam between points D and T, resulting in the following integral in the limit where **Δx** goes to zero:

$$\delta_{DT} = \lim_{\Delta x \to 0} \sum x\phi(x)\Delta x = \int_D^T x\phi(x)dx \tag{12.7}$$

The integral term in Eq. (12.7) represents the first moment of the area underneath the curvature diagram between points D and T taken about point D. This quantity can be obtained by multiplying the area under the curvature diagram between points D and T, then multiplying this area by the distance between its centroid and point D, $\bar{x}_{DT}$ .This is mathematically represented using the following equation:

$$\delta_{DT} = \int_D^T x\phi(x)dx = \bar{x}_{DT}\int_D^T \phi(x)dx \tag{12.8}$$

Eq. (12.8) is the second Moment Area Theorem, which is illustrated in Fig. 23.3 and states:

> ***For any two points, called D and T, along the length of a deflected beam, the deviation of point D from the tangent drawn at point T equals the area under the curvature diagram between points D and T, times the distance from the centroid of the diagram to point D (i.e., the first moment of area about point D).***

Although the second Moment Area Theorem does not allow us to directly calculate the displacements of a beam, it is possible to express the desired displacement in terms of tangential deviations, $\boldsymbol{\delta_{DT}}$, which can be calculated using Eq. (12.8). When using the theorem, points D and T must be correctly indicated in order to obtain the desired value:

- D is the location where the tangential deviation is being measured
- T is the location where the tangent is drawn

Based on these definitions, the curvature diagram is integrated between points D and T, and that area is multiplied by the distance between its centroid and point D, the location where the deviation is being measured.

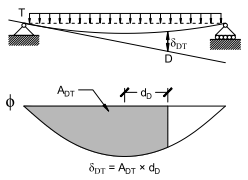

Fig. 23.3 – Summary of Moment Area Theorem #2.

Areas and Centroids of Common Shapes

When using the Moment Area Theorems, the areas and centroids of many different curvature distributions will need to be obtained. Table 23.1 provides a series of simple expressions for the areas and centroids of many common shapes, and is a convenient alternative to analytically integrating the curvature diagram. For distributions which are not shown in the table but can be broken up into **n** simpler subcomponents, the two theorems can be applied by summing of the contributions of the smaller parts to **Δθ** or **δ**. This modifies Eqs. (23.3) and (23.8) to be the following:

$$\Delta\theta_{AB} = \int_A^B \phi(x)dx = \sum_{i=1}^{n}\left[\int \phi(x)dx\right]_i \tag{23.9}$$

$$\delta_{DT} = \int_D^T x\phi(x)dx = \bar{x}_{DT}\int_D^T \phi(x)dx = \sum_{i=1}^{n}\left[\bar{x}\int \phi(x)dx\right]_i \tag{23.10}$$

Table 23.1 – Areas and centroids of common shapes.

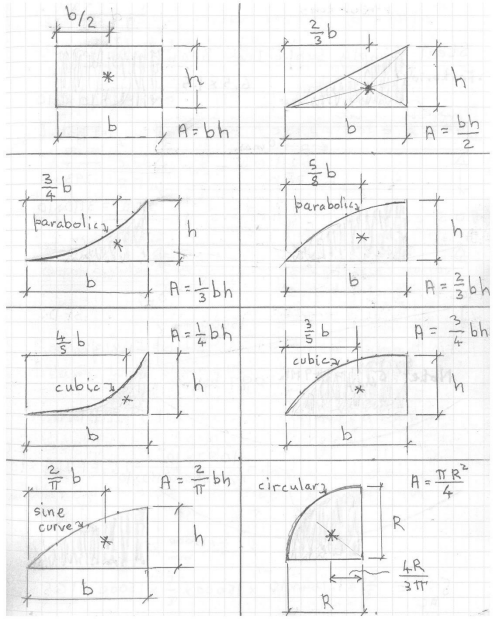

Lecture 24 – Using Moment Area Theorems

Overview:
This chapter demonstrates how to use the Moment Area Theorems presented in Lecture 23 to solve for displacements and rotations in simple structures under common loading situations.

General Procedure
In addition to being designed for strength structures must also have adequate stiffness so they do not experience unreasonable deformations when carrying loads. Two measures of a member's deformation are its slope, **θ**, and how much it has displaced from its original position, **Δ**.

The two Moment Area Theorems introduced in Lecture 23 provide the means to obtain quantities related to the displaced shape of a loaded member. The first Moment Area Theorem (MAT1) allows us to calculate the change in angle between two locations, $\Delta\theta_{AB}$, by finding the area under the curvature diagram between these two points. This is mathematically represented in Eq. (24.1):

$$\Delta\theta_{AB} = \theta_B - \theta_A = \int_A^B \phi(x)dx \tag{24.1}$$

The second Moment Area Theorem (MAT2) allows us to calculate the vertical distance between a point on the displaced member, point D, and a tangent which is drawn from another point on the displaced member, point T. This distance, the tangential deviation of point D from a tangent drawn at point T, is equal to the area of the curvature diagram between points D and T multiplied by the distance between its centroid and point D:

$$\delta_{DT} = \int_D^T x\phi(x)dx \tag{24.2}$$

Although the two Moment Area Theorems allow displacement-related quantities about the structure to be obtained, they do not allow us to directly calculate the slope or deflection of the deformed member at a specific point of interest. Instead, they must be used together with other information about the structure – such as how it is loaded and how it is supported – to obtain the displacements and slopes.

A general procedure for calculating the slopes and displacements of a loading member is the following:

i. Calculate the reaction forces and draw the shear force, bending moment, and curvature diagrams.
ii. Sketch out an approximate shape of the deformed structure.
iii. Identify any locations where the deflection and slope of the member are known by considering the supports and loading conditions. Locations where the tangent is horizontal are particularly helpful.
iv. Calculate the slope at a location of interest by using a known angle and Moment Area Theorem no. 1.
v. Express the desired displacement in terms of tangential deviations which can be calculated using Moment Area Theorem no. 2 and solve.

This general procedure will be illustrated using three common scenarios.

Scenario 1 – Known Horizontal Tangent due to a Support Condition
Consider the cantilever structure shown in Fig. 24.1 which is carrying a point load which is located at its tip. The fixed end restrains the member from rotating, and hence the slope of the member at the support remains flat even when the member curves under the load. Therefore, a tangent which touches this point will be horizontal, as shown in the second drawing in Fig. 24.1. Since the fixed end also prevents the member from translating at this point, the tangent effectively acts along the undeformed length of the member.

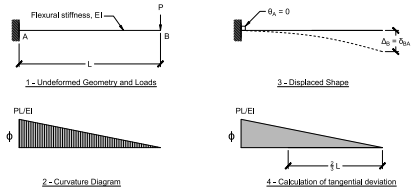

Fig. 24.1 – Undeformed (left) and deformed (right) geometry of a loaded cantilever.

Calculating the slope at any point along the member can be done using MAT1 using the knowledge that $\theta_A = 0$ due to the fixed end. For example, the slope of the member at the tip, θ_B, is equal to the area under the full curvature diagram as shown below:

$$\Delta\theta_{AB} = \theta_B - 0 \rightarrow \theta_B = \int_{x=0}^{x=L} \phi(x)dx \tag{24.3}$$

Evaluating this integral results in the following expression for the slope at the tip:

$$\theta_B = \frac{1}{2} \times L \times \frac{PL}{EI} = \frac{PL^2}{2EI} \tag{24.4}$$

The horizontal tangent at the fixed end is also useful for evaluating the vertical displacement of the cantilever at any point because the deviation of the displaced member from that horizontal tangent is simply equal to the displacement. For example, the displacement of the tip, Δ_B, can be written as the tangential deviation of point B from a tangent drawn at the fixed end:

$$\Delta_B = \delta_{BA} \tag{24.5}$$

Evaluating the tangential deviation results in the following expression for Δ_B:

$$\Delta_B = \left(\frac{1}{2} \times L \times \frac{PL}{EI}\right) \times \left(\frac{2}{3} \times L\right) = \frac{PL^3}{3EI} \tag{24.6}$$

Scenario 2 – Known Horizontal Tangent due to Symmetrical Loading Conditions
When a structure is subjected to symmetrical loading conditions, this sometimes results in the location of a horizontal tangent being known. Consider the symmetrical beam shown in Fig. 24.2 which supports a point load at its midspan. It can be deduced that the maximum displacement occurs at the midspan, which implies that a tangent which touches this point is horizontal. The deformed shape of the beam and this horizontal tangent are shown in the Fig. 24.2 as well.

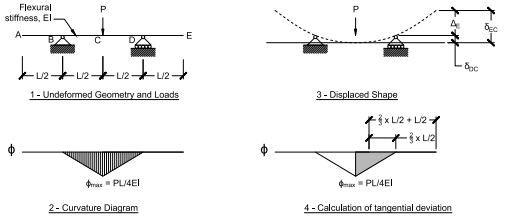

Fig. 24.2 - Undeformed (left) and deformed (right) geometry of a symmetrically loaded beam.

As with the previous scenario, the slope of the member at any location along its length can be determined by using the slope at the midspan, $\theta_C = 0$, as a reference. For example, the slope at the right support, θ_D, is equal to the area underneath the curvature diagram between points C and D:

$$\Delta\theta_{CD} = \theta_D - 0 \rightarrow \theta_D = \int_C^D \phi(x)dx \tag{24.7}$$

Evaluating the area underneath the curvature diagram between points C and D results in the following expression for θ_C:

$$\theta_D = \frac{1}{2} \times \frac{L}{2} \times \frac{PL}{4EI} = \frac{PL^2}{16EI} \tag{24.8}$$

The horizontal tangent at the midspan is also useful for determining the vertical displacements at other points along the member. Suppose the upwards displacement of the tip, Δ_E, is desired. As shown in Fig. 24.2, this displacement can be calculated by taking the tangential deviation of point E from the tangent at C, and subtracting the deviation of the support, point D, from the same tangent:

$$\Delta_E = \delta_{EC} - \delta_{DC} \tag{24.9}$$

δ_{EC} and δ_{DC} are calculated by obtaining the area beneath the curvature diagram between points EC and DC respectively and multiplying this area by the distance from the centroid of the area to the location where the deviation is being calculated. In the case of δ_{EC}, this results in the following:

$$\delta_{EC} = \left(\frac{1}{2} \times \frac{L}{2} \times \frac{PL}{4EI}\right) \times \left(\frac{2}{3} \times \frac{L}{2} + \frac{L}{2}\right) = \frac{5PL^3}{96EI} \tag{24.10}$$

δ_{DC} is calculated as:

$$\delta_{DC} = \left(\frac{1}{2} \times \frac{L}{2} \times \frac{PL}{4EI}\right) \times \left(\frac{2}{3} \times \frac{L}{2}\right) = \frac{PL^3}{48EI} \tag{24.11}$$

Substituting the results of Eqs. (24.10) and (24.11) into Eq. (24.9) results in Δ_E being equal to:

$$\Delta_E = \frac{5PL^3}{96EI} - \frac{PL^3}{48EI} = \frac{PL^3}{32EI} \tag{24.12}$$

Scenario 3 – No Known Horizontal Tangents
In many instances, structures will be subjected to nonsymmetric loading, which means that the location of the maximum displacement (and therefore the horizontal tangent) cannot be determined without detailed calculations. An example of this is the simply supported beam carrying a point load located L/3 away from its right support in Fig. 24.3.

Note: The maximum displacement does not occur right underneath the applied load. It occurs where the slope of the beam is equal to zero (which cannot usually be determined from inspection).

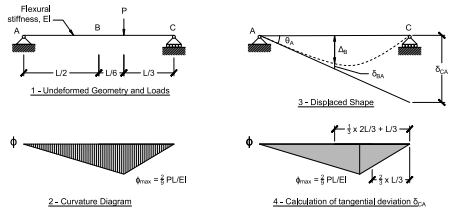

Fig. 24.3 - Undeformed (left) and deformed (right) geometry of an asymmetrically loaded beam.

Despite the lack of a known angle or flat tangent, the displacements and slopes can still be obtained by determining the deviation of one support from a tangent to the other support, like in the top right drawing in Fig. 24.3. If we assume that the beam is experiencing small deformations, then the slope at support A is approximately equal to:

$$\theta_A \cong \frac{\delta_{CA}}{L} \tag{24.13}$$

The tangential deviation $\boldsymbol{\delta_{CA}}$ can be calculated by dividing the curvature diagram into two triangles, resulting in the following expression:

$$\delta_{CA} = A_1 d_1 + A_2 d_2 = \left(\frac{1}{2}\times\frac{2}{3}L \times \frac{2PL}{9EI}\right)\times\left(\frac{L}{3}+\frac{1}{3}\times\frac{2}{3}L\right) + \left(\frac{1}{2}\times\frac{L}{3}\times\frac{2PL}{9EI}\right)\times\left(\frac{2}{3}\times\frac{L}{3}\right) = \frac{4PL^3}{81EI} \tag{24.14}$$

Therefore, $\boldsymbol{\theta_A}$ can be calculated using Eq. (24.13) and used as a reference to find the slope anywhere else along the member:

$$\theta_A = \frac{4PL^2}{81EI} \tag{24.15}$$

Suppose the displacement at the midspan, $\boldsymbol{\Delta_B}$, was of interest. This displacement can be obtained by drawing a similar triangle which relates the triangle outlined by the tangent and $\boldsymbol{\delta_{CA}}$ to another triangle outlined by the tangent and the vertical distance between the tangent and the original position of the beam at the midspan. Using similar triangles results in the following equation:

$$\theta_A = \frac{\delta_{CA}}{L} = \frac{\Delta_B + \delta_{BA}}{0.5L} \tag{24.16}$$

Therefore, if the deviation of the midspan from a tangent drawn at support A is known, then $\boldsymbol{\Delta_B}$ can be calculated by using Eq. (24.16). This deviation, $\boldsymbol{\delta_{BA}}$, can be found by using MAT2, resulting in:

$$\delta_{BA} = \left(\frac{1}{2}\times\frac{L}{2}\times\left(\frac{3}{4}\right)\times\frac{2PL}{9EI}\right)\times\left(\frac{1}{3}\times\frac{L}{2}\right) = \frac{PL^3}{72EI} \tag{24.17}$$

Re-arranging Eq. (24.16) substituting our results from Eqs. (24.14) and (24.17) allows $\boldsymbol{\Delta_B}$ to be obtained:

$$\Delta_B = \frac{1}{2}\times\delta_{CA} - \delta_{BA} = \frac{7PL^3}{648EI} \tag{24.18}$$

Note: the 3/4 factor in Eq. (24.17) is used to obtain the curvature at the midspan by scaling the curvature underneath the point load.

Lecture 25 – Shear Stresses in Beams

Overview

High shear forces carried by short members can lead to shear failures. In this chapter, the concept of shear stresses is introduced and Jourawski's equation for obtaining these shear stresses is derived.

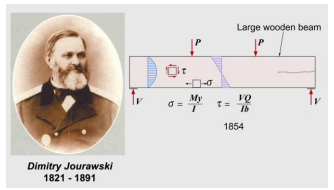

Fig. 25.1 – Summary of Jourawski's equation for shear stresses in beams.

Shear Stresses

Shear stresses are the stresses which occur in structures which are carrying a shear force which is perpendicular to their longitudinal axis. Like axial stresses, $\boldsymbol{\sigma}$, the shear stress, $\boldsymbol{\tau}$, is equal to the force applied parallel to a surface, **V**, divided by the area over which it acts, **A**:

$$\tau = \frac{V}{A} \tag{25.1}$$

Fig. 25.2 shows a small square element cut from a larger beam which is carrying vertical shear stresses on its left and right faces. Although the stresses on the two sides satisfy vertical equilibrium, they produce a couple which tends to cause the element to rotate. Therefore, ***complementary shear stresses*** exist on the top and bottom faces to satisfy rotational equilibrium. These shear stresses can be resolved into tensile and compressive stresses which act diagonally.

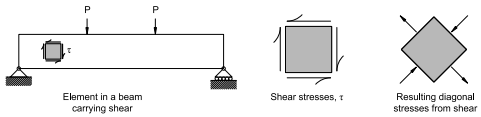

Fig. 25.2 – Shear stresses in beams (left), elements in pure shear (centre), resulting diagonal stresses (right).

Axial stresses, which are associated with axial strains, $\boldsymbol{\varepsilon}$, tend to cause materials to change volume by causing an expansion or contraction of the material. This volume change does not however affect the overall shape of the material. Shear stresses, which are associated with shear strains, $\boldsymbol{\gamma}$, tend to cause materials to change shape while maintaining their volume. This is illustrated in Fig. 25.3.

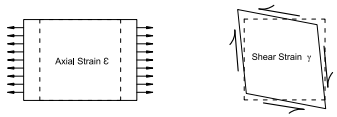

Fig. 25.3 – Comparison of axial deformations (left) and shear deformations (right).

Shear stresses produce failures which are very different than the failures caused by axial loads and bending moments, which are instead associated with axial stresses. Some of examples of how shear causes structural failures are illustrated in Fig. 25.4. The first mode of failure, which can occur in wooden members, is a failure caused by the sliding of adjacent elements due to the horizontal complementary shear stresses. The second mode of failure is caused by the diagonal tensile stresses associated with shear, which can lead to failures in brittle materials like concrete. A third mode of failure which is not shown is caused by the diagonal compressive stresses associated with shear, which may lead to diagonal buckling of thin members.

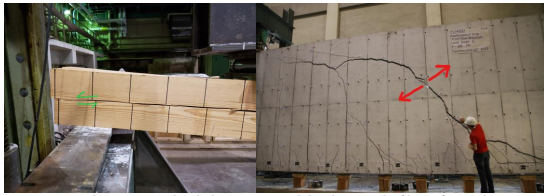

Fig. 25.3 – Failures associated with shear stresses – sliding between the fibres of a wooden beam (left) and diagonal cracking in a concrete beam (right).

Although Eq. (25.1) is a simple definition of the shear stress, calculating these stresses in beams which carry shear forces is more complicated because these shear stresses are not constant over the cross section. Instead, Jourawski's equation, shown below in Eq. (25.2), must be used to find them:

$$\tau = \frac{VQ}{Ib} \tag{25.2}$$

Derivation of Jourawski's equation

Consider a beam which is carrying loads that are perpendicular to its longitudinal axis. Recall that the relationship between the bending moment and the shear force is:

$$V = \frac{dM}{dx} \tag{25.3}$$

Therefore, in regions where there are shear forces, the moment will be changing along the length of the beam. This changing moment means that the flexural stresses will also be varying along the member as well.

Fig. 25.5 shows a portion of a beam which has a length of $\boldsymbol{\Delta x}$ which has been sliced out of a region of a beam which is carrying shear. For simplicity, the cross-section of the beam is a rectangle with width **b** and second moment of area **I**. On the left side of the beam, the moment will be equal to **M**, while on the right side of the beam, the moment carried by the section will be slightly larger, $\mathbf{M + \Delta M}$.

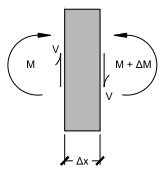

Fig. 25.5 – Slice of a beam carrying bending moments and shear forces.

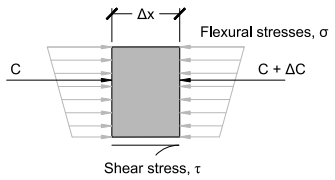

Fig. 25.6 – Free body diagram showing how shear stresses provide horizontal equilibrium.

We can obtain an expression for the shear stress at a particular depth of this beam by drawing a free body diagram which cuts through this body to an arbitrary depth of interest, like the one shown in Fig. 25.6. The flexural stresses applied to this body cause it to be in compression, and because the moment is higher on the right side, the body will have a tendency to be pushed to the left. The net force which pushes the body to the left, $\boldsymbol{\Delta C}$, is caused by the increment in moment, $\boldsymbol{\Delta M}$, and is equal to:

$$\Delta C = \int_{y=y_o}^{y=y_{top}} \sigma(y)dy = \int_{y=y_o}^{y=y_{top}} \frac{\Delta M y}{I} dy \tag{25.4}$$

Eq. (25.4) can be simplified by removing the constants $\boldsymbol{\Delta M}$ and **I** from the integral, and representing the integral, which is a first moment of area about the centroidal axis of the member, as the quantity **Q**:

$$\Delta C = \frac{\Delta M}{I}\int_{y=y_o}^{y=y_{top}} y dy = \frac{\Delta M}{I} Q \tag{25.5}$$

In order to satisfy horizontal equilibrium, there must be a companion force which resists $\boldsymbol{\Delta C}$. This resisting force is provided by the shear stresses acting on the underside of the body, which produce an equal and opposite force resulting in the following:

$$\Delta C = \tau b \Delta x \tag{25.6}$$

Equating Eqs. (25.5) and (25.6) and isolating for the shear stress results in the following:

$$\tau = \frac{\Delta M}{\Delta x}\frac{Q}{Ib} \tag{25.7}$$

*Note: The area over which the shear stress acts is equal to the width of the beam, **b**, multiplied by the length of the body, **Δx**.*

If the length of our body approaches zero, then the term ΔM/Δx becomes equal to the shear force **V** due to Eq. (25.3), resulting in Jourawski's equation which is reproduced below:

$$\tau = \lim_{\Delta x \to 0} \frac{\Delta M}{\Delta x} \frac{Q}{Ib} = \frac{VQ}{Ib} \tag{25.8}$$

Calculating the First Moment of Area, Q

Q is defined as the first moment of area of the portion of the cross-sectional area about the centroidal axis of the member. The area considered is taken as the area from the depth of interest to the top or the member, or the area from the bottom of the member to the depth of interest, $\mathbf{y_o}$:

$$Q(y = y_o) = \int_{y_{bot}}^{y_o} y dA = \int_{y_o}^{y_{top}} y dA \tag{25.9}$$

Q can be evaluated by following the procedure outlined below:

i. Determine the depth of interest where **Q** is being calculated.
ii. Calculate the area, **A**, of the cross section between the depth of interest to the top of the member; alternatively, the area of the cross section between the depth of interest to the bottom of the member.
iii. Determine the distance between the centroid of the area found in step ii and the centroid of the cross section, **d**.
iv. Calculate **Q** using Eq. (25.10):

$$Q = Ad \tag{25.10}$$

Distribution of Shear Stresses

Like the axial stresses caused by bending moments, the shear stresses carried in a member are not constant over the depth of the cross section. This is because **Q** depends on where the shear stress is being calculated, and the width of the member, **b**, may vary over the height of the member.

Consider a rectangular cross section, shown in Fig. 25.8, which has a height of **h**, a width of **b**, and whose centroidal axis is located at a height of **h/2** above the base. The value of **Q** calculated for an arbitrary depth located a distance **y** from the bottom of the cross section is:

$$Q = Ad = (by) \times \left(\frac{h}{2} - \frac{y}{2}\right) = \frac{1}{2} by(h - y) \tag{25.11}$$

From Eq. (25.11), we can deduce three properties of **Q** which generally apply to all cross-sectional shapes:

i. **Q** varies parabolically over the height of the member.
ii. **Q** is equal to 0 at y = 0 and y = h, i.e., **Q** is equal to zero at the top and the bottom of the member.
iii. The largest value of **Q** occurs at y = h/2. In general, **Q** is maximized at the centroidal axis of the member.

For rectangular members, **b** is a constant, and hence the shear stress distribution will be parabolic.

*Note: When calculating **Q**, the area under consideration can be broken up into n smaller areas whose local centroid is easier to calculate. If this is done, then Eq. (25.10) becomes:*

$$Q = \sum_{i=1}^{n} A_i d_i \tag{25.11}$$

Fig. 25.7 shows the application of Eq. (25.11) to find the shear stress at the mid-height of a T-beam

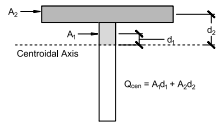

Fig. 25.7 – Calculating Q for more complex shapes.

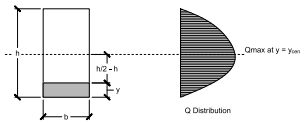

Fig. 25.8 – Derivation of Q for a rectangular cross section and resulting distribution over the member height.

Lecture 26 – Wood Beams

Overview

Along with steel and concrete, wood is one of the most commonly used materials for building structures. In this chapter, the various structural properties of wood are discussed, and tables of wood properties are presented and explained.

Properties of Wood

Wood has historically been used as a building material since perhaps the beginning of civilization due to its strength, workability, and abundance in nature in many parts of the world. Woods can be classified as being ***softwoods*** or ***hardwoods***, with softwoods typically coming from coniferous trees and hardwoods from deciduous species. Hardwoods are typically stronger, stiffer, heavier, and more difficult to work with than softwoods. Due to their relatively low cost and ease of use, softwoods tend to be used extensively in construction, while the more expensive hardwoods tend to be used for furniture, high-end finishes, and musical instruments due to their durability. Examples of softwood and hardwood species are shown in Fig. 26.1.

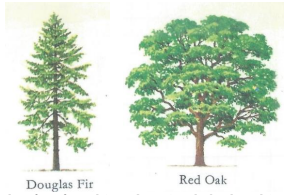

Fig. 26.1 – Examples of a softwood (Douglas Fir) and a hardwood (Red Oak).

The internal structures of both types of woods, shown in Fig. 26.2, resemble a series of fibres oriented along the height of a growing tree. Within the hardwood, there is a mixture of larger vessels embedded in a tightly packed matrix of smaller fibres, while the softwoods are composed of uniformly distributed vessels which are hollow to allow water and nutrients to move throughout the tree. The dense fibres in the hardwood give the material its strength, stiffness, and weight, while the relatively soft tubes in the softwood make it easier to work with.

Wood, being a naturally occurring material, differs in many ways from an engineered material like steel. Since the structure of wood is biased along the height of the tree, the material properties of wood are different depending on the direction of loading relative to the orientation of the fibres; this is unlike the uniform response which steel exhibits. The property of having different mechanical properties in various directions makes wood an ***anisotropic*** material, unlike steel which is an ***isotropic*** material.

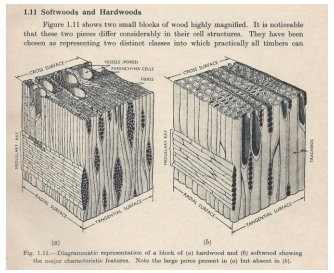

Fig. 26.2 – Schematic showing the structure of hardwoods (left) and softwoods (right).

*Note: The strength and stiffness of wood generally differ parallel to the grain and perpendicular to the grain; because these directions are orthogonal, wood is example of an **orthotropic** material, which is a subset of anisotropic materials.*

Another important aspect to consider when working with timber structures is that wood has a wide range of mechanical properties which cannot be precisely specified in design. Therefore, appropriate values of strength and stiffness to use in design must be obtained by extensive testing, and larger factors of safety are typically employed.

Response of Wood to Loading

Timber members, often used as beams or columns in structures, typically need to support axial loads, bending moments, and shear forces. Wooden members tend to perform well when loaded in ways which resemble the forces which trees must resist in nature, namely high bending moments and axial forces which act along the direction of the fibres. When subjected to axial forces which act parallel to the grain, wooden members are strong and stiff. This allows them to carry high tensile forces, which occur in a wooden truss structures, and high compression forces, which occur in columns in buildings.

In construction, large heavy objects are often placed on the ground and supported from below by smaller wooden pieces. This loads the wood in compression perpendicular to the grain. Under this loading condition, the response of the wood is much softer and ductile than when loaded parallel to the grain, especially in softwoods. This property makes wood an ideal material to use when placing delicate objects on the ground. The differences in the compression response of woods when loaded parallel to the grain and perpendicular to the grain is illustrated in Fig. 26.3.

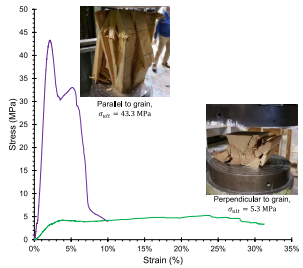

Fig. 26.3 – Comparison of stress-strain response of wooden members loaded in compression parallel to the grain and perpendicular to the grain.

When used in beams, timber members must carry significant bending moments and shear forces. Wooden members are strong in bending because the resulting flexural stresses act along the fibres of the material. However, they are susceptible to failing in shear because the fibres can be separated by the resulting shear stresses relatively easily. An example of a wooden beam failing in shear can be seen in Fig. 26.4.

Fig. 26.4 – Timber beam loaded under four-point bending. Note the shear failure on the left side of the beam which has caused the previously vertical lines to separate, and the flexural failure at the midspan.

Wood Design Tables

As noted earlier in the chapter, wood is not an engineering product and hence has great variability in its material properties. Fig. 26.5, which shows the failure stresses of 2110 small wooden specimens when loaded in flexure, illustrates the range of strengths which may exist for specimens cut from the same tree. The measured strengths, which are roughly normally distributed, were on average 50.2 MPa. However, the weakest specimens were less than half of the average strength, and the strongest ones were approximately 60% stronger. **To account for the variability in strength, the 5th percentile strength is typically used in design, along with a factor of safety of 1.5.**

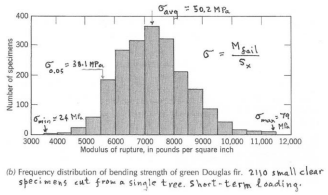

Fig. 26.5 – Distribution of flexural strengths obtained by testing 2110 small wooden specimens.

Tables of material properties of many types of wood are shown in Table 26.1 and in Appendix D. The tables are categorized as being for smaller members (top) and for larger members (bottom). This is because the material strengths used in design vary depending on the size of the wooden members used. The 5th percentile strengths of smaller members tend to be weaker because they are more strongly influenced by the presence of knots and other defects.

In the tables, the 5th percentile Young's modulus, $\mathbf{E_{05}}$, and the average Young's modulus, $\mathbf{E_{50}}$, are provided in the far-right columns. When determining the strength of a member, like when estimating its buckling load, $\mathbf{E_{05}}$ should be used. Deflection calculations on the other hand should be done using $\mathbf{E_{50}}$.

Table 26.1 – Wood Properties. Small specimens (top) and large specimens (bottom)

Section 9 Wood Structures 259

5th Percentile estimates of strength under one month loading. For safe working stresses reduce these breaking stresses by factor of safety of 1.5.

9 – 11.2 (a) Specified strength and modulus of elasticity for dimension lumber, thickness 38 to 77 mm, MPa**

Species or Species Combination	Grade	Bending f_{bu}	Shear Longitudinal f_{vu}	Compression Parallel to Grain f_{pu}	Compression Perpendicular to Grain f_{qu}	Tension Parallel to Grain f_{tu}	Modulus of Elasticity E_{50}	Modulus of Elasticity E_{05}
Douglas Fir-Larch	Select Structural	17.5	1.1	16.5	3.6	13.5	11,000	8,000
	No. 1 and No. 2	10.0	1.1	9.0	3.6	9.0	9,500	6,000
Hem-Fir	Select Structural	16.0	0.8	14.5	1.9	13.5	11,000	7,500
	No. 1 and No. 2	11.5	0.8	10.5	1.9	9.0	10,500	7,000
Lodgepole Pine, or Ponderosa Pine	Select Structural	16.0	1.0	14.5	1.9	13.5	10,000	7,000
	No. 1 and No.2	11.5	1.0	10.5	1.9	9.0	9,000	6,000
Jack Pine	Select Structural	16.0	1.0	14.5	2.6	13.5	10,500	7,000
	No. 1 and No. 2	11.5	1.0	10.5	2.6	9.0	9,500	6,000
Red Pine	Select Structural	11.5	0.8	10.0	1.9	10.0	7,000	5,000
	No. 1 and No. 2	8.0	0.8	7.0	1.9	7.0	6,000	4,000
White Pine*	Select Structural	6.0	0.8	–	1.9	–	5,500	4,000
	No. 1 and No. 2	4.5	0.8	–	1.9	–	4,500	3,500

* For use in stress-laminated decks only.
** Dimension lumber with thickness of 89 mm or greater shall have specified strengths in accordance with Table 13–11.2 (b).

9 – 11.2 (b) Specified strength and modulus of elasticity for beams & stringers, post & timbers, minimum dimension 140 mm, MPa

Species or Species Combination	Grade	Bending f_{bu}	Shear Longitudinal f_{vu}	Compression Parallel to Grain f_{pu}	Compression Perpendicular to Grain f_{qu}	Tension Parallel to Grain f_{tu}	Modulus of Elasticity E_{50}	Modulus of Elasticity E_{05}
Douglas Fir-Larch	Select Structural	24.0	1.1	16.5	3.6	13.0	11,000	7,500
	No. 1	20.0	1.1	9.0	3.6	9.0	9,500	6,500
Hem-Fir	Select Structural	20.0	0.8	14.5	1.9	13.0	11,000	7,500
	No. 1	18.0	0.8	10.5	1.9	9.0	10,500	7,000
Lodgepole Pine, or Ponderosa Pine	Select Structural	18.5	1.0	14.5	1.9	13.0	10,000	7,000
	No. 1	13.0	1.0	10.5	1.9	9.0	9,000	6,000
Jack Pine	Select Structural	18.5	1.0	14.5	2.6	13.0	10,500	7,000
	No. 1	13.0	1.0	10.5	2.6	9.0	9,500	6,000
Red Pine	Select Structural	13.0	0.8	10.0	1.9	10.0	7,000	5,000
	No. 1	9.0	0.8	7.0	1.9	7.0	6,000	4,000

Lecture 27 – Shear Stresses in I Beams and Box Beams

Overview
In this lecture, procedures for calculating the shear stresses for more complex shapes are discussed.

Shear Stresses in Complex Shapes
For a member with second moment of area **I** and subjected to a shear force **V**, Jourawski's equation can be used to determine the shear stresses, **τ**:

$$\tau = \frac{VQ}{Ib} \tag{27.1}$$

When Eq. 27.1 was used to find the shear stresses for a rectangular member in Lecture 25, **b** was constant over the height and the change in shear stresses over the height was due to the varying first moment of area, **Q**, defined as:

$$Q(y = y_o) = \int_{y_{bot}}^{y_o} ydA = \int_{y_o}^{y_{top}} ydA \tag{27.2}$$

*Note: Recall that **Q** can be calculated by integrating from the bottom of the member up to the depth of interest, or by integrating from the top of the member down to the depth of interest. Both will produce the same result; this is reflected in Eq. 27.2.*

In Eq. (27.2), $\mathbf{y_o}$ is the depth of interest, $\mathbf{y_{bot}}$ and $\mathbf{y_{top}}$ refer to the bottom and top of the cross section respectively, and **y** is the vertical distance measured from the centroid of the cross section. For complex shapes, **Q** is typically calculated by subdividing the area of interest into **n** smaller areas, $\mathbf{A_i}$, whose centroids are each a distance $\mathbf{d_i}$ away from the centroid of the cross section. **Q** is then calculated as:

$$Q = \sum_{i=1}^{n} A_i d_i \tag{27.3}$$

When calculating the shear stresses in more complex shapes like I beams, T beams or box beams, Eqs. (27.1) to (27.3) are still valid. However, **Q** must account for the geometry more carefully and **b** is the width of the cross section at the location of interest. Fig. 27.1 illustrates an example of how **Q** and **b** are obtained when calculating the shear stresses in the web of an I beam.

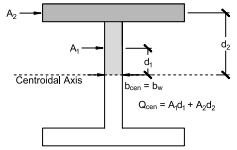

Fig. 27.1 – Calculation of shear stresses in an I beam.

Built-Up Sections with Glued Components
It is common to construct larger cross sections by fastening together smaller components together using glue or mechanical fasteners like screws or nails. For these built-up sections, the ability of these connections to resist shear stresses is crucial for the section to behave together as a whole instead of as several smaller pieces.

Note: The methods described in Figs. 27.2 and 27.3 can be used together when determining the shear stresses on glued surfaces with both horizontal and vertical components.

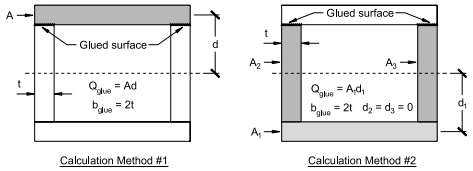

Fig. 27.2 – Calculating shear stresses for built-up sections with horizontal glued surfaces. Either method will produce the correct value.

For horizontal glued surfaces, like those shown in Fig. 27.2, determining the shear stresses simply involves using Jourawski's equation at the depth of interest and taking **b** as the combined width of the interfacing surfaces. When the surfaces are vertical, like in the situations shown in Fig. 27.3, the typical procedure for calculating **Q** still applies, however the value of **b** to use is the total width of the vertical glued surfaces. In this case, the area of interest in the calculation of **A** is now best described as the area of the cross section which will slide longitudinally if the glue fails.

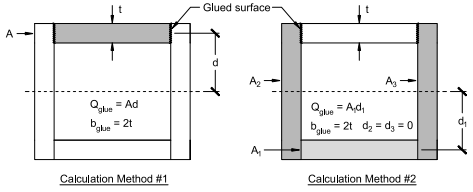

Fig. 27.3 – Calculating shear stresses for built-up sections with vertical glued surfaces Either method will produce the correct value.

Distribution of Shear Stresses
Having a variable width over the height of a member has a pronounced effect on the shear stress distribution. For these shapes, **Q** is still equal to zero at the top and bottom of the member, reaches its maximum at the centroid, and varies parabolically in between. Applying Jourawski's equation results in the somewhat unusual shear stress distributions shown in Fig. 27.4. The shear stress distribution largely follows the shape of **Q**, but suddenly increases when there is an abrupt reduction in width, and suddenly decreases for abrupt increases in width.

Note: When determining the maximum shear stress in a member with varying width, a good strategy is to check both the narrowest part of the member, where b is minimized, and at the centroidal axis, where Q is maximized.

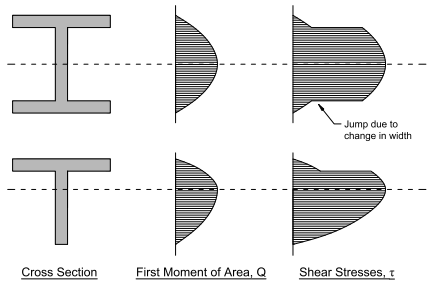

Fig. 27.4 – Shear stress distributions for a wide flange (top) and T-shaped (bottom) sections.

Lecture 28 – Thin-Walled Box Girders

Overview

Hollow structures are efficient, being lightweight yet strong and stiff. In this chapter, the development and use of hollow members made from assemblies of thin plates is discussed.

Advantages of Hollow Structures

The obvious advantage of using hollow members is that they weigh less than solid members which share the same outside dimensions. This reduction in weight however does not coincide with an equivalent reduction in strength and stiffness. Consider a hollow square member which has outside dimensions **b**, and thickness **t**. Its cross-sectional area, which is related to its weight, is equal to:

$$A = b^2 - (b - 2t)^2 \tag{28.1}$$

The second moment of area, **I**, which is related to the member's flexural stiffness and buckling strength, is equal to:

$$I = \frac{b^4}{12} - \frac{(b-2t)^4}{12} \tag{28.2}$$

Eqs. (28.1) and (28.2) show that **A** and **I** do not decrease at the same rate as a solid member gradually becomes hollow; in the case of the area, it reduces quadratically while the second moment of area follows a quartic relationship. These relationships are plotted in Fig. 28.1.

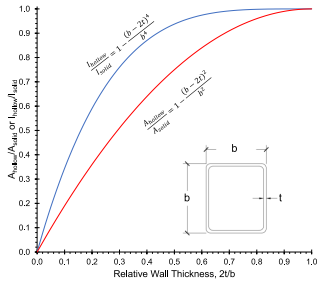

Fig. 28.1 – Relationship between A (red) and I (blue) and the wall thickness of a hollow square member.

As shown in Fig. 28.1, reducing the area, and hence the weight, of members by making them hollow leads to smaller reductions in the flexural stiffness. This makes hollow members useful for situations where the bending stiffness is important, like in beams or slender columns which tend to fail by buckling.

Design Considerations

In many ways, thin-walled hollow structures behave in the same way as solid members: they may fail by yielding in tension, buckling is a possibility when in compression, and they may also fail due to high flexural or shear stresses. An additional consideration for hollow members is that they may also fail due to ***local buckling*** of the thin walls. This kind of buckling is characterized by an instability of the walls themselves, as opposed to instability of the complete member, which is the case with Euler buckling. Thin plate buckling is discussed in more detail in Lectures 29 and 30.

Historical Development

A significant advance in the use of thin-walled box girders was in the Brittania Bridge, which was designed by the English engineer Robert Stevenson and built between 1847 and 1850. Stevenson's bridge, shown under construction in Fig. 28.2, consisted of two iron tubes running side by side over a clear span of 460 ft. This was a significant engineering accomplishment because the previous record for the longest box girder was only 31 ft.

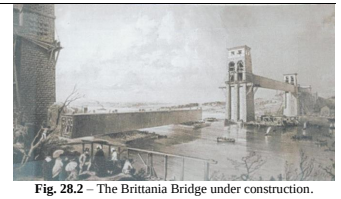

Fig. 28.2 – The Brittania Bridge under construction.

The elevation, plan, and cross section views of the bridge are shown in Fig. 28.3. The structure ran continuously over several intermediate supports, being subjected to both large positive and negative bending moments along its full span. In regions of positive moments, which typically occurred between the supports, the top of the bridge carried flexural compression stresses. The negative moment regions occurred over the supports, and typically resulted in slightly smaller compressive stresses which instead acted on the bottom of the member. To prevent the thin plates on the top and bottom of the bridge from locally buckling, Stevenson had vertical stiffeners fastened to them, restraining them from moving up and down. These stiffeners, which are visible in the cross section of the bridge, were more closely spaced on the top flange because the flexural compression stresses were higher in these areas.

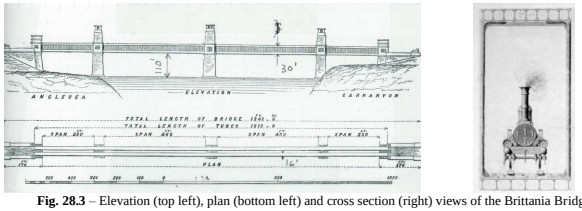

Fig. 28.3 – Elevation (top left), plan (bottom left) and cross section (right) views of the Brittania Bridge.

Fig. 28.4 – Surviving segment of the original Brittania Bridge.

Lecture 29 – Buckling of Thin Plates

Overview

Buckling of thin plates is a phenomenon which occurs in thin-walled sections which are subjected to axial compression, moment, or shear. In this chapter, the basic equations for characterizing the strength of plates are presented for common cases.

Theoretical Background

In Lecture 14, the derivation of Euler's equation for slender members was presented. Euler's equation, which is applicable for one-dimensional members with length **L** and flexural stiffness **EI**, states that the buckling load for a member free to rotate on its two ends is:

$$P_e = \frac{pi^2 EI}{L^2} \tag{29.1}$$

For a plate which has a width of **b** and thickness **t** like the one shown in Fig. 29.1, the second moment of area will be equal to $bt^3/12$. Substituting this into Eq. (29.1) and rearranging terms results in the following equation for the buckling stress, σ_{crit}:

$$\sigma_{crit} = \frac{\pi^2 E}{12}\left(\frac{t}{L}\right)^2 \tag{29.2}$$

Consider the plate shown in Fig. 29.2 which is subjected to a horizontal compression stress which acts along its left and right faces. In addition to the restraints on its two horizontal edges, the two vertical sides of the plate are restrained from moving in the out-of-plane direction. For this scenario, if the width of the plate, **b**, is larger than its unrestrained length **L**, then the required stress to buckle the plate will be equal to the following:

$$\sigma_{crit} = \frac{k\pi^2 E}{12(1-\mu^2)}\left(\frac{t}{b}\right)^2 \tag{29.3}$$

Eq. (29.3) is the solution to a fourth order partial differential equation for the displaced shape of a thin plate subjected to compressive stresses. This equation, whose solution was formulated by the American-Russian-Ukrainian engineer Stephen Timoshenko, is a two-dimensional extension of Euler's equation for slender one-dimensional members buckling under compressive loads. Although the derivation of the solution is beyond the scope of CIV102, the key idea is that **k** depends on the applied loading conditions (i.e., distribution of compressive stresses) and the boundary conditions (i.e., how the edges of the plate are restrained from moving).

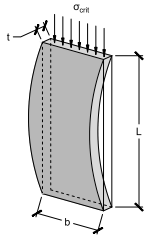

Fig. 29.1 – Rectangular plate loaded in compression with no restraints on the sides

Note: μ is the Poisson's ratio of the material, which is a measure of how much a material deforms in the directions orthogonal to an applied load. For example, for a 2-D material which is being stressed in the x-direction, the transverse strain ε_y is equal to:

$$\varepsilon_y = -\mu\varepsilon_x = -\mu\frac{\sigma_x}{E} \tag{29.4}$$

Because the vertical surfaces are restrained from moving, ε_y is equal to zero. This means that an additional y-direction stress must be provided to make the net strain equal to zero:

$$\sigma_y = -\varepsilon_y E = \mu\sigma_x \tag{29.5}$$

This produces a carryover effect in the x-direction, reducing the longitudinal strain ε_x to be the following:

$$\varepsilon_x = \frac{\sigma_x(1-\mu^2)}{E} \tag{29.6}$$

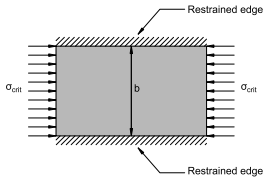

Fig. 29.2 – Rectangular plate loaded in compression and restrained along its two horizontal edges.

Plate Buckling Equations:

For the plate shown in Fig. 29.2 whose sides are restrained from movement both in and out of plane, the solution to the buckling coefficient **k** is the following equation:

$$k = \left(\frac{1}{n}\cdot\frac{L}{b} + n\frac{b}{L}\right)^2 \tag{29.7}$$

In Eq. (29.7), **n** is the number of half cycles which the buckled plate assumes, which is similar to Euler's solution for the buckled shape of one-dimensional struts. This equation is plotted in Fig. 29.3, and although it assumes a wide range of values for different values of L/b and n, the lowest possible value is k = 4. Therefore, a reasonable lower bound of the buckling stress which is appropriate for design is:

$$\sigma_{crit} = \frac{4\pi^2 E}{12(1-\mu^2)}\left(\frac{t}{b}\right)^2 \tag{29.8}$$

Fig. 29.4 shows a rectangular plate which is loaded with a constant compressive stress on its vertical boundaries like the one shown Fig. 29.2. However, only one edge is restrained from moving while the other edge is free to move. In this situation, the free edge greatly weakens the plate under compressive stresses, and it fails at a stress of:

$$\sigma_{crit} = \frac{0.425\pi^2 E}{12(1-\mu^2)}\left(\frac{t}{b}\right)^2 \tag{29.9}$$

This factor, $(1-\mu^2)$, therefore appears in the plate buckling equation to account for the extra rigidity provided by the restrained edges and the Poisson effect.

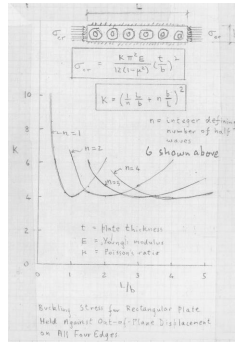

Fig. 29.3 – Plot of k values for different L/b and n values

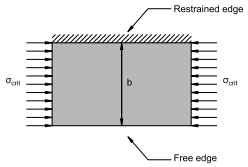

Fig. 29.4 - Rectangular plate loaded in compression with only one restrained horizontal edge.

Fig. 29.5 show a rectangular plate which, unlike the ones shown in Figs. 29.2 and 29.4, carries compressive stresses which vary linearly from zero to a maximum on each side. The magnitude of the maximum stress which causes buckling is:

$$\sigma_{crit} = \frac{6\pi^2 E}{12(1-\mu^2)}\left(\frac{t}{b}\right)^2 \tag{29.10}$$

High shear stresses carried by thin plates can also cause buckling due to the diagonal compressive stresses which are caused by shear. The shear stress which causes a thin plate to buckle is:

$$\tau_{crit} = \frac{5\pi^2 E}{12(1-\mu^2)}\left(\left(\frac{t}{h}\right)^2 + \left(\frac{t}{a}\right)^2\right) \tag{29.11}$$

In Eq. (29.11), **h** is the height of the plate, and **a** is the spacing between vertical stiffeners which prevent the plate from moving in the out-of-plane direction. These terms are illustrated in Fig. 29.6.

Summary of Plate Buckling Equations
Fig. 29.7 contains a complete summary of the buckling stresses for the four situations discussed in Eqs. (29.8) to (29.11). The figure shows the various situations in which they can be used in the design of thin-walled box girder. The first two equations apply to the flange which is in compression due to the flexural compression. The compressive stresses from the moment may also cause the webs to buckle; the third equation can be used to predict when this might happen. Finally, the fourth equation should be used to determine if the shear stresses cause the webs to buckle. The application of these examples in design are discussed in more detail in Lecture 30.

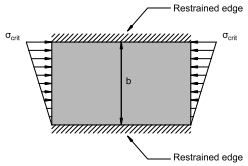

Fig. 29.5 - Rectangular plate loaded in compression and restrained on its two horizontal edges, but loaded with linearly varying compressive stresses

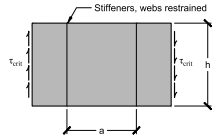

Fig. 29.6 - Rectangular plate subjected to shear stresses, with a height of h. The plate is restrained from buckling in the out-of-plane direction by vertical stiffeners which are spaced apart by a distance a.

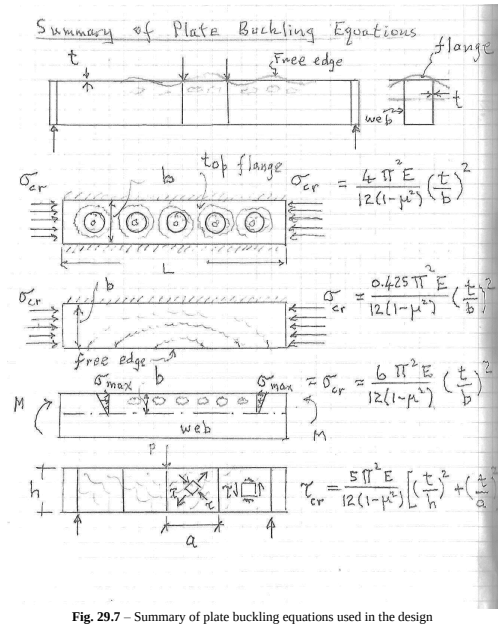

Fig. 29.7 – Summary of plate buckling equations used in the design of a thin-walled box girder.

Lecture 30 – Design of a Thin-Walled Box Girder

Overview
In this chapter, the procedures described in the previous lectures are summarized and applied to the design of a thin-walled box girder. Failures associated with both failure of the materials and buckling the thin plates are considered.

Basic Design Considerations
Consider the simply supported thin-walled box girder shown in Fig. 30.1 which is subjected to a single point load at its midspan. It is subjected to a constant shear force over its entire length and bending moments which linearly increase to a maximum at the midspan.

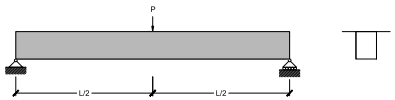

Fig. 30.1 – Example of a thin-walled box girder. Elevation (left) and cross section (right) views.

If the tensile strength of the material, σ_{ult}^{+}, the compressive strength of the material, σ_{ult}^{-}, the shear strength of the material, τ_{ult}, and the shear strength of the material used to fasten the walls together, τ_m, are known, then there are four modes of material failure which are summarized in Table 30.1.

The design of thin-walled structures must also consider the possibility of buckling of the walls. Recall from Lecture 15 that when a structure is subjected to compressive stresses, it will fail at the lower of the ultimate compressive stress or the critical buckling stress:

$$\sigma_{\text{fail}} = \min\{\sigma_{ult}^{-}, \sigma_{crit}\} \tag{30.1}$$

When designing struts for compression, we used the critical buckling stress, σ_{crit}, as the Euler buckling stress. For the two-dimensional plates which make up the walls of a thin-walled box girder, σ_{crit} is instead taken as the appropriate plate buckling equation from Lecture 29.

Table 30.1 – Summary of material failure modes

No.	Failure Mode	Failure Condition	Relevant Design Equation
1	Tensile failure of walls	$\sigma = \sigma_{ult}^{+}$	$\sigma = \frac{My}{I}$
2	Compressive failure of walls	$\sigma = \sigma_{ult}^{-}$	
3	Shear failure of walls	$\tau = \tau_{ult}$	$\tau = \frac{VQ}{Ib}$
4	Shear failure of fastening material	$\tau = \tau_m$	

Note: Some examples of fastening materials include glue, screws, bolts, or nails.

Table 30.2 – Summary of plate buckling failure modes

No.	Failure Mode	Failure Condition	Relevant Design Equation
5	Buckling of the compressive flange between the webs	$\sigma = \frac{4\pi^2 E}{12(1-\mu^2)}\left(\frac{t}{b}\right)^2$	$\sigma = \frac{My}{I}$
6	Buckling of the tips of the compressive flange	$\sigma = \frac{0.425\pi^2 E}{12(1-\mu^2)}\left(\frac{t}{b}\right)^2$	
7	Buckling of the webs due to the flexural stresses	$\sigma = \frac{6\pi^2 E}{12(1-\mu^2)}\left(\frac{t}{b}\right)^2$	
8	Shear buckling of the webs	$\tau = \frac{5\pi^2 E}{12(1-\mu^2)}\left(\left(\frac{t}{h}\right)^2 + \left(\frac{t}{a}\right)^2\right)$	$\tau = \frac{VQ}{Ib}$

As noted in Lecture 29, large shear stresses can also cause the thin plates to buckle due to the resulting diagonal compressive stresses. Therefore, the walls will fail at the lower of the shear strength or the critical shear buckling stress:

$$\tau_{\text{fail}} = \min\{\tau_{ult}, \tau_{crit}\} \tag{30.2}$$

Including the additional buckling considerations results in the four more possible failure modes which must be considered in the design of the box girder, which are summarized in Table 30.2.

To illustrate the design process, we will try to determine the lowest value of P which causes our example bridge to fail. To do this, we will express the maximum shear force and bending moments in terms of **P** and substitute these relationships into the appropriate design equations:

$$V = \frac{P}{2} \tag{30.3}$$

$$M = \frac{PL}{4} \tag{30.4}$$

Flexural and Shear Strength
The most straightforward modes of failure are associated with tensile and compressive failures caused by flexure. Combining Navier's equation with Eq. (30.4) and noting the top of the girder is in compression and bottom of the girder is in tension results in the following values of **P** causing failure. Note that the subscripts on **P** correspond to the failure modes described in Tables 30.1 and 30.2.

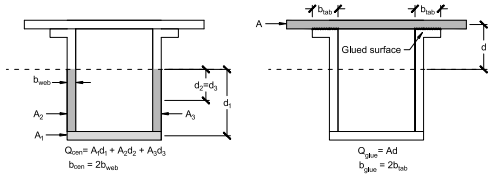

Fig. 30.2 – Calculation of Q to determine the shear stresses in the web (left) and in the glue (right).

$$\sigma_{ult}^{+} = \frac{\left(\frac{P_1 L}{4}\right) y_{bot}}{I} \rightarrow P_1 = 4\frac{\sigma_{ult}^{+} I}{L y_{bot}} \tag{30.5}$$

$$\sigma_{ult}^{-} = \frac{\left(\frac{P_2 L}{4}\right) y_{top}}{I} \rightarrow P_2 = 4\frac{\sigma_{ult}^{-} I}{L y_{top}} \tag{30.6}$$

The shear failures of the webs or the fastening material can be determined by using Jourawski's equation and calculating the appropriate values of **Q** and **b**. For the box girder being considered in this example, which is glued together, the areas and distances used to calculate **Q** and **b** are shown in Fig. 30.2. Using these values, the forces causing the shear failures of the web material and glue respectively are:

$$\tau_{ult} = \frac{\left(\frac{P_3}{2}\right) Q_{cen}}{I b_{cen}} \rightarrow P_3 = 2\frac{\tau_{ult} I b_{cen}}{Q_{cen}} \tag{30.7}$$

$$\tau_m = \frac{\left(\frac{P_4}{2}\right) Q_{glue}}{I b_{glue}} \rightarrow P_4 = 2\frac{\tau_m I b_{glue}}{Q_{glue}} \tag{30.8}$$

Failure Modes Associated with Plate Buckling

Calculating the loads which cause the structure to fail due to plate buckling is a matter of identifying which parts of the structure are carrying compressive (or shear) stresses, and then selecting the appropriate equation based on the distribution of these stresses and how the plate is restrained if applicable.

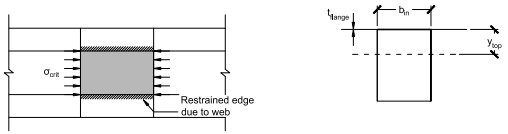

Fig. 30.3 – Buckling of the flange between the two webs. Top (left) and cross section (right) views.

Consider the region of the compression flange shown in Fig. 30.3 which is located between the two webs. Because the flange is located at constant height above the centroidal axis, the flange experiences uniform compressive stresses along its width from the bending moment. The webs, which are securely fastened to the flange from below, provide a restraint which prevents the region between the webs to move up or down. These boundary conditions suggest that the plate buckling equation with a coefficient of **k = 4** is appropriate for determining when failure occurs. Therefore, failure of this region of the bridge takes place at the following load:

$$\frac{4\pi^2 E}{12(1-\mu^2)}\left(\frac{t_{\text{flange}}}{b_{in}}\right)^2 = \frac{\left(\frac{P_5 L}{4}\right) y_{top}}{I} \rightarrow P_5 = \frac{16\pi^2 EI}{12 L y_{top}(1-\mu^2)}\left(\frac{t_{\text{flange}}}{b_{in}}\right)^2 \tag{30.9}$$

*Note: Recall that the compressive stresses caused by bending do not vary over the width of the member because they are only a function of the vertical distance from the centroidal axis, **y**.*

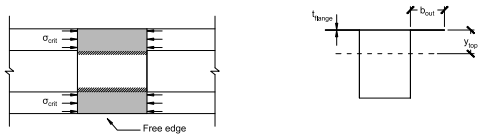

Fig. 30.4 – Buckling of the free edges of the flange. Top (left) and cross section (right) views.

The tips of the flange, shown in Fig. 30.4, may also buckle due to the flexural compressive stresses. Like the flange between the webs, they are also subjected to uniform stresses over their width. However, they have a free edge on one side which can move up or down, meaning the plate buckling equation with a coefficient of **k = 0.425** is more appropriate for determining their strength. Therefore, the load causing these tips to buckle, $\mathbf{P_6}$, is equal to:

$$\frac{0.4254\pi^2 E}{12(1-\mu^2)}\left(\frac{t_{\text{flange}}}{b_{out}}\right)^2 = \frac{\left(\frac{P_6 L}{4}\right) y_{top}}{I} \rightarrow P_6 = \frac{1.7\pi^2 EI}{12 L y_{top}(1-\mu^2)}\left(\frac{t_{\text{flange}}}{b_{out}}\right)^2 \tag{30.10}$$

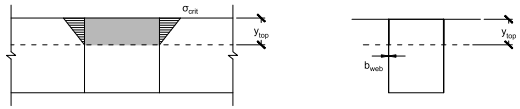

Fig. 30.5 – Buckling of the webs due to flexural compressive stresses. Side (left) and cross section (right) views.

The flexural compressive stresses can also cause the webs of the structure to buckle. These webs, which are oriented vertically, will experience compressive stresses which increase linearly from zero at the centroidal axis to a maximum at the top of the web. This linear gradient of stresses suggests that the plate buckling with the coefficient **k = 6** is the most appropriate. The load causing these webs to buckle, $\mathbf{P_7}$, is therefore equal to:

$$\frac{6\pi^2 E}{12(1-\mu^2)}\left(\frac{b_{web}}{y_{top}}\right)^2 = \frac{\left(\frac{P_7 L}{4}\right) y_{top}}{I} \rightarrow P_7 = \frac{24\pi^2 EI}{12 L y_{top}(1-\mu^2)}\left(\frac{b_{web}}{y_{top}}\right)^2 \tag{30.11}$$

*Note: Even when there is more than one web in the structure, the width of **one** web is used in the plate buckling equations. This is because the equations are used to describe the strength of each individual plate which may buckle independently of each other.*

*Note: In Eq. 30.11, the value of **y** used to calculate the flexural stresses should be $y_{top} - t_{flange}$. If the thickness of the flange is small compared to y_{top}, then the following approximation is appropriate:*

$$t_{\text{flange}} \ll y_{top} \rightarrow y_{top} \approx y_{top} - t_{\text{flange}}$$

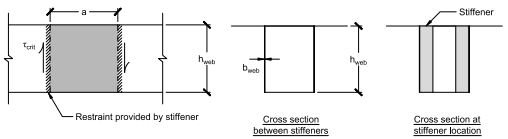

Fig. 30.6 – Buckling of the webs due to shear stresses. Side (left) and cross section (right) views.

Choosing the appropriate equation to determine when the webs buckle in shear is straightforward because only one of the four plate buckling equations is related to the shear stresses. Using Jourawski's equation and equating the critical shear buckling stress to the shear stresses in the web results in the following expression for $\mathbf{P_8}$, where **a** is the spacing of stiffeners which restrain the web from moving side to side:

$$\frac{5\pi^2 E}{12(1-\mu^2)}\left(\left(\frac{b_{web}}{h_{web}}\right)^2 + \left(\frac{b_{web}}{a}\right)^2\right) = \frac{\left(\frac{P_8}{2}\right) Q_{cen}}{2 I b_{web}} \rightarrow P_8 = \frac{20\pi^2 EI b_{web}^3}{12 Q_{cen}(1-\mu^2)}\left(\left(\frac{1}{h_{web}}\right)^2 + \left(\frac{1}{a}\right)^2\right) \tag{30.12}$$

The strength of the structure is governed by the lowest value of **P** obtained from the eight calculations. Note that under more complex loading and support conditions, more calculations will be required to obtain the failure load.

*Note: In design, appropriate factors of safety must be used to determine the lowest value of **P** which can be safely resisted by the structure.*

Lecture 31 – Building with Stone and Concrete

Overview

In this chapter, the unique characteristics of stone and concrete structures are discussed. Stone-like materials are typically strong in compression, have low tensile strength, and have significant self-weight. The theory used to design of arches and towers is presented.

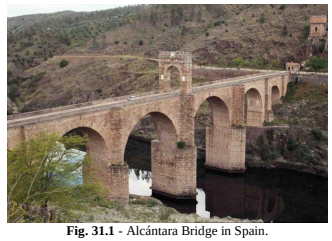

Fig. 31.1 - Alcántara Bridge in Spain.

Note: Masonry construction refers to the use of stones joined by mortar to build structures. The mortar is used to position the stone blocks together and fill in gaps as needed.

Unique Characteristics of Stone

The existence of stone structures which date back hundreds or thousands of years is evidence of the many strengths of these materials. Unlike organic materials like wood, or metallic materials like iron, stone is very durable and capable of surviving for many years under harsh weather conditions. An example of a stone structure which has survived over the centuries is the Alcántara Bridge in Spain, shown in Fig. 31.1, which was built in 106 AD, almost two thousand years ago.

Although stone is strong and durable, it is difficult to transport, and shape. Furthermore, stones suitable for construction are only found in certain geographical regions. A common alternative is to instead use ***concrete***, a Roman invention, which is manmade stone which addresses these shortcomings of natural stone. Concrete, which is made by mixing cement, water, air, fine aggregate (i.e., sand) and coarse aggregate (i.e., larger rocks), can be readily formed into any shape. Transporting its component ingredients is comparatively easy, making it a versatile material commonly used in modern construction. The Romans, however, were also experts of using concrete for their structures. An example of a Roman structure which demonstrates their mastery of the material is the Pantheon in Rome, which was built in 125 AD and still stands despite many wars and natural disasters occurring during its lifetime.

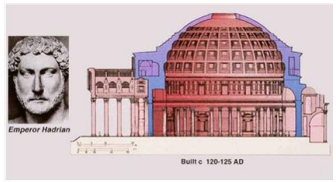

Fig. 31.2 – Pantheon in Rome.

Stone-like materials, like concrete, limestone, granite, etc., share many common material properties. They are heavy and tend to be formed into large structures, resulting in a substantial self-weight which must be included in their design. They tend to be strong in compression but weak in tension, and when they fail in tension, they exhibit little to no ductility. Stone structures have essentially the opposite characteristics of slender wires used to carry tensile loads, as they favour compression instead of tension, they are heavy instead of light, and they are brittle instead of tough.

True Theory of Arches

One common structural system used in buildings and bridges which uses stone is the arch. When designing arches, the shape must allow the applied loads from above to travel to the supports below without causing any tensile stresses in the structure. Although the Romans were experts at building arches, Robert Hooke later summarized his true theory of arches with the following statement:

"As hangs a flexible cable, so, inverted, stand the touching pieces of an arch"

Hooke's theory, shown in Fig. 31.3, illustrates the idea shape of an arch when supporting one, two, three, or four point loads. Under a uniformly distributed load, the ideal shape becomes a parabola, the same way a suspension bridge carries the uniformly distributed weight of a deck using a parabolic cable. The famous Catalan architect, Antoni Gaudí, made use of Hooke's theory of arches when designing his stone cathedrals. Fig. 31.4 shows one of his string models that he used to determine the form of his buildings.

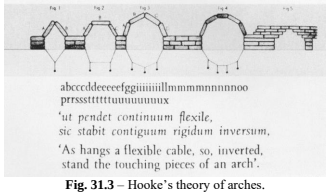

Fig. 31.3 – Hooke's theory of arches.

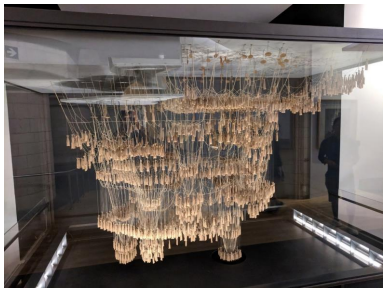

Fig. 31.4 – Model used by Antoni Gaudí to design stone cathedrals. The built shape was obtained by flipping the model upside down.

Design for Combined Axial Load and Bending Moment

Although the poor tensile strength of stone reduces the ability of masonry structures to resist large bending moments, their substantial self-weight allows some structures, like towers, to overcome this weakness. Consider the tower shown in Fig. 31.5, which is subjected to large horizontal forces from a severe windstorm. At the base of the structure, there must be a significant bending moment, $\mathbf{M_{base}}$, to prevent the tower from tipping over, and a high horizontal shear force, $\mathbf{V_{base}}$, to prevent it from sliding. There must also be a large vertical reaction force provided by the ground to support the self-weight of the tower, which places the tower in compression.

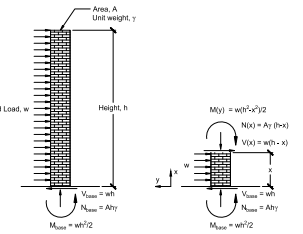

Fig. 31.5 – Stone tower subjected to high wind forces (left) and free body diagram at the base (right).

At the bottom of the tower, the axial force, **N**, is equal to the weight of the tower above. Using the unit density of the material, **γ**, the stress at the base caused by the axial load, σ_N, can be calculated to be:

$$\sigma_N = -\frac{N}{A} = -\frac{V_o\gamma}{A} \tag{31.1}$$

In Eq. (31.1), $\mathbf{V_o}$ is the volume of the tower, and the minus sign indicates that these stresses are compressive. In addition to the stress from the self-weight, there will also be stresses at the base of the tower due to the presence of the bending moment. These stresses, σ_M, can be calculated by using Navier's equation:

$$\sigma_M = \frac{My}{I} \tag{31.2}$$

The total stress in the tower at its base can be obtained by simply adding the two effects together if it is linear elastic. Therefore, the stress on the side where the wind blows, which would normally be in tension, is:

$$\sigma = -\frac{N}{A} + \frac{My_{\text{left}}}{I} \tag{31.3}$$

And the stress on the side opposite to the wind, which would normally be in compression, is:

$$\sigma = -\frac{N}{A} - \frac{My_{\text{right}}}{I} \tag{31.4}$$

Although the tower is subjected to a high moment, the stresses may remain compressive if the tower is heavy enough.

*Note: If the cross-sectional area of the tower is constant over its height, **h**, then the stress at the base can be calculated as:*

$$\sigma = \frac{V_o\gamma}{A} = \frac{Ah\gamma}{A} = h\gamma$$

Note: Due to the axial load, the stress in the member at the centroidal axis will no longer be equal to zero. This can be shown in Fig. 31.6.

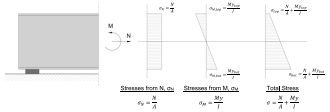

Fig. 31.6 – Stress distribution under combined axial load and bending moment

Lecture 32 – Reinforced Concrete: Material Properties

Overview

In this chapter, the material properties of concrete, steel, and reinforced concrete are discussed.

Reinforced Concrete

Concrete is the most commonly used building material in the world, having applications in the construction of roads, bridges, buildings, dams, tunnels and more. Besides being both strong and durable, concrete can be formed into any shape, offering a versatility which cannot be matched by other materials like steel and timber.

Although concrete, being a stone-like material, has poor tensile strength, this weakness can be addressed by providing reinforcement in the form of steel bars which are cast into the concrete. Concrete containing internal reinforcement is typically referred to as ***reinforced concrete***, while concrete without reinforcement is typically referred to as ***plain concrete***.

Material Properties of Concrete

The stress-strain response of concrete under axial load is shown in Fig. 32.2. In compression, the stress-strain response is linear until a stress of approximately 40% of the ultimate compressive stress is reached; after this, the behaviour is highly nonlinear. In tension, the behaviour is linear elastic until the concrete fails by cracking, which typically occurs at a stress around 2 to 3 MPa.

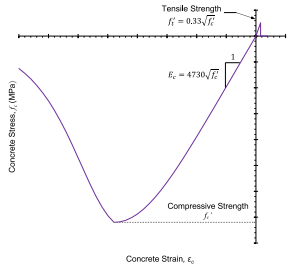

Fig. 32.2 – Stress-strain response of plain concrete under axial load.

When building concrete structures, it is customary to cast small concrete cylinders made from the same concrete, which are tested later to measure the material properties of the concrete present in the actual structure. These cylinders are tested in compression to determine the compressive strength of the concrete, f_c', which is then correlated to other

Fig. 32.1 – Large reinforced concrete beam in the Bahen Centre for Information Technology at the University of Toronto. Details of the internal reinforcement are shown.

Note: Although steel is typically used as reinforcement, other materials can be used as well. Common alternatives include using glass fibre reinforced polymer (GFRP) bars or embedding steel or polymer fibers into the concrete to create Fiber Reinforced Concrete (FRC).

*Note: The notation for stresses for concrete structures differs from the notation used for the rest of the course. Axial stresses are represented as **f** and shear stresses are represented as **v**, instead of σ and τ respectively.*

properties using empirical equations. Concrete which has a compressive strength of less than 40 MPa is ***normal strength concrete***. Special circumstances may necessitate the use of ***high strength concrete***, which has a higher compressive strength that can exceed 100 MPa.

Given the concrete compressive strength, f_c', a common empirical equation to estimate the tensile strength of the concrete, f_t', is:

$$f_t' = 0.33\sqrt{f_c'} \tag{32.1}$$

Like the tensile strength, the Young's modulus of the concrete, $\mathbf{E_c}$, can also be correlated with the compressive strength of the concrete. Although there are many equations in the literature which express $\mathbf{E_c}$ as a function of f_c', a common expression used for concrete whose strength is 40 MPa or less is:

$$E_c = 4730\sqrt{f_c'} \tag{32.2}$$

When using Eq. (32.1) and (32.2), f_t' and $\mathbf{E_c}$ will be in units of MPa if f_c' is also in MPa.

Material Properties of Reinforcing Steel

To reinforce concrete members, steel reinforcing bars are bent and tied together to form complex, interlocking cages like the one shown in Fig. 32.3. The stress-strain response of these steel reinforcing bars under axial load is shown in Fig. 32.4. Reinforcing steel bars, colloquially referred to as ***rebars***, are made of mild steel and are manufactured to have surface deformations to help anchor them into the surrounding concrete. The Young's modulus of the steel is taken as $\mathbf{E_s}$ **= 200,000 MPa**, and the yield strength of Canadian reinforcing bars is typically f_y **= 400 MPa** in both tension and compression.

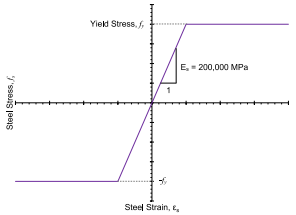

Fig. 32.4 – Stress-strain response of reinforcing steel under axial load.

Note: Performing tensile tests on stone-like materials is very difficult. For this reason, it is more common to correlate the cracking stress with the compressive strength.

Note: Another equation for E_c which appeared in previous versions of the CIV102 notes is the following:

$$E_c = 3320\sqrt{f_c'} + 6900 \tag{32.3}$$

When solving reinforced concrete problems which do not provide E_c in the question, use Eq. (32.2) to estimate E_c if needed.

Note: Although E_s is 200,000 MPa for all types of steel, different countries use different steel strengths. For example, in USA, it is customary to use steel which has a yield strength of 60 ksi (414 MPa).

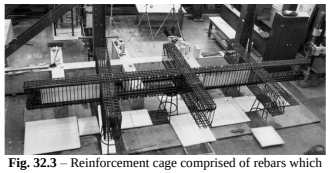

Fig. 32.3 – Reinforcement cage comprised of rebars which are bent and tied together.

Table 32.1 – Common Canadian Reinforcing Bar Information

Designation	Linear Density (kg/m)	Nominal Diameter (mm)	Cross-Sectional Area (mm^2)
10M	0.785	11.3	100
15M	1.570	16.0	200
20M	2.355	19.6	300
25M	3.925	25.2	500
30M	5.495	29.9	700
35M	7.850	35.7	1000
45M	11.775	43.7	1500
55M	19.625	56.4	2500

Steel producers fabricate rebar into many standardized sizes. Table 32.1, which is also found in Appendix G, shows the common types of rebar which are available in Canada. The bar number roughly refers to the diameter of the bar, although the actual diameter is usually slightly larger. The smaller bars (10M and 15M) are usually used for reinforcement which needs to be bent into compact shapes, while the larger bars are more difficult to bend and are usually used where straight bars are needed.

Material Properties of Reinforced Concrete

Fig. 32.4 shows the stress-strain response of a concrete member which is reinforced with steel bars. Its response under compression is similar to that of plain concrete because the steel only provides a small increase in compressive strength. In tension however, the response is substantially different, especially after the concrete cracks. When this occurs, the tensile force is carried by the steel instead of by the cracked concrete, which allows substantial tensile forces to be carried by the material. The response of the material becomes also ductile because failure in tension occurs due to the steel yielding instead of the concrete cracking. The presence of steel also affects the pattern of cracking and the sizes of the individual cracks. As the amount of steel in the concrete increases, more cracks form which have smaller widths because the elongation of the member is distributed over many cracks, instead of being localized at one location.

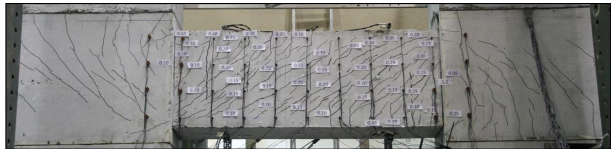

Fig. 32.6 – Heavily reinforced coupling beam tested at the University of Toronto by Fischer et al. Electronic measuring gauges are attached to the surface of the concrete, and labels indicate the measured crack widths in mm.

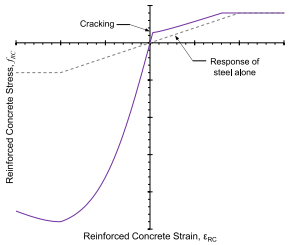

Fig. 32.5 – Stress-strain response of reinforced concrete under axial load.

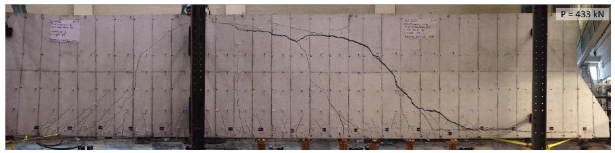

32.7 – Large slab strip tested at the University of Toronto by Quach et al. The right-hand side contained no vertical reinforcement and failed in a brittle manner.

The heavily reinforced beam shown in Fig. 32.6 illustrates the ability of internal reinforcement to improve the behaviour of concrete members after cracking. This beam, loaded under moment and shear, was capable of carrying significant forces after cracking. Because large amounts of steel were used to reinforce it, the shear and flexural deformations are distributed over many narrow cracks. This member failed in a ductile manner once the steel began to yield.

Fig. 32.7 shows a reinforced concrete beam built without vertical reinforcement in its East (right) span. Because there was no vertical reinforcement, the deformations caused by the shear forces were concentrated at a single wide crack, which ultimately caused its failure. This member failed in a brittle manner once widening and sliding along the crack reduced its load-carrying capacity to be less than the applied load.

The benefits of using steel reinforcement in concrete can be summarized below:

i. It provides tensile capacity in a member after the concrete cracks.
ii. It controls the crack widths after cracking occurs, so that tensile deformations are distributed over multiple narrow cracks, instead of fewer wide cracks.

In design, it is customary to use different factors of safety associated with the stresses in the concrete and in the steel. Concrete, whose strength can be affected by factors like how it was cast, variances in the mix and the curing environment, is typically associated with a larger factor of safety compared to steel, which is a typically manufactured in controlled conditions. ***In CIV102, we will account for these by using partial safety factors to reduce the strength of concrete by 0.5 and reduce the strength of steel by 0.6 when designing reinforced concrete members.***

Lecture 33 – Reinforced Concrete Members – Design for Flexure

Overview

In this chapter, the behaviour of reinforced concrete structures subjected to bending moments is described. A simple procedure which can be used to design the flexural reinforcement or estimate the flexural strength of a reinforced concrete member is presented.

Overview of Flexural Behaviour

The response of a reinforced concrete member subjected to bending moments can be described as having three distinct phases, which are shown in Fig. 33.1. For small loads, the stresses in the concrete will be low and the member will exhibit linear elastic behaviour. During this portion of the member's life, the presence of the reinforcing steel has little influence of the flexural response, and Navier's equation can be used to determine the stresses in the concrete.

At larger loads, the flexural stresses obtained by using Navier's equation will exceed the tensile strength of the concrete, and vertical cracks will form. After this happens, the member will continue to carry bending moments with the concrete carrying the compression forces on one side of the member, and the longitudinal steel reinforcement carrying the tension forces on the other side of the member. During this stage, the compressive stresses in the concrete and the tensile stresses in the steel are relatively low, and they will both behave in a linear elastic manner. This sort of load-carrying mechanism is sometimes referred to as the cracked elastic state of the member.

Under larger loads, the reinforcement will begin to yield, and the concrete will begin to crush, which results in a nonlinear response being observed. If the steel yields before the concrete crushes, then the failure mode will be ductile, and large deformations will occur before the beam finally breaks. If the opposite is true, then the member may fail more suddenly. Analyzing the nonlinear behaviour requires more advanced tools and is beyond the scope of CIV102.

The primary task involved when designing for flexure is to determine how much longitudinal steel is needed to carry the bending moments. This steel is provided on the side of the beam experiencing tension, so that the tensile forces in the steel and the compressive forces in the concrete together resist the applied moments.

Cracked Elastic Response

To analyze the flexural behaviour of a reinforced concrete member after it has cracked, the following assumptions are made:

i. Plane sections remain plane, and hence there are longitudinal strains which vary linearly over the height of the member
ii. The concrete cannot carry any tensile stresses
iii. The steel is perfectly bonded to the concrete, so that the concrete and steel experience the same strain at every point

Consider the cracked reinforced concrete beam shown in Fig. 33.2 which bends as it supports the applied loads. The bending moments carried by the member causes vertical cracks to form on the bottom of the beam. To resist the applied loads after cracking occurs, longitudinal steel reinforcement is required. The steel carrying the flexural tension has a total area of $\mathbf{A_s}$ and the distance from the extreme compression fibre of the beam to the centroid of this reinforcement is equal to **d**.

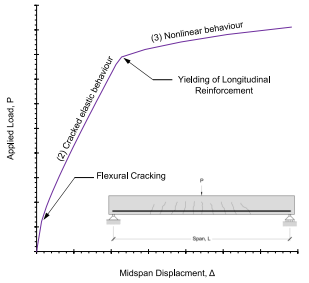

Fig. 33.1 – Typical load-displacement plot of a reinforced concrete beam subjected to bending.

Fig. 33.2 – A reinforced concrete beam tested by Garratt et al. which failed in flexure. Note the large cracks and displacements, as well as the crushed concrete at the top of the beam.

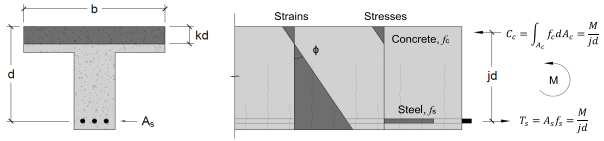

Fig. 33.3 – Schematic of a cracked reinforced concrete beam subjected to bending moments, showing the distribution of strains, stresses and forces.

As the cracked beam curves, there will be longitudinal strains which vary linearly over the height of the member. If the curvature, $\boldsymbol{\phi}$, is known, then the longitudinal strain, $\boldsymbol{\varepsilon}$, at a distance **y** from the neutral axis will be equal to:

$$\varepsilon = \phi y \tag{33.1}$$

Although this is the same equation which we used in Lecture 10 for elastic beams, the neutral axis of the cracked member will not align with the centroidal axis of the cross section because the cracked concrete cannot carry any tensile stresses. To determine the location of the new neutral axis of the cracked member, we need to find the corresponding strain conditions which guarantee that the net axial force in the member is zero.

If we define the distance from the extreme compression fibre to the neutral axis as **kd**, then we can express the curvature of the section as:

$$\phi = \frac{\varepsilon_{c,top}}{kd} = \frac{\varepsilon_{c,top} + \varepsilon_s}{d} \tag{33.2}$$

In Eq. (33.2), $\boldsymbol{\varepsilon_{c,top}}$ is the concrete strain at the top of the section, and $\boldsymbol{\varepsilon_s}$ is the strain in the steel, which is located a distance **d** from the top of the section. Rearranging Eq. (33.2) results in the following equations for these strains in terms of the curvature and **kd**:

$$\varepsilon_{c,top} = \phi kd \tag{33.3}$$

$$\varepsilon_s = \phi d(1-k) \tag{33.4}$$

Using Hooke's law, the stresses in the concrete and steel can be obtained once these strains are known. The concrete carries compressive stresses which increase linearly from 0 at the depth of compression to a maximum at the top of the section, and the steel carries a tensile stress at the location of the bars. The net compressive force in the concrete, $\mathbf{C_c}$, can be obtained by integrating the concrete stresses over the cross section, resulting in:

Note: Here, the strains in the compression region, like $\varepsilon_{c,top}$, are taken as positive numbers even though it is understood that they are compressive.

$$C_c = \int_{A_c} f_c dA_c = \int_{A_c} E_c \varepsilon_c dA_c = \frac{1}{2} bkd E_c \varepsilon_{c,top} \quad (33.5)$$

The net tensile force in the steel, $\mathbf{T_s}$, can be obtained by multiplying the steel stresses over the cross section, which results in:

$$T_s = f_s A_s = E_s \varepsilon_s A_s \quad (33.6)$$

For a member subjected to pure bending, there will be no net axial force and therefore the compressive force in the concrete must equal to the tensile force carried by the steel. Therefore, setting Eqs. (33.5) and (33.6) to equal each other and substituting the expressions for $\varepsilon_{c,top}$ and ε_s into the resulting equation yields:

$$\frac{1}{2}\phi b(kd)^2 E_c = \phi E_s A_s d(1-k) \quad (33.7)$$

Eliminating ϕ from Eq. (33.7) and rearranging terms results in the following quadratic equation for **k**:

$$\frac{1}{2}k^2 + k\frac{E_s}{E_c}\frac{A_s}{bd} - \frac{E_s}{E_c}\frac{A_s}{bd} = 0 \quad (33.8)$$

We can abbreviate Eq. (33.8) by defining the modular ratio, **n**, as the following:

$$n = \frac{E_s}{E_c} \quad (33.9)$$

Furthermore, we will define the quantity of longitudinal reinforcement, **ρ**, as:

$$\rho = \frac{A_s}{bd} \quad (33.10)$$

Substituting these new quantities into Eq. (33.8) allows it to be rewritten in the following form:

$$\frac{1}{2}k^2 + kn\rho - n\rho = 0 \quad (33.11)$$

Solving for Eq. (33.11) using the quadratic equation results in the following equation for **k**:

$$k = \sqrt{(n\rho)^2 + 2n\rho} - n\rho \quad (33.12)$$

Having found the required value of **k** so that the net axial force carried by the member equals to zero under pure moment, the bending moment carried by the member, **M**, can now be obtained by using fact that the compression

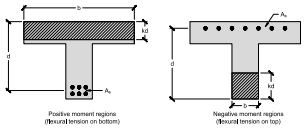

Fig. 33.4 – Definition of b.

Note: b is defined as the width of the of the compression side of the member. Therefore, for this T-beam, b is the width of the flange when it is carrying positive moments, and width of the stem when it is carrying negative moments.

force in the concrete, $\mathbf{C_c}$, is equal and opposite to the tension force in the steel, $\mathbf{T_s}$. Together, they form a couple which has the following properties:

$$M = C_c jd = T_s jd \quad (33.13)$$

In Eq. (33.11), **jd** is the vertical distance between the compressive and tensile forces and is called the ***flexural lever arm***. Because the concrete stresses, are distributed in a triangular pattern over the height **kd**, the resultant compressive force is located at a distance of kd/3 from the top of the member. Therefore, **jd** is equal to:

$$jd = d - \frac{1}{3}kd \rightarrow j = 1 - \frac{1}{3}k \quad (33.14)$$

Knowing the value of the flexural lever arm is important as it provides the necessary link between the bending moment carried by the member and the stress in the reinforcement, $\boldsymbol{f_s}$. This relationship can be determined by combining Eqs. (33.6) and (33.13):

$$M = A_s f_s jd \rightarrow f_s = \frac{M}{A_s jd} \quad (33.15)$$

If the steel is still linear elastic, the strain in the steel can be obtained by using Hooke's law and dividing $\boldsymbol{f_s}$ by the Young's modulus of steel, $\mathbf{E_s}$. Substituting the steel strain into Eq. (33.4), results in the following equation for the curvature of the member:

$$\phi = \frac{M}{A_s E_s jd^2(1-k)} \quad (33.16)$$

Substituting Eq. (33.16) in Eq. (33.3) and multiplying the concrete strain by $\mathbf{E_c}$ results in a compact equation for the maximum concrete stress when the member is carrying the bending moment:

$$f_c = \frac{k}{1-k}\frac{M}{nA_s jd} \quad (33.15)$$

Finally, the maximum moment which can be carried by the member if it fails by yielding of the flexural reinforcement can be determined if we use Eq. (33.13) and let the steel stress $\boldsymbol{f_s}$ equal the yield stress $\boldsymbol{f_y}$:

$$M_{yield} = A_s f_y jd \quad (33.16)$$

Design Process Summary

The following steps outline a procedure for proportioning the longitudinal reinforcement in a beam to safely resist bending moments which result from applied loads.

i. Obtain the bending moment diagram and determine the moment which must be resisted by the beam, **M**.
ii. Using a provided value of **d**, estimate **k** and **j** to be **k = 3/8** and **j = 7/8**. If it is assumed that the maximum allowable tensile stress in the steel is $\mathbf{0.6}\boldsymbol{f_y}$, then the required area of steel is:

$$A_{s,min} = \frac{M}{0.6 f_y jd}$$

iii. Using the rebar table in Appendix G, select the number of bars needed so that the area of longitudinal steel, $\mathbf{A_s}$, is greater or equal to $\mathbf{A_{s,min}}$.
iv. Calculate the actual value of **k**. Recall that $\mathbf{n = E_s/E_c}$ and $\boldsymbol{\rho = A_s/bd}$.

$$k = \sqrt{(n\rho)^2 + 2n\rho} - n\rho$$

v. Calculate the actual length of the flexural lever arm, **jd**:

$$jd = d\left(1 - \frac{1}{3}k\right)$$

vi. Check to ensure that the steel stress, $\boldsymbol{f_s}$, does not exceed $0.6\boldsymbol{f_y}$:

$$f_s = \frac{M}{A_s jd} \leq 0.6 f_y$$

vii. Check to ensure that the concrete stress, $\boldsymbol{f_c}$, does not exceed $0.5\boldsymbol{f_c'}$:

$$f_c = \frac{k}{1-k}\frac{M}{nA_s jd} \leq 0.5 f_c'$$

When checking if a design is safe, only steps i and iv to vii need to be performed.

Lecture 34 – Reinforced Concrete Members – Design for Shear

Overview

In this chapter, the behaviour of reinforced concrete members subjected to shear is discussed. The Simplified Method for shear design in the Canadian concrete design code, CSA A23.3:19, is presented, and its application for both designing members for shear and evaluating the shear strength of existing structures is explained.

Historical Background

Shear stresses in reinforced concrete members can cause failure due to the resulting diagonal tensile and compressive stresses. If a member does not contain adequate amounts of shear reinforcement, vertical bars which run perpendicular to the longitudinal steel, then it may fail suddenly without obvious signs of distress. The mechanism by which reinforced concrete members carry shear is complex, and there have been significant structural failures in the 20th century due to inadequate design and construction practices. Some notable shear failures include the collapse of the Sleipner A offshore platform in 1991, which imploded while under construction, leading to an estimated cost of $700 million (USD), and the collapse of the De la Concorde overpass in 2006, which killed five people and left six others with serious injuries. Photos of these collapses are shown in Fig. 34.1.

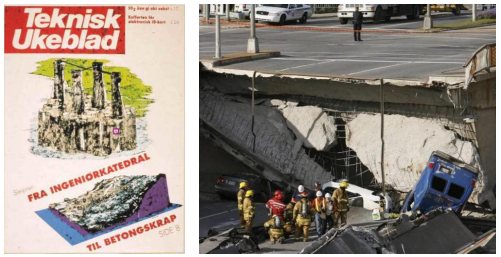

Fig. 34.1 – Collapse of the Sleipner A platform (left) and De la Concorde overpass (right). The magazine title translates to "From Engineering Cathedral to Concrete Scrap".

Research work performed at the University of Toronto has led to significant advances in the understanding of how reinforced concrete carries shear stresses. Experiments performed on concrete specimens using unique equipment like the Panel Element Tester and Shell Element Tester, shown in Fig. 34.2, have led to the development of the ***Modified Compression Field Theory,*** which serves as the theoretical basis for the Canadian and Australian concrete design codes, the fib Model Code 2010 and the American bridge design code.

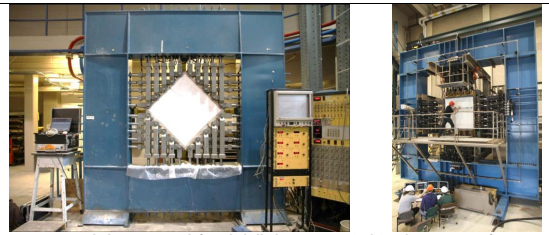

Fig. 34.2 – Panel Element Tester (left) and Shell Element Tester (right) at the University of Toronto.

Overview of Shear Behaviour

Recall from Lecture 25 that shear stresses in beams cause diagonal compressive and tensile stresses. Because concrete has a low tensile strength, these tensile stresses cause diagonal cracks to form. After cracking, the reinforced concrete has two basic mechanisms for carrying shear stresses:

i. **Aggregate Interlock** – shear stresses acting along the crack surfaces, which are rough due to the aggregate embedded in the concrete, along with tensile stresses in the longitudinal steel carry tension across the crack.
ii. **Shear Reinforcement** – steel reinforcement which is perpendicular to the longitudinal reinforcement carry tensile stresses which, along with the tensile stresses in the longitudinal steel, carry tension across the crack.

The first mechanism is the predominant method of carrying shear for members which do not have shear reinforcement and its strength is strongly influenced by the width of the cracks which form under shear loading. A close-up photo showing interlocking of the aggregate is shown in Fig. 34.3.

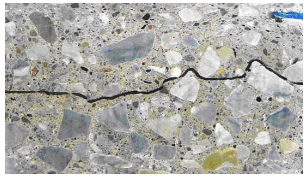

Fig. 34.3 – Interlocking of aggregate in a concrete member, preventing sliding along the crack.

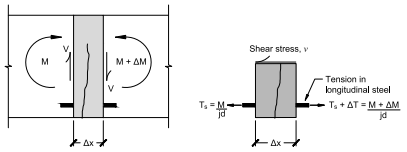

Fig. 34.5 – Derivation of shear stresses in a cracked concrete member.

After cracking, the shear stress distribution no longer follows the shape predicted by Jourawski's equation because the tensile capacity of the concrete is severely reduced. Consider a slice of a beam with a width **Δx** shown from elevation view, like in Fig. 34.5. Recall that the shear force, **V**, is related to the bending moment **M**, by:

$$V = \frac{dM}{dx} \tag{34.1}$$

The change in moment leads to an increase in the tensile forces in the longitudinal steel, which is related to the tension in the steel, $\mathbf{T_s}$, by the flexural lever arm, **jd**. Therefore, Eq. (34.1) can be rewritten in terms of the change in tension force in the longitudinal steel, $\mathbf{\Delta T_s}$:

$$M = T_s jd \rightarrow V = \frac{\Delta T_s jd}{\Delta x} \tag{34.2}$$

The change in tension force in the longitudinal steel is due to the shear stresses which act over the area defined by the web width, $\mathbf{b_w}$, and the length of our slice, **Δx**. Horizontal equilibrium requires that the shear stresses, ***v***, must be defined as:

$$v b_w \Delta x = \Delta T_s \tag{34.3}$$

Substituting Eq. (34.2) in Eq. (34.3) and eliminating **Δx** from the equation results in the following equation for the maximum shear stress in a cracked concrete member, which occurs in its web:

$$v = \frac{V}{b_w jd} \tag{34.4}$$

A shear failure in a member occurs when the shear stress exceeds its shear capacity. As previously noted, the shear capacity is related to the strength offered by the aggregative interlock, $\mathbf{v_c}$, and the shear strength offered by the steel shear reinforcement, $\mathbf{v_s}$. In heavily reinforced members which contain large amounts of reinforcement, then another

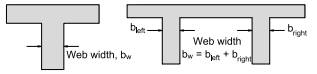

Fig. 34.6 – Effective web width, b_w.

Note: the web width may consider adjacent webs, like in the case of the double-tee beam shown in Fig. 34.6.

possible failure mode is if the diagonal compression from the shear causes crushing to take place. The shear stress which causes this to occur, $\mathbf{v_{max}}$, is defined in the Canadian concrete design code as:

$$v_{max} = 0.25 f_c' \tag{34.5}$$

Where $\mathbf{f_c'}$ is the compressive strength of the concrete. Putting these concepts together, the shear strength of a member, $\mathbf{V_r}$, is equal to strength attributed to the concrete, $\mathbf{V_c}$, plus the strength attributed to the steel, $\mathbf{V_s}$, which must be less than $\mathbf{V_{max}}$. To provide an adequate factor of safety in design, the terms associated with the concrete strength are also multiplied by 0.5, and the terms associated with the steel strength are multiplied by 0.6, which results in the following equation:

$$V_r = 0.5V_c + 0.6V_s \leq 0.5V_{max} \tag{34.6}$$

Finally, when designing for shear, the value of the shear force at the location of a reaction force or concentrated point load is typically not used. These regions are "disturbed" by local compressive stresses, since the forces tend to compress the member in the transverse direction where they are applied. Because shear failures are typically associated with diagonal tension, the additional compression helps to prevent a failure from occurring in these regions. Instead, the shear force which is located a distance **d** away from the reaction force or point load is typically used for analysis and design, where **d** is the distance between the longitudinal steel and the compression face of the member as used for flexural design. Fig. 34.7 illustrates the shear force which should be used in design.

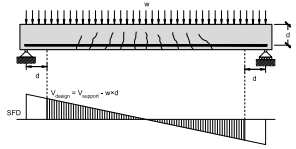

Fig. 34.7 – Design shear force.

Shear Capacity of Members Without Shear Reinforcement

Slabs, which are used commonly used in floors or foundations of a building, are often built without shear reinforcement. Therefore, their shear strength solely depends on the ability of the concrete to carry stresses across the cracks via aggregate interlock. The shear strength is strongly related to how thick the member is, because larger members tend to have wider cracks. Since aggregate interlocking becomes less effective as the cracks get larger, the shear strength, $\mathbf{v_c}$, tends to become smaller as the overall depth of the member increases. This is called the ***size effect*** and has been observed in experiments done at the University of Toronto and other institutions. Fig. 34.8 shows the effect of member depth on predicted shear strength using the Canadian code, as well as the shear strengths of many experiments.

Note: $\mathbf{v_c}$ and $\mathbf{v_s}$ correspond to the shear strengths associated with the concrete and steel respectively in units of MPa. To determine the corresponding shear force, $\mathbf{V_c}$ and $\mathbf{V_s}$ respectively, these quantities should be multiplied by $b_w jd$ in accordance with Eq. (34.4)

Note: The maximum shear force causing crushing is equal to:

$$V_{max} = 0.25 f_c' b_w jd$$

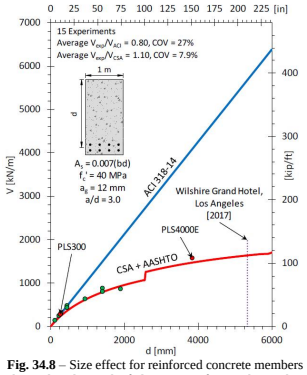

Fig. 34.8 – Size effect for reinforced concrete members subjected to shear. The failure stress of a member without shear reinforcement decreases as it becomes deeper.

The equation for the shear strength of members without shear reinforcement is given in Eq. (34.7). This equation is based on the Modified Compression Field Theory and is used for shear design in Canada.

$$V_c = v_c b_w jd = \frac{230\sqrt{f_c'}}{1000 + 0.9d} b_w jd \tag{34.7}$$

In Eq. (34.7), $\mathbf{V_c}$ is the shear strength in units of force, $\mathbf{f_c'}$ is the compressive strength of the concrete in MPa, **d** is the effective depth in mm, $\mathbf{b_w}$ is the width of the web and **jd** is the flexural lever arm.

Shear Capacity of Members Containing Shear Reinforcement

Shear reinforcement are bars which are perpendicular to the direction of the longitudinal reinforcement. They are commonly inserted into reinforced concrete members by bending bars to form hoops or U-shapes, which are commonly referred to as ***stirrups*** in North America. Some examples of shear reinforcement are shown in Fig. 34.9. The area of shear reinforcement, $\mathbf{A_v}$, refers to the total cross-sectional area of the bars which are oriented vertically, and the primary task of an engineer is to determine their spacing to ensure that the member has adequate shear strength.

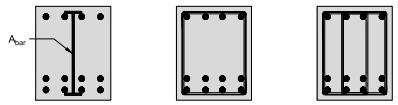

Fig 34.9 – Types of shear reinforcement and corresponding values of A_v.

Providing shear reinforcement has two benefits: the bars themselves provide additional shear strength, $\mathbf{V_s}$, and they control the width of the diagonal cracks, which improves the aggregate interlocking strength and hence increases $\mathbf{V_c}$ as well. The shear strength provided by the stirrups can be described by visualizing how the stresses in a cracked reinforced concrete beam are carried, with fields of diagonal compression in the concrete being equilibrated by the tensile stresses in the shear reinforcement, which have an area of $\mathbf{A_v}$ and spacing **s**. This is shown in the left diagram in Fig. 34.10.

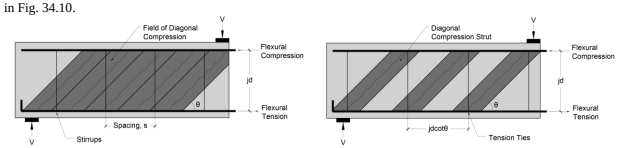

Fig. 34.10 – Diagonal stress fields in a cracked reinforced concrete beam (left) and Simplified truss model for concrete members subjected to shear (right).

Note: the shear strength (in MPa) attributed to the concrete, $\mathbf{v_c}$, is equal to:

$$v_c = \frac{230\sqrt{f_c'}}{1000 + 0.9d}$$

The right diagram in Fig. 34.10 shows a simplified representation of the left diagram. Here, the member is treated as a truss with a height of **jd** and contains discrete diagonal compression members inclined at an angle of **θ** from the longitudinal axis. Given these geometric constraints, the vertical tension members in this equivalent truss model must be spaced at **jdcotθ** and have a cross sectional area, **A**, equal to the following:

$$\frac{A}{jd\cot\theta} = \frac{A_v}{s} \rightarrow A = \frac{A_v jd\cot\theta}{s} \tag{34.8}$$

If yielding of these vertical tension members governs the failure of the member, then the maximum shear force which can be carried in the equivalent truss, $\mathbf{V_s}$, will occur when the stress in these bars reaches the yield stress, $\boldsymbol{f_y}$:

$$V_s = \frac{A_v f_y jd}{s}\cot\theta \tag{34.9}$$

In the Canadian design code, the angle of the diagonal stresses is assumed to be equal to θ = 35°, resulting in the following equation for $\mathbf{V_s}$:

$$V_s = \frac{A_v f_y jd}{s}\cot 35° \tag{34.10}$$

For small amounts of shear reinforcement, $\mathbf{V_c}$ is still calculated by using Eq. (34.7). However, if the quantity of shear reinforcement exceeds a threshold value, then the size effect disappears, and an improved equation can be used. This minimum reinforcement requirement is:

$$\frac{A_v f_y}{b_w s} \geq 0.06\sqrt{f_c'} \tag{34.11}$$

If Eq. (34.11) is satisfied, then $\mathbf{V_c}$ is instead calculated as:

$$V_c = v_c b_w jd = 0.18\sqrt{f_c'} b_w jd \tag{34.12}$$

Although there are many concepts covered in this chapter, applying them to solve problems is relatively straightforward. There are two primary uses of the equations, which are to (1) evaluate the shear strength of a member or (2) design the shear reinforcement by selecting the appropriate spacing of stirrups. Each process is described in the following summary sections.

Note: The shear strength (in MPa) attributed to the steel, $\mathbf{v_s}$, is equal to:

$$v_s = \frac{V_s}{b_w jd} = \frac{A_v f_y}{b_w s}\cot 35°$$

Note: The equation for $\mathbf{v_c}$ when at least a minimum amount of shear reinforcement is present is equal to:

$$v_c = 0.18\sqrt{f_c'}$$

Summary - Evaluating the Shear Strength of a Member

This procedure applies when the failure load of a member is needed. Because we are dealing with structural failure, the partial safety factors, 0.5 for concrete and 0.6 for steel, are not used.

i. Solve for the reaction forces and obtain the shear force and bending moment diagrams. Determine the maximum shear force, **V**, which is not located within **d** of a reaction force or applied point load.
ii. Calculate the relevant parameters used for flexural behaviour, such as **n**, **ρ**, **k** and **j**. Recall that:

$$k = \sqrt{(n\rho)^2 + 2n\rho} - n\rho$$

$$j = 1 - \frac{1}{3}k$$

iii. Check if the provided amount of reinforcement meets or exceeds the minimum reinforcement requirement described in Eq. (34.11). Calculate $\mathbf{V_c}$ using the appropriate equation.

$$V_c = \begin{cases} \dfrac{230\sqrt{f_c'}}{1000 + 0.9d} b_w jd & \dfrac{A_v f_y}{b_w s} < 0.06\sqrt{f_c'} \text{ or no stirrups} \\ 0.18\sqrt{f_c'} b_w jd & \dfrac{A_v f_y}{b_w s} \geq 0.06\sqrt{f_c'} \end{cases}$$

iv. If shear reinforcement is present, calculate $\mathbf{V_s}$:

$$V_s = \frac{A_v f_y jd}{s}\cot 35°$$

v. Calculate the shear strength of the member, $\mathbf{V_r}$:

$$V_r = V_c + V_s \leq V_{max} = 0.25 f_c' b_w jd$$

vi. Failure of the member occurs when the applied shear force is equal to the shear resistance.

$$V = V_r$$

Summary – Designing the Shear Reinforcement of a Member

The first two steps of this procedure are the same as the procedure for evaluating the shear strength of a member, which are finding the shear force diagram and determining the flexural properties **k** and **j**. Once these are found, then the required task involves determining if shear reinforcement is needed, and if so, the calculating the required spacing **s**.

i. Same as step i in the previous procedure.
ii. Same as step ii in the previous procedure.
iii. Check if the shear demand, **V**, exceeds $\mathbf{0.5V_{max}}$. If so, the cross section is too small and needs to be resized. Otherwise, proceed to step iv.

$$0.5 \times V_{max} = 0.125 f_c' b_w jd$$

iv. Check to see if the shear force can be resisted by the $\mathbf{V_c}$ alone. If so, the design is complete.

$$V_r = 0.5V_c = 0.5\frac{230\sqrt{f_c'}}{1000 + 0.9d} b_w jd$$

v. If the shear force cannot be carried by $\mathbf{V_c}$ alone, provide the minimum amount of shear reinforcement and check if this results in enough capacity to carry the shear demand. Remember that providing the minimum amount of shear reinforcement permits Eq. (34.12) to be used when calculating $\mathbf{V_c}$ instead of Eq. (34.7)

$$\frac{A_v f_y}{b_w s} = 0.06\sqrt{f_c'} \rightarrow s = \frac{A_v f_y}{0.06\sqrt{f_c'} b_w}$$

$$V_r = 0.5V_c + 0.6V_s = 0.5 \times 0.18\sqrt{f_c'} b_w jd + 0.6 \times \frac{A_v f_y jd}{s}\cot 35°$$

vi. If the shear capacity is still too low, then a smaller spacing must be obtained to carry the shear force. This spacing, **s**, can be obtained by letting **V** = $\mathbf{V_r}$ and re-arranging the equation, resulting in the following:

$$s = \frac{0.6 \times A_v f_y jd\cot 35°}{V - 0.5 \times 0.18\sqrt{f_c'} b_w jd}$$

Lecture 35 – Prestressed Concrete Structures

Overview

In this chapter, the fundamental behaviour of prestressed concrete members is discussed. The force-in-the-tendon method to determine the stresses in a prestressed concrete member subjected to bending moments is presented.

Prestressed Concrete

In many ways, prestressed concrete is similar to reinforced concrete. Steel reinforcement is cast into the concrete and after the concrete cracks under loads, the steel carries tensile forces to increase the structure's load-carrying capacity. Unlike reinforced concrete however, prestressing the reinforcement results in the steel carrying significant tensile forces before the external loads are applied. Because the steel is embedded into the concrete, these tensile forces in the steel cause the concrete to be in a state of compression. Prestressed reinforcement is sometimes referred to as ***active reinforcement*** because the steel is actively in a state of tension, which contrasts with ***passive reinforcement***, which is only engaged once the concrete cracks.

The precompression applied to the concrete by the prestressed reinforcement has a significant impact on its load-deformation response because significant tensile forces are now needed to overcome the precompression and cause cracking. Therefore, under the loads which are expected under typical daily situations, the concrete will remain uncracked and behave in a linear elastic manner. Figure 35.1 illustrates the difference prestressing can make for a beam carrying a uniform load. For loads which are about half of the predicted failure load, which corresponds to a typical factor of safety, the reinforced concrete beam deflects significantly more than the equivalent prestressed beam.

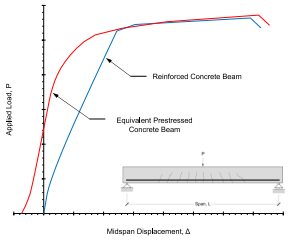

Fig. 35.1 – Comparison of load-deformation response of equivalent reinforced and prestressed concrete members.

The stresses in the concrete and steel caused by prestressing are said to be self-equilibrating, meaning that they balance each other out without the influence of external loads. Therefore, the total stresses in the concrete can be calculated as the sum of the stresses caused by prestressing and the stresses caused from axial loads, shear forces, and moments.

Note: Prestressed concrete requires using high-strength steel and high strength concrete. This is so the steel can be stressed to carry large forces to compress the concrete and not yield or rupture. The steel must also be able to sustain these stresses over the lifetime of the structure and minimize losses due to effects like creep. The concrete must have a high compressive strength to avoid crushing under the combined effects of the applied loads and the prestress.

Fig. 35.2 – Skilled worker post-tensioning cables in a concrete member using a hydraulic jack.

*Note: There are two primary means of prestressing concrete. The first method, called **pre-tensioning**, involves casting concrete around strands of steel which are being pulled. Once the concrete hardens, the steel is cut from the bed and embedded parts compress the concrete. The second method, called **post-tensioning**, involves casting hollow ducts into the concrete. Once the concrete hardens, steel strands are inserted into the ducts where they are stressed and anchored.*

*Note: The prestressed reinforcement in a prestressed concrete member is sometimes referred to as **tendons**.*

Calculating Stresses in Prestressed Concrete Members with Concentric Tendons

Consider the prestressed member shown in Fig. 35.3, which has a tendon running along its centroidal axis. The tendon is stressed to carry a tensile force, **P**, which compresses the concrete. The member is simply supported over a span **L** and carries a uniformly distributed load along its span, **w**, causing a bending moment of $wL^2/8$ at the midspan.

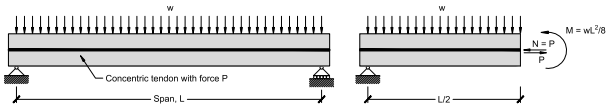

Fig. 35.3 – Prestressed member with a concentric tendon. Elevation view (left) and free body diagram at midspan (right). Note the tension force acting to the right should be aligned with the tendon.

Consider the stresses in the member at the midspan, also shown in Fig. 35.3. In addition to the bending moment, there is also an axial load applied to the section due to the prestressing force. If the concrete is uncracked, and therefore behaving in a linear elastic manner, the stresses in the concrete, $\boldsymbol{\sigma_c}$, can be calculated by using the basic definition of stress and Navier's equation:

$$\sigma_{c,top} = -\frac{P}{A} - \frac{My_{top}}{I} \tag{35.1}$$

$$\sigma_{c,bot} = -\frac{P}{A} + \frac{My_{bot}}{I} \tag{35.2}$$

In Eqs (35.1) and (35.2), $\boldsymbol{\sigma_{c,top}}$ and $\boldsymbol{\sigma_{c,top}}$ refer to the concrete stresses at the top and bottom of the beam respectively, **A** is the cross sectional area, **I** is the second moment of area, and $\mathbf{y_{top}}$ and $\mathbf{y_{bot}}$ are the distances to the top and bottom of the beam from the centroidal axis. This method is appropriate for finding the stresses if, using these equations, they are found to be less than the cracking strength of the concrete.

Calculating Stresses in Prestressed Concrete Members with Eccentric Tendons

Arranging the tendons in a prestressed concrete member so that they do not align with the centroidal axis is an effective strategy when designing for bending. Consider the beam shown in Fig. 35.4 which has a straight tendon that is eccentric by a distance **e** from the centroidal axis. In the absence of applied forces, the prestressing force will compress the member at the location of the steel, causing it to curve upwards. This counteracts the downwards displacements caused by gravity loads, as shown in Fig. 35.5.

Note: If the stresses exceed the tensile strength of the concrete, it will crack, and more advanced analysis procedures are required to analyze the behaviour.

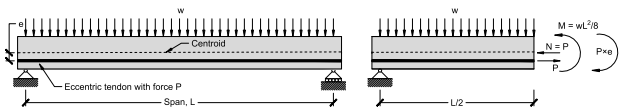

Fig. 35.4 – Prestressed concrete member with eccentric tendons. Elevation view (left) and free body diagram at midspan (right).

When the tendon is eccentric, the member curves because the axial force in the concrete, which resists the eccentric tensile force in the steel, must act through the centroid of the cross section. Since the two forces are equal and opposite, but separated by a distance **e**, they produce a couple which counteracts the bending moment caused by the loads. The stresses in the concrete can then be taken as the sum of those caused by the prestressing force, those caused by the eccentricity of the tendon, and those caused by the applied loads:

$$\sigma_{c,top} = -\frac{P}{A} + \frac{Pey_{top}}{I} - \frac{My_{top}}{I} \tag{35.3}$$

$$\sigma_{c,bot} = -\frac{P}{A} - \frac{Pey_{bot}}{I} + \frac{My_{bot}}{I} \tag{35.4}$$

Eqs. (35.3) and (35.4) can be used to calculate the stresses in the concrete at any location along the length of the member. Note that in regions where the bending moment is low, like near the supports, the stresses caused by the eccentricity of the tendons may cause the top of the member to crack. Therefore, it is common to have the tendons follow a curved profile so that the eccentricity varies to match the demand from the applied loads.

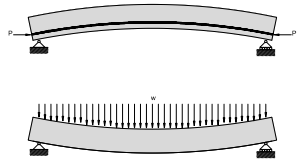

Fig. 35.5 – Curving of prestressed member due to eccentric tendons (top), which opposes the deflections caused by applied loads (bottom)

Appendices

Appendix A – Common Material Properties

Average Properties of Some Typical Materials Note that except for density, stiffness and coefficient of thermal expansion, all values have a considerable range

Material	Weight (kN/m^3)	Stiffness E (MPa)	Tensile Strength (MPa)		Compressive Strength (MPa)	Resilience (MJ/m^3)	Toughness (MJ/m^3) tens./comp.	Ductility Max. Elong. (%) Plastic/Elastic	α $10^{-6}/^oC$	Cost $/kg	Comment
			Yield	Ultimate							
Low Alloy Steel	77	200,000	420	560	420	0.44	135	25/0.21	12	0.60	Used in buildings, bridges, cars, etc.
High Tensile Steel	77	200,000	1650	1860	1650	6.8	55	4/0.83	12	1.50	Wire ropes, cables
High Alloy Steel	77	200,000	700	800	700	1.22	200	25/0.35	12	2.00	Pressure Vessels and tanks
Piano Wire	77	200,000	-	3000	-	22	22	0.2/1.50	12	1.50	Brittle material, not used in structures
Cast Iron	70	150,000	-	110	770	0.04	0.06/6	1/0.7	11	0.50	Traditional cast iron, moulded
Wrought Iron	75	185,000	200	350	200	0.11	90	30/0.11	12	1.00	99% pure iron, hammered, fibrous
Aluminum	27	69,000	40	80	60	0.012	19	40/0.06	24	1.80	Light, ductile, non-corrosive, soft metal
Aluminum Alloy	27	73,000	470	580	500	1.51	50	11/0.64	24	2.50	Used for canoes, aircraft, etc.
Copper	88	124,000	70	230	200	0.02	85	55/0.06	20	7.47	Very ductile metal – rounded curve
Bronze	79	105,000	200	390	350	0.2	40	12/0.19	17	2.80	Tin + copper alloy – stronger
Gold	189	82,000	40	220	180	0.01	80	50/0.05	14	40k	Heavy, expensive metal
Granite	26	52,000	-	11	140	0.001	0.01/0.26	0/0.02	8	0.15	Strongest and most durable building stone
Limestone	25	58,000	-	8	62	0.0006	0.01/0.09	0/0.01	6	0.03	Soft, useful building store
Slate	28	95,000	-	60	100	0.019	0.02/0.10	0/0.06		0.08	Stratified rock with high tensile strength
Brick	19	20,000	-	3	20	0.0002	0.01/0.03	0/0.01	9	0.10	Fired clay
Concrete	24	30,000	-	3	35	0.002	0.01/0.10	0/0.01	9	0.12	Mixture of cement, sand, stone, water
Glass	27	69,000	-	100	200	0.072	0.07/0.8	0/0.15	20	1.50	Solidified liquid sand
Oak	7.5	14,000	75	90	60	0.23	0.3/2.5	0.5/0.47	3	3.2	Strong, tough, heavy hardwood
Spruce	4.4	11,000	55	70	50	0.19	0.2/2.2	0.5/0.50	7	2.0	Light, strong, durable softwood
Tendon	10	900	70	80	-	2.7	4	1/7.8		-	Used as tension ties in mammals
Bone	20	17,000	150	180	180	0.66	1	0.5/0.9		-	Used as struts and beams in mammals
Rubber	9.2	7	-	20	20	15	20	4/300	500	2.0	Strange, useful material – low stiffness
Spider's Silk	10	4,000	-	1400	-	160	170	10/35		-	Most resilient material
Carbon Fibre	15	160,000	-	1800	-	10	10	0.1/1.1		50.0	Carbon fibre composites used in aircraft
Nylon Fibre	11	5,500	-	900	-	74	75	2/16	80	8.00	Excellent if stiffness not required
Kevlar Fibre	14	130,000	-	3600	-	50	60	1/2.7		50.00	Super material in many ways

Appendix B – HSS Tables

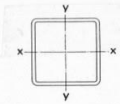

STEEL

SQUARE Hollow Structural Sections **METRIC Dimensions and Properties**

Designation	Size	Mass	Dead Load	Area	I	S	r	Z	Torsion J	Surface Area	Shear C_{rt}
mm x mm x mm	mm x mm x mm	kg/m	kN/m	mm^2	$10^6\ mm^4$	$10^3\ mm^3$	mm	$10^3\ mm^3$	$10^3\ mm^4$	m^2/m	mm^2
HSS 305x305x13	HSS 305x305x12.7	113	1.110	14 400	202	1 330	118	1 560	324 000	1.18	6 450
x 11	x 11.1	100	0.982	12 800	181	1 190	119	1 390	288 000	1.18	5 790
x 9.5	x 9.53	86.5	0.848	11 000	158	1 040	120	1 210	250 000	1.19	5 080
x 8.0	x 7.95	72.8	0.714	9 280	135	886	121	1 030	211 000	1.19	4 340
x 6.4	x 6.35	58.7	0.576	7 480	110	723	121	833	171 000	1.20	3 550
HSS 254x254x13	HSS 254x254x12.7	93.0	0.912	11 800	113	888	97.6	1 060	183 000	0.972	5 160
x 11	x 11.1	82.4	0.808	10 500	102	799	98.4	945	163 000	0.978	4 660
x 9.5	x 9.53	71.3	0.699	9 090	89.3	703	99.1	825	142 000	0.983	4 110
x 8.0	x 7.95	60.1	0.590	7 660	76.5	602	99.9	702	121 000	0.989	3 530
x 6.4	x 6.35	48.6	0.476	6 190	62.7	494	101	571	97 900	0.994	2 900
HSS 203x203x13	HSS 203x203x12.7	72.7	0.713	9 260	54.7	538	76.8	650	90 700	0.769	3 870
x 11	x 11.1	64.6	0.634	8 230	49.6	488	77.6	584	81 200	0.775	3 530
x 9.5	x 9.53	56.1	0.550	7 150	43.9	432	78.4	513	71 000	0.780	3 150
x 8.0	x 7.95	47.5	0.465	6 050	37.9	373	79.2	438	60 500	0.786	2 730
x 6.4	x 6.35	38.4	0.377	4 900	31.3	308	79.9	359	49 300	0.791	2 260
HSS 178x178x13	HSS 178x178x12.7	62.6	0.614	7 970	35.2	396	66.4	484	59 200	0.668	3 230
x 11	x 11.1	55.7	0.547	7 100	32.1	361	67.2	436	53 200	0.673	2 970
x 9.5	x 9.53	48.5	0.476	6 180	28.6	322	68.0	385	46 700	0.678	2 660
x 8.0	x 7.95	41.1	0.403	5 240	24.8	279	68.8	330	39 900	0.684	2 320
x 6.4	x 6.35	33.4	0.327	4 250	20.6	231	69.6	271	32 700	0.689	1 940
x 4.8	x 4.78	25.5	0.250	3 250	16.1	181	70.3	209	25 200	0.695	1 520
HSS 152x152x13	HSS 152x152x12.7	52.4	0.514	6 680	21.0	275	56.0	341	36 000	0.566	2 580
x 11	x 11.1	46.9	0.460	5 970	19.3	253	56.8	310	32 500	0.571	2 400
x 9.5	x 9.53	40.9	0.401	5 210	17.3	227	57.6	275	28 700	0.577	2 180
x 8.0	x 7.95	34.8	0.341	4 430	15.1	198	58.4	237	24 600	0.582	1 920
x 6.4	x 6.35	28.3	0.278	3 610	12.6	166	59.2	195	20 300	0.588	1 610
x 4.8	x 4.78	21.7	0.213	2 760	9.93	130	59.9	152	15 700	0.593	1 270
HSS 127x127x11	HSS 127x127x11.1	38.0	0.373	4 840	10.4	164	46.4	205	18 000	0.470	1 840
x 9.5	x 9.53	33.3	0.327	4 240	9.47	149	47.2	183	16 000	0.475	1 690
x 8.0	x 7.95	28.4	0.279	3 620	8.35	132	48.0	159	13 900	0.481	1 510
x 6.4	x 6.35	23.2	0.228	2 960	7.05	111	48.8	132	11 500	0.486	1 290
x 4.8	x 4.78	17.9	0.175	2 280	5.60	88.1	49.6	103	8 920	0.492	1 030
HSS 102x102x9.5	HSS 102x102x9.53	25.7	0.252	3 280	4.44	87.4	36.8	110	7 740	0.374	1210
x 8.0	x 7.95	22.1	0.217	2 820	3.98	78.4	37.6	96.6	6 780	0.379	1110
x 6.4	x 6.35	18.2	0.178	2 320	3.42	67.3	38.4	81.3	5 670	0.385	968
x 4.8	x 4.78	14.1	0.138	1 790	2.75	54.2	39.2	64.3	4 450	0.390	789
HSS 89x89x9.5	HSS 88.9x88.9x9.53	21.9	0.215	2 790	2.79	62.7	31.6	80.2	4 970	0.323	968
x 8.0	x 7.95	18.9	0.186	2 410	2.53	57.0	32.4	71.2	4 390	0.328	908
x 6.4	x 6.35	15.6	0.153	1 990	2.20	49.5	33.2	60.5	3 700	0.334	806
x 4.8	x 4.78	12.2	0.119	1 550	1.79	40.3	34.0	48.2	2 930	0.339	667
HSS 76x76x8.0	HSS 76.2x76.2x7.95	15.8	0.155	2 010	1.49	39.0	27.2	49.7	2 630	0.278	706
x 6.4	x 6.35	13.1	0.129	1 670	1.31	34.4	28.0	42.7	2 250	0.283	645
x 4.8	x 4.78	10.3	0.101	1 310	1.08	28.5	28.8	34.4	1 800	0.288	546
HSS 64x64x6.4	HSS 63.5x63.5x6.35	10.6	0.104	1 350	0.701	22.1	22.8	28.0	1 230	0.232	484
x 4.8	x 4.78	8.35	0.082	1 060	0.593	18.7	23.6	22.9	1 000	0.238	424
x 3.8	x 3.81	6.85	0.067	872	0.506	15.9	24.1	19.2	836	0.241	368
x 3.2	x 3.18	5.82	0.057	741	0.441	13.9	24.4	16.5	717	0.243	323
HSS 51x51x6.4	HSS 50.8x50.8x6.35	8.05	0.079	1 030	0.317	12.5	17.6	16.3	580	0.181	323
x 4.8	x 4.78	6.45	0.063	821	0.278	10.9	18.4	13.8	485	0.187	303
x 3.8	x 3.81	5.33	0.052	679	0.242	9.54	18.9	11.7	410	0.190	271
x 3.2	x 3.18	4.55	0.045	580	0.214	8.42	19.2	10.2	355	0.192	242
x 2.8	x 2.79	4.05	0.040	516	0.194	7.64	19.4	9.15	318	0.194	221
HSS 38x38x4.8	HSS 38.1x38.1x4.78	4.54	0.044	578	0.100	5.27	13.2	6.91	184	0.136	181
x 3.8	x 3.81	3.81	0.037	485	0.091	4.77	13.7	6.04	160	0.139	174
x 3.2	x 3.18	3.28	0.032	418	0.082	4.31	14.0	5.34	141	0.141	161
x 2.5	x 2.54	2.71	0.026	345	0.071	3.71	14.3	4.51	118	0.144	142
HSS 32x32x3.8	HSS 31.8x31.8x3.81	3.06	0.030	389	0.048	3.01	11.1	3.92	87.0	0.114	126
x 3.2	x 3.18	2.65	0.026	338	0.044	2.77	11.4	3.51	77.6	0.116	121
x 2.5	x 2.54	2.20	0.022	281	0.039	2.44	11.7	3.01	66.1	0.118	110
HSS 25x25x3.2	HSS 25.4x25.4x3.18	2.01	0.020	257	0.020	1.56	8.79	2.05	36.3	0.091	80.6
x 2.5	x 2.54	1.69	0.017	216	0.018	1.41	9.12	1.79	31.6	0.093	77.4

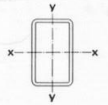

STEEL

RECTANGULAR Hollow Structural Sections **METRIC Dimensions and Properties**

Designation	Size	Mass	Dead Load	Area	I_x	S_x	r_x	Z_x	I_y	S_y	r_y	Z_y	Torsion J	Shear C_{rt}
mm x mm x mm	mm x mm x mm	kg/m	kN/m	mm^2	$10^6\ mm^4$	$10^3\ mm^3$	mm	$10^3\ mm^3$	$10^6\ mm^4$	$10^3\ mm^3$	mm	$10^3\ mm^3$	$10^3\ mm^4$	mm^2
HSS 305x203x13	HSS 305x203x12.7	93.0	0.912	11 800	147	964	111	1 190	78.1	769	81.2	896	167 000	6 450
x 11	x 11.1	82.4	0.808	10 500	132	867	112	1 060	70.5	693	81.9	802	149 000	5 790
x 9.5	x 9.53	71.3	0.699	9 090	116	762	113	925	62.1	611	82.7	701	130 000	5 080
x 8.0	x 7.95	60.1	0.590	7 660	99.4	652	114	787	53.3	524	83.4	596	111 000	4 340
x 6.4	x 6.35	48.6	0.476	6 190	81.5	535	115	640	43.8	431	84.1	486	89 800	3 550
HSS254x152x13	HSS254x152x12.7	72.7	0.713	9 260	75.2	592	90.1	746	33.6	441	60.2	522	78 200	5 160
x 11	x 11.1	64.6	0.634	8 230	68.2	537	91.0	671	30.6	401	61.0	470	70 200	4 660
x 9.5	x 9.53	56.1	0.550	7 150	60.3	475	91.9	589	27.2	357	61.7	413	61 600	4 110
x 8.0	x 7.95	47.5	0.465	6 050	52.0	409	92.7	503	23.5	309	62.4	353	52 600	3 530
x 6.4	x 6.35	38.4	0.377	4 900	42.9	338	93.6	411	19.5	256	63.1	290	43 000	2 900
HSS 203x152x13	HSS 203x152x12.7	62.6	0.614	7 970	43.0	123	73.4	528	27.3	358	58.5	432	56 400	3 870
x 11	x 11.1	55.7	0.547	7 100	39.1	385	74.2	476	24.9	327	59.3	390	50 800	3 530
x 9.5	x 9.53	48.5	0.476	6 180	34.8	343	75.1	419	22.3	292	60.0	344	44 600	3 150
x 8.0	x 7.95	41.1	0.403	5 240	30.2	297	75.9	360	19.3	254	60.7	295	38 200	2 730
x 6.4	x 6.35	33.4	0.327	4 250	25.0	246	76.7	295	16.1	211	61.5	243	31 200	2 260
x 4.8	x 4.78	25.5	0.250	3 250	19.5	192	77.5	228	12.6	165	62.2	188	24 100	1 760
HSS 203x102x13	HSS 203x102x12.7	52.4	0.514	6 680	31.2	307	68.4	405	10.2	201	39.1	246	27 000	3 870
x 11	x 11.1	46.9	0.460	5 970	28.7	282	69.3	367	9.46	186	39.8	224	24 600	3 530
x 9.5	x 9.53	40.9	0.401	5 210	25.8	253	70.3	325	8.56	168	40.5	199	21 900	3 150
x 8.0	x 7.95	34.8	0.341	4 430	22.5	221	71.2	281	7.54	148	41.2	172	18 900	2 730
x 6.4	x 6.35	28.3	0.278	3 610	18.8	185	72.2	232	6.35	125	42.0	143	15 600	2 260
x 4.8	x 4.78	21.7	0.213	2 760	14.7	145	73.1	180	5.03	99.0	42.7	111	12 200	1 760
HSS 178x127x13	HSS 178x127x12.7	52.4	0.514	6 680	26.4	297	62.8	377	15.5	243	48.1	298	33 600	3 230
x 11	x 11.1	46.9	0.460	5 970	24.2	272	63.7	342	14.2	224	48.8	270	30 400	2 970
x 9.5	x 9.53	40.9	0.401	5 210	21.7	244	64.6	303	12.8	202	49.6	240	26 900	2 660
x 8.0	x 7.95	34.8	0.341	4 430	18.9	213	65.4	261	11.2	177	50.3	207	23 100	2 320
x 6.4	x 6.35	28.3	0.278	3 610	15.8	178	66.2	216	9.40	148	51.1	171	19 000	1 940
x 4.8	x 4.78	21.7	0.213	2 760	12.4	140	67.1	167	7.41	117	51.8	133	14 700	1 520
HSS 152x102x11	HSS 152x102x11.1	38.0	0.373	4 840	13.6	179	53.1	230	7.13	140	38.4	172	16 300	2 400
x 9.5	x 9.53	33.3	0.327	4 240	12.4	162	54.0	205	6.50	128	39.1	154	14 500	2 180
x 8.0	x 7.95	28.4	0.279	3 620	10.9	143	54.8	178	5.76	113	39.9	134	12 600	1 920
x 6.4	x 6.35	23.2	0.228	2 960	9.18	121	55.7	148	4.88	96.1	40.6	112	10 500	1 610
x 4.8	x 4.78	17.9	0.175	2 280	7.28	95.6	56.5	116	3.89	76.6	41.3	87.8	8 160	1 270
HSS 127x76x9.5	HSS 127x76.2x9.53	25.7	0.252	3 280	6.12	96.4	43.2	126	2.69	70.5	28.6	87.5	6 600	1 690
x 8.0	x 7.95	22.1	0.217	2 820	5.49	86.4	44.1	111	2.43	63.8	29.4	77.2	5 810	1 510
x 6.4	x 6.35	18.2	0.178	2 320	4.70	74.0	45.1	93.3	2.10	55.1	30.1	65.2	4 890	1 290
x 4.8	x 4.78	14.1	0.138	1 790	3.78	59.5	45.9	73.8	1.70	44.7	30.8	51.7	3 860	1 030
HSS 127x64x9.5	HSS 127x63.5x9.53	23.8	0.234	3 030	5.28	83.2	41.7	112	1.70	53.6	23.7	67.4	4 640	1 690
x 8.0	x 7.95	20.5	0.201	2 610	4.77	75.1	42.7	98.9	1.56	49.1	24.4	60.0	4 130	1 510
x 6.4	x 6.35	16.9	0.166	2 150	4.11	64.8	43.7	83.6	1.36	42.9	25.1	51.0	3 510	1 290
x 4.8	x 4.78	13.1	0.129	1 670	3.33	52.4	44.6	66.3	1.12	35.2	25.9	40.7	2 800	1 030
HSS 127x51x9.5	HSS 127x50.8x9.53	21.9	0.215	2 790	4.45	70.0	39.9	97.7	0.961	37.8	18.6	48.9	2 930	1 690
x 8.0	x 7.95	18.9	0.186	2 410	4.05	63.8	41.0	86.9	0.897	35.3	19.3	44.0	2 650	1 510
x 6.4	x 6.35	15.6	0.153	1 990	3.53	55.5	42.1	73.8	0.798	31.4	20.0	37.9	2 290	1 290
x 4.8	x 4.78	12.2	0.119	1 550	2.87	45.3	43.1	58.9	0.665	26.2	20.7	30.5	1 850	1 030
HSS 102x76x9.5	HSS 102x76.2x9.53	21.9	0.215	2 790	3.41	67.2	35.0	87.6	2.15	56.3	27.7	71.3	4 710	1 210
x 8.0	x 7.95	18.9	0.186	2 410	3.10	61.0	35.8	77.7	1.96	51.4	28.5	63.5	4 170	1 110
x 6.4	x 6.35	15.6	0.153	1 990	2.68	52.8	36.7	65.9	1.71	44.8	29.3	54.0	3 530	968
x 4.8	x 4.78	12.2	0.119	1 550	2.18	43.0	37.5	52.5	1.39	36.6	30.0	43.1	2 800	789
HSS 102x51x8.0	HSS 102x50.8x7.95	15.8	0.155	2 010	2.21	43.5	33.2	58.8	0.709	27.9	18.8	35.4	1 950	1 110
x 6.4	x 6.35	13.1	0.129	1 670	1.95	38.4	34.2	50.6	0.638	25.1	19.5	30.7	1 690	968
x 4.8	x 4.78	10.3	0.101	1 310	1.61	31.8	35.1	40.8	0.536	21.1	20.3	24.9	1 370	789
x 3.8	x 3.81	8.37	0.082	1 070	1.36	26.8	35.7	33.9	0.456	18.0	20.7	20.8	1 140	658
x 3.2	x 3.18	7.09	0.069	903	1.17	23.1	36.1	29.0	0.397	15.6	21.0	17.9	979	565
HSS 89x64x8.0	HSS 88.9x63.5x7.95	15.8	0.155	2 010	1.87	42.1	30.5	54.9	1.09	34.3	23.3	43.2	2 450	908
x 6.4	x 6.35	13.1	0.129	1 670	1.65	37.1	31.4	47.1	0.966	30.4	24.0	37.2	2 100	806
x 4.8	x 4.78	10.3	0.101	1 310	1.36	30.6	32.3	38.0	0.803	25.3	24.8	30.1	1 690	667
x 3.8	x 3.81	8.37	0.082	1 070	1.15	25.8	32.8	31.5	0.679	21.4	25.2	25.0	1 400	561
x 3.2	x 3.18	7.09	0.069	903	0.990	22.3	33.1	27.0	0.588	18.5	25.5	21.4	1 190	485
HSS 76x51x8.0	HSS 76.2x50.8x7.95	12.6	0.123	1 600	1.01	26.6	25.1	35.9	0.522	20.5	18.0	26.7	1 270	706
x 6.4	x 6.35	10.6	0.104	1 350	0.917	24.1	26.1	31.4	0.477	18.8	18.8	23.5	1 110	645
x 4.8	x 4.78	8.35	0.082	1 060	0.774	20.3	27.0	25.7	0.407	16.0	19.6	19.3	911	546
x 3.8	x 3.81	6.85	0.067	872	0.660	17.3	27.5	21.6	0.349	13.8	20.0	16.3	762	465
HSS 51x25x3.2	HSS 50.8x25.4x3.18	3.28	0.032	418	0.122	4.81	17.1	6.33	0.040	3.14	9.77	3.84	106	242
x 2.5	x 2.54	2.71	0.026	345	0.105	4.15	17.5	5.35	0.035	2.75	10.1	3.27	89.8	206

Appendix C – Steel Wide Flange Beams and Sawn Timber Section Tables

Wide Flange Rolled Steel Beams
Dimensions and Section Properties

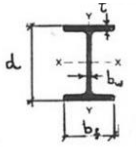

Designation	Dimensions				Dead Load	Area	Strong Axis x-x			Weak Axis y-y			Torsion Constant	Shear Depth
	d	b_f	t	b_w			I_x	S_x	r_x	I_y	S_y	r_y	J	I_x/Q
mm × kg/m	mm	mm	mm	mm	kN/m	mm²	10^6 mm⁴	10^3 mm³	mm	10^6 mm⁴	10^3 mm³	mm	10^3 mm⁴	mm
W920 × 446	933	423	43	24.0	4.38	57000	8470	18200	385	540	2550	97.3	26800	822
× 365	916	419	34	20.3	3.57	46400	6710	14600	380	421	2010	95.3	14400	813
× 313	932	309	34	21.1	3.06	39800	5480	11800	371	170	1100	65.4	11600	806
× 238	915	305	26	16.5	2.33	30400	4060	8880	365	123	806	63.6	5140	796
W840 × 329	862	401	32	19.7	3.23	42000	5350	12400	357	349	1740	91.2	11500	764
× 210	846	293	24	15.4	2.06	26800	3110	7340	341	103	700	62.0	4050	738
× 176	835	292	19	14.0	1.72	22400	2460	5900	331	78.2	536	59.1	2220	722
W760 × 257	773	381	27	16.6	2.52	32800	3420	8840	323	250	1310	87.3	6380	689
× 173	762	267	22	14.4	1.70	22100	2060	5400	305	68.7	515	55.8	2690	663
× 147	753	265	17	13.2	1.44	18700	1660	4410	298	52.9	399	53.2	1560	651
W690 × 217	695	355	25	15.4	2.13	27700	2340	6740	291	185	1040	81.7	4560	618
× 152	688	254	21	13.1	1.49	19400	1510	4380	279	57.8	455	54.6	2200	604
× 125	678	253	16	11.7	1.23	16000	1190	3500	273	44.1	349	52.5	1180	594
W610 × 195	622	327	24	15.4	1.91	24900	1680	5400	260	142	871	75.5	3970	554
× 155	611	324	19	12.7	1.51	19700	1290	4220	256	108	666	74.0	1950	545
× 125	612	229	20	11.9	1.22	15900	985	3220	249	39.3	343	49.7	1540	537
× 101	603	228	15	10.5	0.99	13000	764	2530	242	29.5	259	47.6	781	527
W530 × 182	551	315	24	15.2	1.78	23100	1240	4480	232	127	808	74.1	3740	492
× 150	543	312	20	12.7	1.47	19200	1010	3710	229	103	659	73.2	2160	487
× 109	539	211	19	11.6	1.06	13900	667	2480	219	29.5	280	46.1	1260	471
× 82	528	209	13	9.5	0.81	10500	479	1810	214	20.3	194	44.0	530	463
W460 × 144	472	283	22	13.6	1.41	18400	726	3080	199	83.6	591	67.4	2440	421
× 97	466	193	19	11.4	0.95	12300	445	1910	190	22.8	237	43.1	1130	408
× 82	460	191	16	9.9	0.80	10400	370	1610	189	18.6	195	42.3	691	404
× 61	450	189	11	8.1	0.60	7760	259	1150	183	12.2	129	39.7	289	395
W410 × 114	420	261	19	11.6	1.12	14600	462	2200	178	57.2	439	62.6	1490	376
× 74	413	180	16	9.7	0.73	9550	275	1330	170	15.6	173	40.4	637	364
× 60	407	178	13	7.7	0.58	7580	216	1060	169	12.0	135	39.8	328	363
× 39	399	140	9	6.4	0.38	4990	127	634	160	4.0	57.7	28.5	111	348
W360 × 314	399	401	40	24.9	3.07	39900	1100	5530	166	426	2120	103	18500	345
× 122	363	257	22	13.0	1.19	15500	365	2010	153	61.5	478	63.0	2100	322
× 79	354	205	17	9.4	0.78	10100	227	1280	150	24.2	236	48.9	814	317
× 64	347	203	14	7.7	0.63	8140	178	1030	148	18.8	186	48.1	438	312
× 45	352	171	10	6.9	0.44	5730	122	691	146	8.18	95.7	37.8	160	313
× 33	349	127	8	5.8	0.32	4170	82.7	474	141	2.91	45.8	26.4	85.9	305
W310 × 253	356	319	40	24.4	2.48	32200	682	3830	146	215	1350	81.7	14800	304
× 118	314	307	19	11.9	1.15	15000	275	1750	135	90.2	588	77.5	1600	282
× 79	306	254	15	8.8	0.77	10100	177	1160	132	39.9	314	62.9	657	277
× 60	303	203	13	7.5	0.59	7590	129	849	130	18.3	180	49.1	397	274
× 39	310	165	10	5.8	0.38	4940	85.1	549	131	7.27	88.1	38.4	126	279
× 21	303	101	6	5.1	0.21	2690	37.0	244	117	0.983	19.5	19.1	29.4	258
W250 × 115	269	259	22	13.5	1.12	14600	189	1410	114	64.1	495	66.3	2130	236
× 49	247	202	11	7.4	0.48	6250	70.6	572	106	15.1	150	49.2	241	223
× 33	258	146	9	6.1	0.32	4170	48.9	379	108	4.73	64.7	33.7	98.5	231
W200 × 59	210	205	14	9.1	0.58	7560	61.1	582	89.9	20.4	199	51.9	465	187
× 36	201	165	10	6.2	0.35	4580	34.4	342	86.7	7.64	92.6	40.8	146	181
× 27	207	133	8	5.8	0.26	3390	25.8	249	87.2	3.30	49.6	31.2	71.3	185
W150 × 30	157	153	9	6.6	0.29	3790	17.2	219	67.4	5.56	72.6	38.3	101	141
× 14	150	100	6	4.3	0.13	1730	6.87	91.5	63.0	0.92	18.4	23.0	17.0	133

Sawn Timber Sections
Dimensions and Section Properties

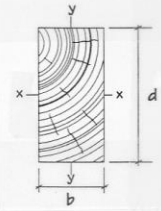

Size and Designation $b \times d$	Nominal Dimensions	Dead Load	Area	Strong Axis x-x			Weak Axis y-y			Torsion Constant
				I_x	S_x	r_x	I_y	S_y	r_y	J
mm	in.	kN/m	mm²	10^6 mm⁴	10^3 mm³	mm	10^6 mm⁴	10^3 mm³	mm	10^6 mm⁴
292 × 495	12 × 20	0.907	145000	2950	11900	143	1030	7030	84.3	2570
× 445	× 18	0.816	130000	2140	9640	129	923	6320	84.3	2190
× 394	× 16	0.722	115000	1490	7550	114	817	5600	84.3	1760
× 343	× 14	0.629	100000	982	5730	99.0	712	4870	84.3	1370
× 292	× 12	0.535	85300	606	4150	84.3	606	4150	84.3	1030
241 × 495	10 × 20	0.749	119000	2440	9840	143	577	4790	69.9	1600
× 445	× 18	0.673	107000	1770	7950	129	519	4310	69.6	1360
× 394	× 16	0.596	95000	1230	6240	114	460	3810	69.6	1130
× 343	× 14	0.519	82700	810	4730	99.0	400	3320	69.6	900
× 292	× 12	0.442	70400	500	3420	84.3	341	2830	69.6	671
× 241	× 10	0.365	58100	281	2330	69.6	281	2330	69.6	476
191 × 495	8 × 20	0.594	94600	1930	7800	143	287	3010	55.1	868
× 445	× 18	0.534	85000	1400	6300	129	258	2710	55.1	751
× 394	× 16	0.472	75300	974	4940	114	229	2400	55.1	636
× 343	× 14	0.411	65500	642	3750	99.0	199	2090	55.1	515
× 292	× 12	0.350	55800	396	2710	84.3	170	1780	55.1	403
× 241	× 10	0.289	46000	223	1850	69.6	140	1470	55.1	285
× 191	× 8	0.229	36500	111	1160	55.1	111	1160	55.1	188
140 × 445	6 × 18	0.391	62300	1030	4620	129	102	1450	40.4	325
× 394	× 16	0.346	55200	714	3620	114	90.1	1290	40.4	279
× 343	× 14	0.301	48000	471	2750	99.0	78.4	1120	40.4	232
× 292	× 12	0.257	40900	290	1990	84.3	66.8	954	40.4	186
× 241	× 10	0.212	33700	163	1360	69.6	55.1	787	40.4	139
× 191	× 8	0.168	26700	81.3	851	55.1	43.7	624	40.4	94.9
× 140	× 6	0.123	19600	32.0	457	40.4	32.0	457	40.4	54.2
89 × 387	4 × 16	0.216	34400	430	2220	112	22.7	511	25.7	77.5
× 337	× 14	0.188	30000	284	1680	97.3	19.8	445	25.7	65.9
× 286	× 12	0.160	25500	174	1210	82.6	16.8	378	25.7	53.8
× 235	× 10	0.131	20900	96.3	819	67.8	13.8	310	25.7	41.9
× 184	× 8	0.103	16400	46.2	502	53.1	10.8	243	25.7	30.1
× 140	× 6	0.078	12500	20.4	291	40.4	8.22	185	25.7	19.8
× 114	× 5	0.064	10200	11.0	193	32.9	6.70	151	25.7	13.8
× 89	× 4	0.050	7920	5.23	118	25.7	5.23	117	25.7	8.85
64 × 337	3 × 14	0.135	21600	204	1210	97.3	7.36	230	18.5	25.8
× 286	× 12	0.115	18300	125	872	82.6	6.25	195	18.5	21.4
× 235	× 10	0.094	15000	69.2	589	67.8	5.13	160	18.5	17.0
× 184	× 8	0.074	11800	33.2	361	53.1	4.02	126	18.5	12.5
× 140	× 6	0.056	8960	14.6	209	40.4	3.06	95.6	18.5	8.68
× 114	× 5	0.046	7300	7.90	139	32.9	2.49	77.8	18.5	6.41
× 89	× 4	0.036	5700	3.76	84.5	25.7	1.94	60.8	18.5	4.29
38 × 337	2 × 14	0.071	12800	121	719	97.3	1.54	81.1	11.0	5.72
× 286	× 12	0.060	10900	74.1	518	82.6	1.31	68.8	11.0	4.79
× 235	× 10	0.049	8930	41.1	350	67.8	1.07	56.6	11.0	3.87
× 184	× 8	0.038	6990	19.7	214	53.1	0.84	44.3	11.0	2.91
× 140	× 6	0.029	5320	8.69	124	40.4	0.64	33.7	11.0	2.11
× 114	× 5	0.024	4330	4.69	82.3	32.9	0.52	27.4	11.0	1.65
× 89	× 4	0.019	3380	2.23	50.2	25.7	0.41	21.4	11.0	1.19
× 64	× 3	0.013	2430	0.83	25.9	18.5	0.29	15.4	11.0	0.73
× 38	× 2	0.008	1440	0.17	9.15	11.0	0.17	9.15	11.0	0.29

Appendix D – Wood Properties

Section 9 | Wood Structures

5th Percentile estimates of strength under one month loading. For safe working stresses reduce these breaking stresses by factor of safety of 1.5.

Page 259

9 – 11.2 (a) Specified strength and modulus of elasticity for dimension lumber, thickness 38 to 77 mm, MPa**

Species or Species Combination	Grade	Bending f_{bu}	Shear Longitudinal f_{vu}	Compression Parallel to Grain f_{pu}	Compression Perpendicular to Grain f_{qu}	Tension Parallel to Grain f_{tu}	Modulus of Elasticity E_{50}	Modulus of Elasticity E_{05}
Douglas Fir-Larch	Select Structural	17.5	1.1	16.5	3.6	13.5	11,000	8,000
	No. 1 and No. 2	10.0	1.1	9.0	3.6	9.0	9,500	6,000
Hem-Fir	Select Structural	16.0	0.8	14.5	1.9	13.5	11,000	7,500
	No. 1 and No. 2	11.5	0.8	10.5	1.9	9.0	10,500	7,000
Lodgepole Pine, or Ponderosa Pine	Select Structural	16.0	1.0	14.5	1.9	13.5	10,000	7,000
	No. 1 and No 2	11.5	1.0	10.5	1.9	9.0	9,000	6,000
Jack Pine	Select Structural	16.0	1.0	14.5	2.6	13.5	10,500	7,000
	No. 1 and No. 2	11.5	1.0	10.5	2.6	9.0	9,500	6,000
Red Pine	Select Structural	11.5	0.8	10.0	1.9	10.0	7,000	5,000
	No. 1 and No. 2	8.0	0.8	7.0	1.9	7.0	6,000	4,000
White Pine*	Select Structural	6.0	0.8	–	1.9	–	5,500	4,000
	No. 1 and No. 2	4.5	0.8	–	1.9	–	4,500	3,500

* *For use in stress-laminated decks only.*

** *Dimension lumber with thickness of 89 mm or greater shall have specified strengths in accordance with Table 13–11.2 (b).*

9 – 11.2 (b) Specified strength and modulus of elasticity for beams & stringers, post & timbers, minimum dimension 140 mm, MPa

Species or Species Combination	Grade	Bending f_{bu}	Shear Longitudinal f_{vu}	Compression Parallel to Grain f_{pu}	Compression Perpendicular to Grain f_{qu}	Tension Parallel to Grain f_{tu}	Modulus of Elasticity E_{50}	Modulus of Elasticity E_{05}
Douglas Fir-Larch	Select Structural	24.0	1.1	16.5	3.6	13.0	11,000	7,500
	No. 1	20.0	1.1	9.0	3.6	9.0	9,500	6,500
Hem-Fir	Select Structural	20.0	0.8	14.5	1.9	13.0	11,000	7,500
	No. 1	18.0	0.8	10.5	1.9	9.0	10,500	7,000
Lodgepole Pine, or Ponderosa Pine	Select Structural	18.5	1.0	14.5	1.9	13.0	10,000	7,000
	No. 1	13.0	1.0	10.5	1.9	9.0	9,000	6,000
Jack Pine	Select Structural	18.5	1.0	14.5	2.6	13.0	10,500	7,000
	No. 1	13.0	1.0	10.5	2.6	9.0	9,500	6,000
Red Pine	Select Structural	13.0	0.8	10.0	1.9	10.0	7,000	5,000
	No. 1	9.0	0.8	7.0	1.9	7.0	6,000	4,000

Table 4.3 *Average clear-wood strength values* for commercial species in air-dry condition*

Species	Relative density† Nominal	Relative density† Oven-dry	Shrinkage, green to air-dry based on dimensions when green (%) Radial	Tangential	Volumetric	Modulus of rupture (MPa)	Modulus of elasticity (MPa)	Compression parallel to grain, crushing strength max. (MPa)	Shear strength (MPa)	Compression perpendicular to grain, fiber stress at proportional limit (MPa)	Tension perpendicular to grain (MPa)
						Property					
SOFTWOODS											
Cedar											
Eastern white	0.30	0.31	–	–	3.8	42.3	4 380	24.8	6.93	2.68	2.63
Western red	0.34	0.34	–	–	4.8	53.8	8 270	33.9	5.58	3.43	1.46
Yellow	0.43	0.46	–	–	5.0	79.7	11 000	45.9	9.21	4.74	3.49
Douglas-fir	0.49	0.51	–	–	7.0	88.6	13 500	50.1	9.53	6.01	3.06
Fir											
Amabilis (Pacific silver)	0.39	0.41	–	–	7.5	68.9	11 400	40.8	7.54	3.61	3.06
Balsam	0.35	0.37	1.2	4.3	5.7	58.3	9 650	34.3	6.25	3.14	2.08
Hemlock											
Eastern	0.43	0.45	2.4	4.7	6.2	67.1	9 720	41.0	8.75	4.28	2.06
Western	0.43	0.47	–	–	8.1	81.1	12 300	46.7	6.48	4.53	2.93
Tamarack	0.51	0.54	–	–	7.1	76.0	9 380	44.8	9.00	6.15	3.47
Larch, western	0.58	0.64	–	–	8.0	107.0	14 300	60.9	9.25	7.31	3.62
Pine											
Eastern white	0.37	0.38	–	–	4.5	65.0	9 380	36.2	6.10	3.39	2.63
Jack	0.44	0.45	2.1	3.8	5.7	77.9	10 200	40.5	8.23	5.70	3.65
Lodgepole	0.41	0.46	–	–	6.6	76.0	10 900	43.2	8.54	3.65	3.78
Ponderosa	0.46	0.49	–	–	6.1	73.3	9 510	42.3	7.03	5.22	3.47
Red	0.40	0.42	1.9	4.1	6.5	69.7	9 450	37.9	7.50	4.96	3.54
Western white	0.37	0.40	–	–	6.0	64.1	10 100	36.1	6.34	3.23	2.64
Spruce											
Black	0.43	0.44	1.7	4.0	6.5	78.3	10 400	41.5	8.65	4.25	3.43
Engelmann	0.40	0.42	–	–	6.8	69.5	10 700	42.4	7.55	3.70	2.72
Red	0.40	0.42	–	–	6.2	71.5	11 000	38.5	9.20	3.77	3.70
Sitka	0.39	0.39	–	–	6.0	69.8	11 200	37.8	6.78	4.10	2.48
White	0.37	0.39	1.4	4.0	6.8	62.7	9 930	36.9	6.79	3.45	3.28
HARDWOODS											
Aspen, trembling	0.41	–	2.7	5.7	8.3	67.6	11 200	36.3	6.76	3.52	4.19
Birch, yellow	0.61	–	–	–	9.9	106.0	14 100	52.1	14.67	7.24	7.52
Maple, sugar	0.66	–	2.9	6.4	9.3	115.0	14 100	56.4	16.71	9.72	9.21
Oak, red	0.61	–	–	–	6.9	98.7	11 900	49.8	14.38	8.89	6.52

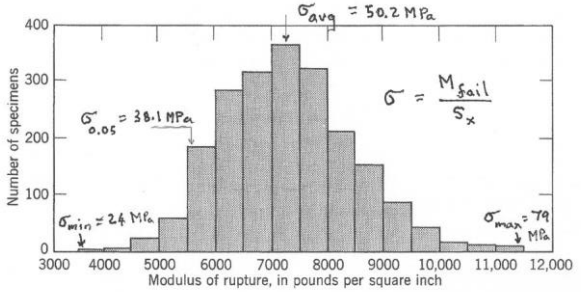

(b) Frequency distribution of bending strength of green Douglas fir. 2110 small clear specimens cut from a single tree. Short-term loading.

Appendix E – Common Unit Conversions

Working with SI units		
Lengths, Strains and Curvatures	Pressures and Stresses	Forces and Moments
1 m = 1,000 mm 1 m^2 = 10^6 mm^2 1 m^3 = 10^9 mm^3 1 mm/m = 10^3 mm/mm 1 rad/m = 10^6 mrad/mm	1 Pa = 1 N/m^2 1 kPa = 1 kN/m^2 1 MPa = 1 MN/m^2 1 MPa = 1 N/mm^2	1 kN = 1,000 N 1 MN = 10^6 N 1 Nm = 1,000 Nmm 1 kNm = 10^6 Nmm
Working with other unit systems and other miscellaneous quantities		
1 foot = 12 inches 1 cubit = 18 inches 1 yard = 3 feet 1 chain = 22 yards 1 furlong = 10 chains 1 mile = 8 furlongs 1 mile = 1,760 yards 1 acre = 10 square chains 1 square mile = 640 acres 1 ha = 10,000 square m	1 inch = 25.4 mm 1 foot = 304.8 mm 1 mile = 1609 m 1 ha = 2.47 acres 1 kg = 2.20 lbs 1 stone = 14.0 lbs 1 lbs/ ft^3 = 16.02 kg/ m^3 100 lbs/ft^3 = 15.72 kN/m^3 1 N = 0.225 lbs (force) 1 kip = 4.45 kN	9.81 m/s^2 = 32.2 $feet/s^2$ 1 kNm = 0.738 kip ft 1 kNm = 8.85 kip in 1 hp = 746 Watt 1 km/h = 0.278 m/s 1 km/h = 0.621 miles/h 1 knot = 1.852 km/h 1 MPa = 145.0 psi 1 kN/m^2 = 20.9 lbs/ft^2

Appendix F – Areas and Centroids of Common Shapes

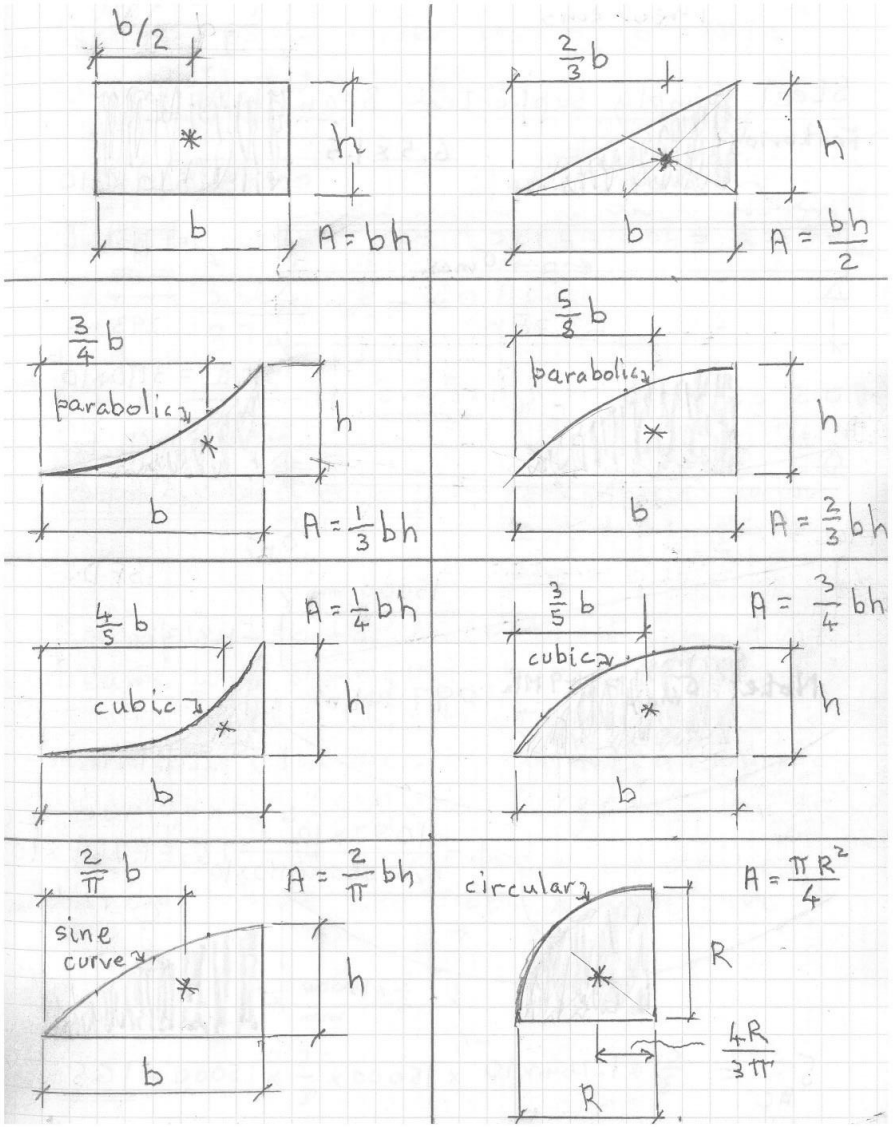

Appendix G – Common Canadian Reinforcing Bar Information

Designation	Linear Density (kg/m)	Nominal Diameter (mm)	Cross-Sectional Area (mm^2)
10M	0.785	11.3	100
15M	1.570	16.0	200
20M	2.355	19.6	300
25M	3.925	25.2	500
30M	5.495	29.9	700
35M	7.850	35.7	1000
45M	11.775	43.7	1500
55M	19.625	56.4	2500